PREPARATION AND PROPERTIES OF INCLUSION COMPLEXES BETWEEN β–CYCLODEXTRIN-MODIFIED HYDROXYALKYLACRYLCHITOSANS AND METHYL ORANGE

MONGKHOL PRAWATBORISUT

A THESIS SUBMITTED IN PARTIAL FULFILLMENT OF THE REQUIREMENT FOR THE DEGREE OF MASTER OF SCIENCE IN POLYMER TECHNOLOGY
DEPARTMENT OF CHEMISTRY
FACULTY OF SCIENCE
KING MONGKUT'S INSTITUTE OF TECHNOLOGY LADKRABANG
2016

KMITL-2016-SC-M-014-020

หัวข้อวิทยานิพนธ์	การเตรียมและสมบัติของสารประกอบเชิงซ้อนระหว่างไฮดรอกซีอัลคิลอะคริลไคโตซานปรับปรุงด้วย β-ไซโคล-เดกซ์ทริน และเมทิลออเรนจ์
ชื่อนักศึกษา	มงคล ประวัติบริสุทธิ์
รหัสประจำตัว	57605052
ปริญญา	วิทยาศาสตรมหาบัณฑิต (เทคโนโลยีพอลิเมอร์)
ภาควิชา	เคมี
พ.ศ.	2559
อาจารย์ที่ปรึกษาวิทยานิพนธ์	ผศ.ดร.ภัทธาวุธ มนต์วิเศษ

บทคัดย่อ

งานวิจัยนี้ศึกษาการเตรียมและสมบัติของสารประกอบเชิงซ้อนระหว่างไฮดรอกซี-อัลคิลอะคริลไคโตซานปรับปรุงด้วย β-ไซโคลเดกซ์ทริน (HAACSs-g-CDs) และเมทิลออเรนจ์ ซึ่งเป็นหนึ่งในสารประกอบเอโซ โดยไฮดรอกซีอัลคิลอะคริลไคโตซาน (HAACSs) เตรียมได้จากปฏิกิริยาการเติมแบบไมเคิลระหว่างไฮดรอกซีอัลคิลอะคริเลต (2-hydroxyethylacrylate, 2-hydroxy-propylacrylate หรือ 4-hydroxybutylacrylate) และไคโตซาน (CS) โดยใช้อัตราส่วนโดยโมลเป็น 6:1 จากนั้นนำไฮดรอกซีอัลคิลอะคริลไคโตซานที่ได้มาทำปฏิกิริยากับ β-ไซโคลเดกซ์ทริน ปรับปรุงด้วยหมู่โทซิล (TsCD) ด้วยปฏิกิริยาการเติมด้วยนิวคลีโอไฟล์เพื่อให้ได้ HAACSs-g-CDs ผลการพิสูจน์เอกลักษณ์เชิงโครงสร้างแสดงให้เห็นว่า β–ไซโคลเดกซ์ทรินสามารถต่อกิ่งบนสายโซ่ของ HAACSs ได้สำเร็จ และมีการเกิดสารประกอบเชิงซ้อนภายในโมเลกุล (Self-inclusion complex) จากนั้นศึกษาความสามารถในการเกิดสารประกอบเชิงซ้อนระหว่าง HAACSs-g-CDs กับเมทิล-ออเรนจ์ ผลการทดลองจากยูวี-วิซิเบิลสเปกทราบ่งบอกว่า HAACSs-g-CDs สามารถเกิดสารประกอบเชิงซ้อนกับเมทิลออเรนจ์ได้เช่นเดียวกับ β–ไซโคลเดกซ์ทริน จากนั้นทำการเตรียมฟิล์มจากกระบวนการขึ้นรูปแบบสารละลาย (Solution-casted films) ของ HAACSs, ไฮดรอกซีบิวทิลอะคริล-ไคโตซานปรับปรุงด้วย β-ไซโคลเดกซ์ทริน (TB-1) และสารประกอบเชิงซ้อนระหว่างเมทิลออเรนจ์ที่ปรับเปลี่ยนปริมาณ กับ TB-1 และทำการพิสูจน์เอกลักษณ์ ผลจาก TGA บ่งบอกว่าอุณหภูมิการสลายตัวของฟิล์ม TB-1 สูงกว่าฟิล์มจากไฮดรอกซีบิวทิลอะคริลไคโตซานและสารประกอบเชิงซ้อน นอกจากนี้ผลจาก DMA ยังแสดงให้เห็นว่าอุณหภูมิจากพีคหลักซึ่งบ่งบอกการระเหยของน้ำ, การเคลื่อนที่ของโมเลกุลในสถานะกึ่งเสถียร (Pseudo-stable stage) และการสลายตัวของโมเลกุล ไม่ปรากฏในเทอร์โมแกรมของฟิล์ม TB-1 แต่พบได้ในเทอร์โมแกรมของฟิล์มของสารประกอบเชิงซ้อน โดยผลการทดลองดังกล่าวแสดงให้เห็นว่าโมเลกุลของเมทิลออเรนจ์สามารถแทนที่สายโซ่ไฮดรอกซี-บิวทิลอะคริเลตในโพรงของ β-ไซโคลเดกซ์ทรินได้

คำสำคัญ : ไคโตซานปรับปรุง, β-ไซโคลเดกซ์ทริน, สารประกอบเชิงซ้อน, เมทิลออเรนจ์

Thesis Title	Preparation and Properties of Inclusion Complexes between β–Cyclodextrin-modified Hydroxyalkylacrylchitosans and Methyl Orange
Student Name	Mongkhol Prawatborisut
Student ID	57605052
Degree	Master of Science (Polymer Technology)
Department	Chemistry
Year	2016
Thesis Advisor	Asst. Prof. Dr. Pathavuth Monvisade

Abstract

This research studied on preparation and properties of inclusion complexes between β–cyclodextrin-modified hydroxyalkylacrylchitosans (HAACSs-g-CDs) and methyl orange, which is one of the azo compounds. Hydroxyalkylacrylchitosans (HAACSs) were synthesized by Michael addition reaction between various hydroxyalkylacrylates (2-hydroxyethylacrylate, 2-hydroxypropylacrylate, or 4-hydroxybutylacrylate) and chitosan (CS) using the mole ratio of 6:1. Thereafter, those HAACSs were reacted with tosyl-modified β–cyclodextrin (TsCD) via nucleophilic addition reaction to obtain HAACSs-g-CDs. The structural results indicated that β–cyclodextrin was successfully grafted onto HAACSs skeleton with the formation of self-inclusion complex. Afterwards, ability on forming inclusion complex of HAACSs-g-CDs with methyl orange was evaluated. The results from UV-Vis spectra suggested that HAACSs-g-CDs could form inclusion complex with methyl orange as same manner as β–cyclodextrin. Subsequently, solution-casted films from HAACSs, β-cyclodextrin modified hydroxybutylacrylchitosan (TB-1), and inclusion complexes between various amounts of methyl orange and TB-1 were prepared and characterized. The TGA results revealed that the degradation temperature of TB-1 film was higher than that of the hydroxybutylacrylchitosan film and the inclusion complex films. In addition to DMA results, the main peak temperature corresponded to water loss and local movement of the molecule in the pseudo-stable stage as well as molecular degradation did not exhibit in the thermogram of the TB-1 film, but it could be observed in the thermograms of the inclusion complex films. This indicated that methyl orange molecules could be able to substitute hydroxybutylacrylate moieties in β-cyclodextrin cavities.

Keywords : Modified Chitosans, β-Cyclodextrin, Inclusion complex, Methyl Orange

Acknowledgements

The author would like to express his deep gratitude to his advisor, Asst. Prof. Dr. Pathavuth Monvisade for his invaluable guidance, attention, and encouragement throughout this thesis. The grateful thanks also go to the thesis committees: Asst. Prof. Dr. Chonlada Ritvirulh, Asst. Prof. Dr. Patchanee Charoenying, and Asst. Prof. Dr. Thanida Trakulsujaritchok for reading and criticizing the manuscript.

The author would like to express his very great appreciation to Prof. Dr. Masayuki Yamaguchi for his constructive suggestions during the JAIST's Asian short-term stay program. This great appreciation is also extended to Japan Advanced Institute of Science and Technology (JAIST) and Japan Student Services Organization (JASSO) for financial support and guidance during the program. Additionally, the author would like to kindly thanks Faculty of Science, King Mongkut's Institute of Technology Ladkrabang for travel expense support.

The author greatly appreciates the entire professors who provided invaluable knowledge while studying in the Department of Chemistry, Faculty of Science, King Mongkut's Institute of Technology Ladkrabang. It goes without saying to all scientific staffs in the department for abundant assistance.

Special thanks to Thai Mitsui Specialty Chemicals Co., Ltd. for kindly supporting hydroxyalkylacrylates. In addition, thanks also go to National Metal and Materials Technology Center (MTEC) and Scientific and Technological Research Equipment Center at Chulalongkorn University for helping in analysis using GPC and NMR.

The author would also like to give the thanks to all people in Polymer Synthesis and Functional Materials Research Unit (PSFMU) and Yamaguchi's lab for their supports, especially Miss Pitchaya Treenate, Miss Rujirek Wiwattananukul, and Mr. Takumi Sako. The thanks are also extended to students in Taniike's lab for their help in teaching the method for operating thermogravimetric analyzer and Dr. Tong Huang for his kindly help on carrying out WAXS analysis. In addition, the author wish to thanks all of his friends who always encourage him during the master's program.

Last but not least, the author cannot express his thanks sincerely enough to his beloved family for their unconditional love, care, and supports, which enabled him to complete this thesis.

ขอบคุณมากครับ | Thank you very much | どうもありがとうございました

Mr. Mongkhol Prawatborisut

Table of Contents

List of Tables

List of Figures

Figure Page

Figure Page

Figure Page

Figure

Abbreviations

Name	Abbreviation
2-Hydroxyethylacrylate	HEA
2-Hydroxypropylacrylate	HPA
4-Hydroxybutylacrylate	HBA
Acetic acid	AcOH
Chitosan	CS
Cyclodextrins	CDs
Dichloromethane	DCM
Dimethylsulfoxide	DMSO
Dynamic mechanical thermal analysis	DMA
Fourier transform infrared spectroscopy	FTIR
Gel permeation chromatography	GPC
Hydroxalkylacrylchitosans	HAACSs
Hydroxybutylacrylchitosan	HBACS
Hydroxyethylacrylchitosan	HEACS
Hydroxypropylacrylchitosan	HPACS
Isopropanol	i-PrOH
Loss tangent	tan δ
Methyl orange	MO
N,N-Dimethylformamide	DMF
Proton nuclear magnetic resonance spectroscopy	^{1}H-NMR
p-Toluenesulfonic acid	TsOH
p-Toluenesulfonyl chloride	TsCl
Temperature in which %weight of the sample is 50	T_{50}
Temperature in which %weight of the sample is 90	T_{90}
Tetrahydrofuran	THF
Thermogravimetric analysis	TGA
Tosyl-modified-β-cyclodextrin	TsCD
Wide angle X-ray scattering	WAXS
β-cyclodextrin modified hydroxyalkylacrylchitosans	HAACS-g-CDs
β-cyclodextrin modified hydroxybutylacrylchitosans	TB-1, TB-2, TB-3
β-cyclodextrin modified hydroxyethylacrylchitosan	TE-1
β-cyclodextrin modified hydroxypropylacrylchitosan	TP-1
β-Cyclodextrin	CD
β-cyclodextrin-modified chitosan	CS-g-CD

Chapter 1
Introduction

1.1 Research Motivation

Cyclodextrins (CDs) are oligosaccharide consisting of glucopyranose units which covalently bond together by α-(1-4) linkage to form torus-like structure. They commonly have 6-8 glucopyranose units in their structure called as α, β, and γ-cyclodextrin, respectively. Each glucopyranose unit has three free hydroxyl groups. The secondary hydroxyl groups (C_2 and C_3) are located on the wider edge of the ring and primary hydroxyl group (C_6) are on the other side of the ring [1-2]. They also have a hydrophilic outer surface and apolar cavity. Therefore, inclusion complexes between cyclodextrins and variety of guest molecules can be formed in the cavity [3-5].

The azo compounds are the largest group of all synthetic colorants. The chromophoric group of the azo compounds is –N=N-, with association of one or more aromatic systems [6-7]. One of those azo compounds is methyl orange. Several researches have been aimed to prepare inclusion complexes between cyclodextrins [8-9] or modified cyclodextrins [3] with methyl orange.

Chitosan (CS) is a natural polysaccharide obtained from deacelylation of chitin which composes of *N*-acetylglucosamine and glucosamine in its structure [10-11]. It has been known that chitosan has biocompatibility properties, mucoadhesive properties and antibacterial properties [12]. Therefore, many researchers have been aimed to combine merit of chitosan and β-cyclodextrin by grafting β-cyclodextrin onto chitosan (CS-g-CD) [13-16]. However, their solubility in water is still poor limiting their applications in many fields.

To improve water solubility of CS-g-CD, chemical modification of chitosan needs to be carried out. Previously, its water solubility has been improved by adding quaternized agents [17] and by reductive amination reaction [18]. However, it has no report attempted to improve water solubility of CS-g-CD by introducing hydrophilic groups to reactive amino groups at the C_{2nd} position. Therefore, in this study, β-cyclodextrin-modified hydroxyalkylacrylchitosans (HAACSs-g-CDs) were prepared by firstly reacting chitosan with various hydroxyalkylacrylates to obtain hydroxyalkylacrylchitosans (HAACSs) [19-20], then reacted HAACSs with tosyl-modified β-cyclodextrin (TsCD) to obtain HAACSs-g-CDs.

Toward this end, we wish to report properties of inclusion complexes between HAACSs-g-CDs and methyl orange. To study these properties, inclusion complex solutions and solution-casted films were prepared. The solutions were prepared using HAACSs-g-CDs and methyl orange with varying mole ratio and then characterized by UV-Vis spectroscopy. For the solution-casted films, they were prepared by mixing β-cyclodextrin-modified hydroxybutylacrylchitosan (TB-1) with different amounts of methyl orange. After that, the films were characterized and tested. The results were then compared with the uncomplexed film (TB-1).

1.2 Objectives of the study

1) To prepare and characterize HAACSs and HAACSs-g-CDs.
2) To prepare and study properties of inclusion complexes between HAACSs-g-CDs and methyl orange in solutions and solution-casted films.

1.3 Scopes of the study

1) HAACSs (i.e., hydroxyethylacrylchitosan, hydroxypropylacrylchitosan, and hydroxybutylacrylchitosan) were synthesized and characterized in terms of solubility, structural properties, and molecular weight.
2) TsCD was prepared and characterized in terms of solubility, structural, and thermal properties.
3) HAACSs-g-CDs were synthesized by the reaction between HAACSs and TsCD. Thereafter, they were characterized in terms of solubility, structural properties, and molecular weight.
4) Inclusion complex solutions were prepared by mixing β-cyclodextrin or HAACSs-g-CDs with methyl orange. Their properties were investigated by UV-Vis spectroscopy.
5) Solution-casted films from HAACSs, TB-1, and inclusion complexes between TB-1 and various amounts of methyl orange were fabricated. Their photo, crystallographic, and thermal properties were determined.

1.4 Benefits of the study

Properties of inclusion complexes between HAACSs-g-CDs and methyl orange were investigated to widen opportunity of using HAACSs-g-CDs as complexing agents.

Chapter 2
Theory and Literature Reviews

2.1 Cyclodextrins

2.1.1 Structure [1-2]

Cyclodextrins (CDs) are cyclic oligosaccharide consisting of glucopyranose units linked by α-(1,4) bonds. The three major cyclodextrins contain 6 (α-cyclodextrin, Schardinger's α-dextrin, cyclomaltohexaose, cyclohexaglucan, cyclohexaamylose, ACD, C6A), 7 (β-cyclodextrin, Schardinger's β-dextrin, cyclomaltoheptaose, cycloheptaglucan, cycloheptaamylose, BCD, C7A), and 8 (γ-cyclodextrin, Schardinger's γ-dextrin, cyclomaltooctaose, cyclooctaglucan, cyclooctaamylose, GCD, C8A) glucopyranose units in their structures. The structures of α-, β-, and γ-cyclodextrins are illustrated in Figure 2.1.

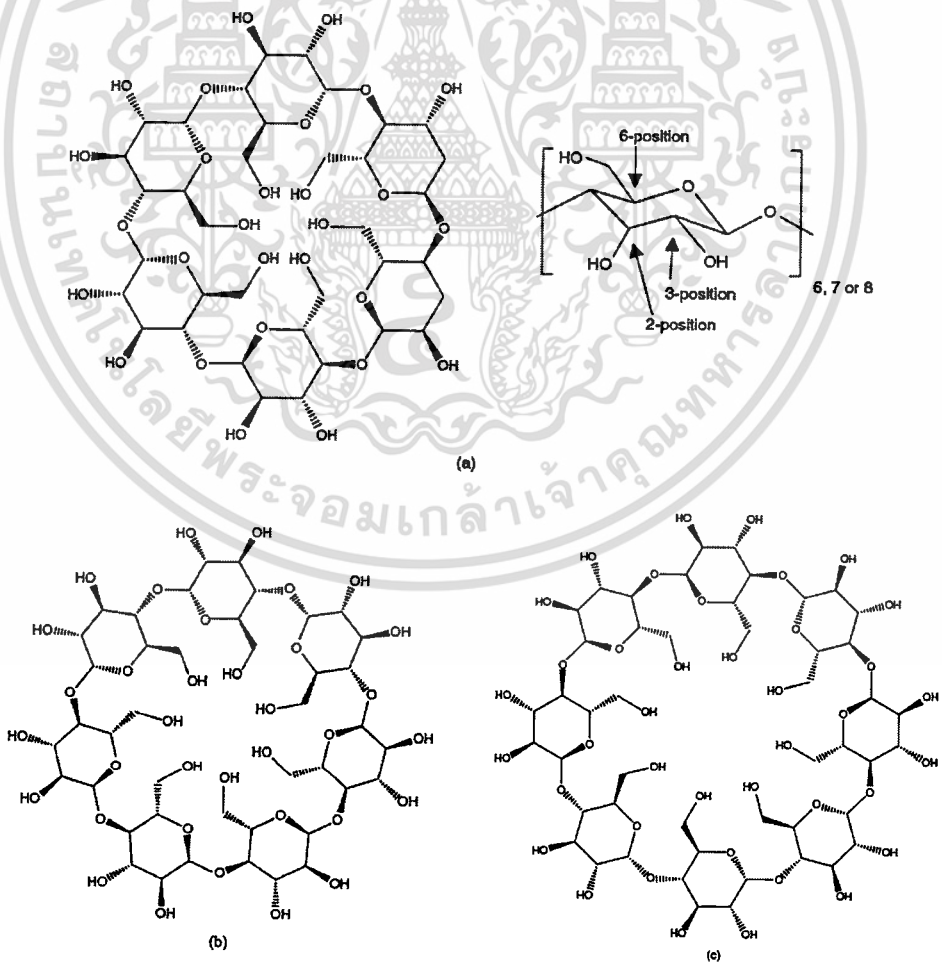

Figure 2.1 Structures of (a) α-, (b) β- and (c) γ-cyclodextrins [21].

Structure of CDs is a macrocycle with a hole in the middle. Data obtained from crystallographic study indicated that the shape of CDs was similar to doughnut or trenched cone owing to $^4C_1$ chair conformation of the glucopyranose units. The conformation makes all primary hydroxyl groups (C_6) locate on the narrow edge and all secondary ones (C_2 and C_3) place on the other edge of the ring, while the apolar C_3 and C_5 hydrogens and ether-like oxygens locate at the inside of the ring. This makes the molecules having both hydrophilic outer surface, which can dissolve in water, and hydrophobic cavity, which provides a hydrophobic matrix similar to crown ethers. Therefore, complexes between CDs and various types of apolar compounds have been able to be prepared. Schematic representation of the hydrophilic and hydrophobic regions of CDs is represented in Figure 2.2.

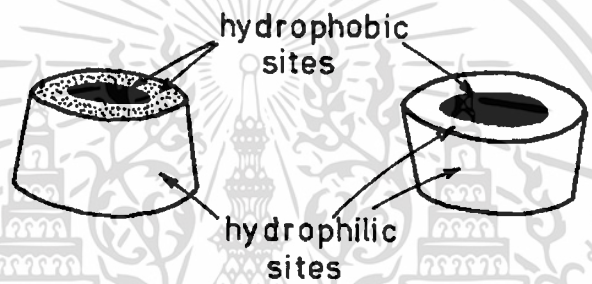

Figure 2.2 Schematic representation of the hydrophilic and hydrophobic regions of CDs [2].

The C2-OH group of each glucopyranose unit can form a hydrogen bond with the C3-OH group at the adjacent unit. These interactions provide a complete secondary belt in the CDs molecule, therefore β-cyclodextrin is a relatively rigid structure. Additionally, the poorest water solubility of β-cyclodextrin compared with all CDs can be also explained by these interactions. Unlike β-cyclodextrin, γ-cyclodextrin is the highest water soluble cyclodextrin from three common CDs because of its quite flexible structure. In terms of α-cyclodextrin, it has incomplete hydrogen bond belt because hydrogen bonds between C2-OH and C3-OH in α-cyclodextrin can establish only 4 bonds instead of 6 bonds. It is because one glucopyronose unit in the molecule is in a distorted position. The water solubility and other interesting information of α-, β-, and γ-cyclodextrin are described in Table 2.1.

Table 2.1 CDs properties [1, 22].

Property	α-CD	β-CD	γ-CD
Number of glucopyranose unts	6	7	8
Molecular weight (g/mol)	972	1135	1297
Solubility in water at 25°C (%w/v)	14.5	1.85	23.2
Outer diameter (Å)	14.6	15.4	17.5
Cavity diameter (ext./int., Å)	5.3/4.7	6.5/6.0	8.3/7.5
Height of torus (Å)	7.9	7.9	7.9
Cavity volume ($Å^3$)	174	262	427

2.1.2 History [1-2, 23]

In 1891, Villiers published a method to prepare a substance which later proved to be CDs. He digested starch with *Bacillus amylobacter*, given 3 g of a crystalline substance from 1000 g of starch. He determined its composition to be $(C_6H_{10}O_5)_2 \cdot 3H_2O$ and named this product as 'cellulosines'. According to other authors, they suggested that the product was produced by *Bacillus macerans*, heat-resistance spores, contaminated in his impure culture.

In 1904, Schardinger reported the preparation of a crystalline solid obtained from digestion of *Bacillus macerans* which seemed to be identical with the cellulosines of Villiers. 25-30% of the starch could be converted to two different crystalline dextrins in his study. He called the major crystalline product as α-dextrin and minor one as β-dextrin. These two products can be distinguished by the iodine reaction. The crystalline α-dextrin/iodine complex in thin layers is blue when damp and gray-green when dry while the crystalline β-dextrin/iodine complex is red-brown both damp and dry.

In the beginning of the 1930s, Freudenberg et al. presented that the crystalline Schardinger dextrins were built from maltose units and linked by α-1,4-glycosidic linkage. They also proposed the cyclic structure of these cyclodextrins in 1936. Subsequently, in 1948-1950, γ-cyclodextrin was discovered.

In the beginning of the 1950s, D. French et al. and F. Cramer et al. began to work intensively on the enzymic production of cyclodextrins. They tried to find method in purifying and characterization in physical and chemical properties. D. French's group discovered that there are even larger CDs, while F. Cramer group's was interested about ability on forming inclusion complex of these cyclic dextrins.

In the end of the 1960s, the methods for the laboratory-scale preparation of cyclodextrins, their structure, physical and chemical properties, as well as their ability on forming inclusion complex had been reported.

From the first discovery by Villiers onward, CDs and their derivatives have been applied in many fields: biomedicine, agriculture, chromatography, stabilizer, catalyst, and so on. The price of CDs is now cheaper than the past due to an advancement in production of CDs. However, despite the fact that many researches about CDs have been carried out, they still have many issues to be studied, especially in their potential applications.

2.1.3 Production [2, 24]

CDs are commercially produced using the enzyme so called CGTase [1,4-α-D-glucan 4-α-D-(1,4-α-D-glucano)-transferase, EC 2.4.1.19] to digest starch. The enzyme is generally found in bacteria and was previously discovered in archaea, which is one of the microbes. The CGTase obtained from *Bacillus macerans* has the biggest market share of the commercially available, while CGTase obtained from *Bacillus* species is most commonly used in industrial production.

Generally, CDs production processes can be classified into two categories: solvent process and non-solvent process.

2.1.3.1 Solvent process

Schematic of solvent process is illustrated in Figure 2.3. This process is almost used in an industrial scale. An organic solvent- mainly toluene, ethanol or acetone- is applied as a complexing agent. The process starts from starch liquefaction process by heat-stable (-amylase, acids (e.g. HCl), mechanical disintegration or thermostable CGTase. Concentration of starch solution used in the process is mostly 20-30%. Thereafter, the solution is cooled down to the enzyme reaction temperature then added CGTase and organic complexing agent. After the conversion process, a CD-agent complex is separated by centrifugation or filtration. The remaining solution contains unused starch, linear dextrins, glucose, maltose, CGTase, unused organic complexing agent, some other by-products and water. Excess complexing agent in the filtrate can be recovered by distillation. The obtained precipitate is then washed, suspended in water, and cleaved by heating. After that, the complexing agent is isolated by either steam distillation or liquid-liquid extraction. The product solution is concentrated using vacuum distillation; sometimes the solution has to be treated with activated carbon. The solution is crystallized to obtain white precipitate of cyclodextrins. The precipitate is filtered, washed and dried.

According to the process, CDs are only separated from the reaction, but different CDs are not separated from each other. Consequently, to receive a desired CD, an appropriate enzyme and complexing agent are needed to be carefully chosen.

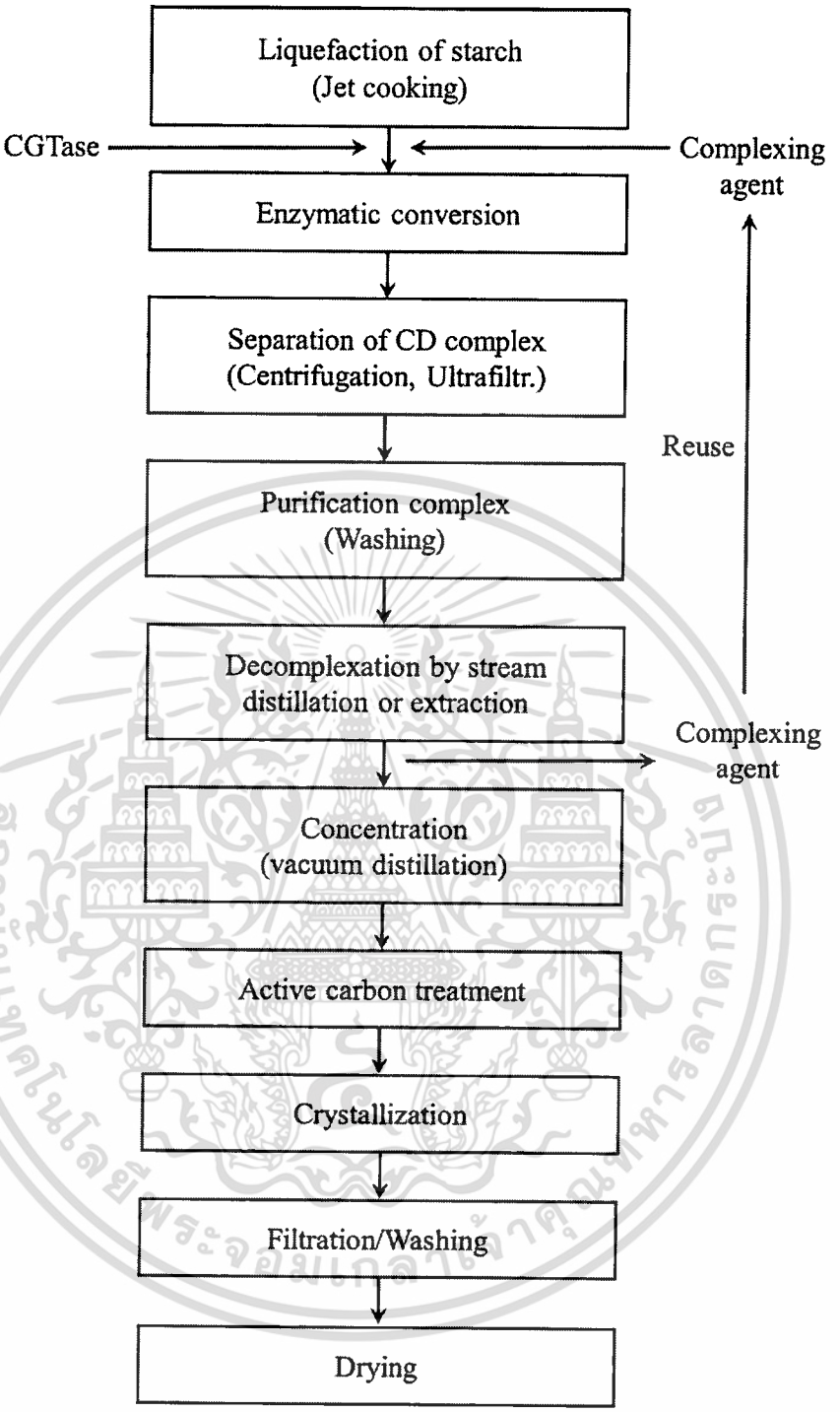

Figure 2.3 Solvent process for CDs production [24].

2.1.3.2 Non-solvent process

Schematic of Non-solvent process is described in Figure 2.4. This process was first developed for production of β-cyclodextrin. Due to its low water solubility, β-cyclodextrin can be easily purified by crystallization, without using chromatography step as α- and β-cyclodextrin. The advantage of this process is that CDs are able to be used in the food industry because they are produced without adding any organic complexing agents, unlike the CDs produced in the solvent process.

To produce β-cyclodextrin by this process, starch liquefaction and enzymatic conversion are carried out, but no complexing agent is applied. After finishing the conversion process, CGTase is inactivated, the pH is reduced and glucoamylase is added. The glucoamylase converts unused starch and other non-cyclic dextrins to glucose and maltose, which are not disturb purification. The solution is then cleared by activated carbon, filtered, and concentrated under reduced pressure. After several rounds of crystallization, β-cyclodextrin is isolated, washed, centrifuged, and dried. In addition, the filtrate, consisting of glucose, maltose, α- and β-cyclodextrin is then concentrated to a syrup for using as a food additive.

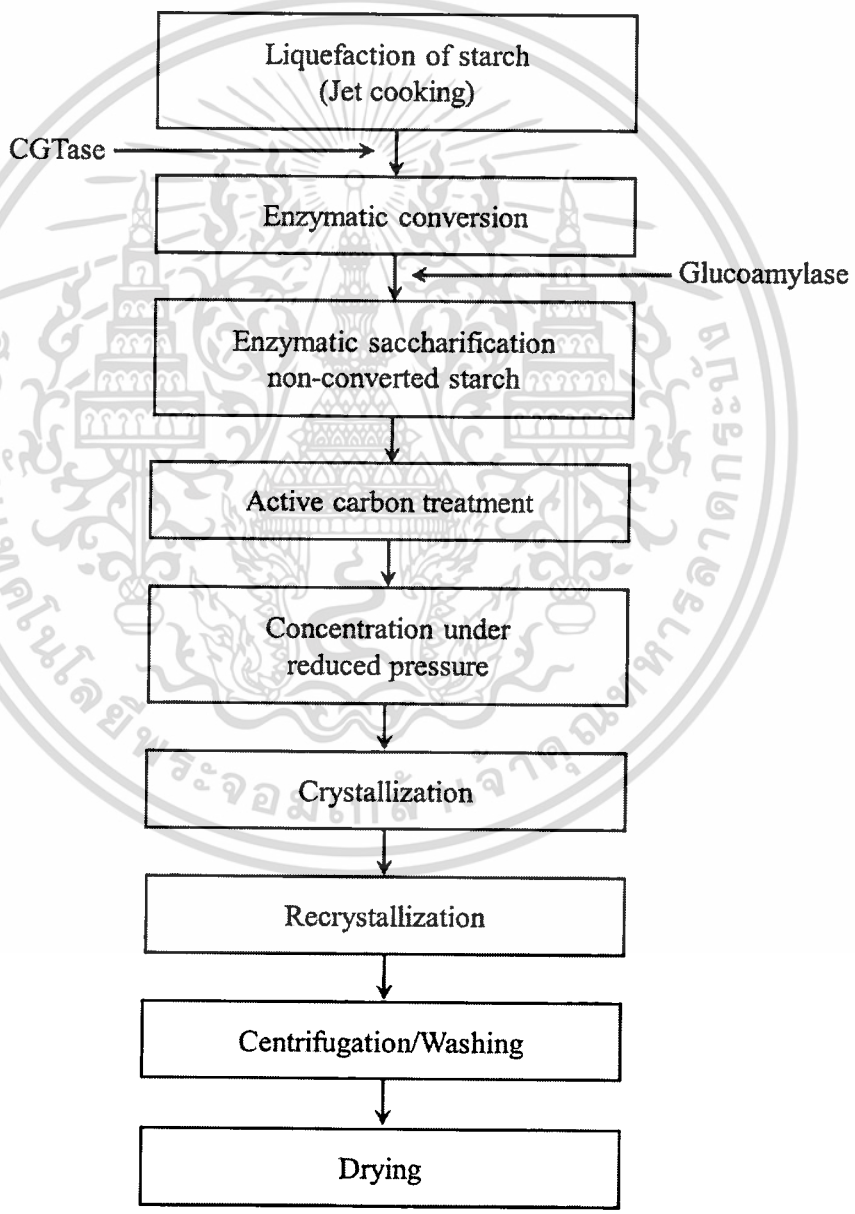

Figure 2.4 Non-solvent process for CDs production [24].

The purity of CDs produced by industrial process is mostly over than 99%. Properties of each CD are described in Table 2.2.

Table 2.2 Quality specification of commercially available α-, β-, and γ-CD of pharmaceutical quality (from Wacker-Chemie, Munich) [2].

	α-CD	β-CD	γ-CD
Appearance	White crystalline powder	White crystalline powder	White crystalline powder
Content	98% min.	98% min.	98% min.
Other cyclodextrins	0.5% max.	0.5% max.	0.5% max.
Residue on ignition	0.1 max.	0.1 max.	0.1 max.
Specific rotation in aqueous solution $[\alpha]_D$	(+) 148°±3°	(+) 161°±3°	(+) 173°±3°
Optical density at a 10% solution at 420 nm	0.1 max.	1% aqueous solution is clear and colorless	0.2 max.
Recuding compounds (determined as dextrose)	0.5% max.	0.5% max.	0.5% max.
Heavy metals	5 ppm max.	5 ppm max.	5 ppm max.
Volatile organics	50 ppm max.	50 ppm max.	50 ppm max.
Water (Karl Fischer)	11% max.	14% max.	11% max.
Microorganisms	1000/g max.	1000/g max.	1000/g max.
Salmonella/*E. Coli*	Negative	Negative	Negative

2.1.4 Inclusion complexes [1-2, 22]

2.1.4.1 Principle of inclusion complexes

As mentioned ealier, CDs have hydrophilic outer surface and apolar cavity. Regarding their apolar cavity, the suitably sized of guest molecules in solid, liquid or gas form can hold within the cavity to form the inclusion complex. The polarity of the cavity has been estimated to be familiar with ethanolic solution [1]. Generally, based on the CDs dimensions, α-cyclodextrin can be usually complexed with low molecular weight molecules or aliphatic compounds, β-cyclodextrin is able to be complexed with aromatics and heterocycles, and γ-cyclodextrin can be complexed with steroids or macrocycles. The schematic representation of inclusion complex is presented in Figure 2.5.

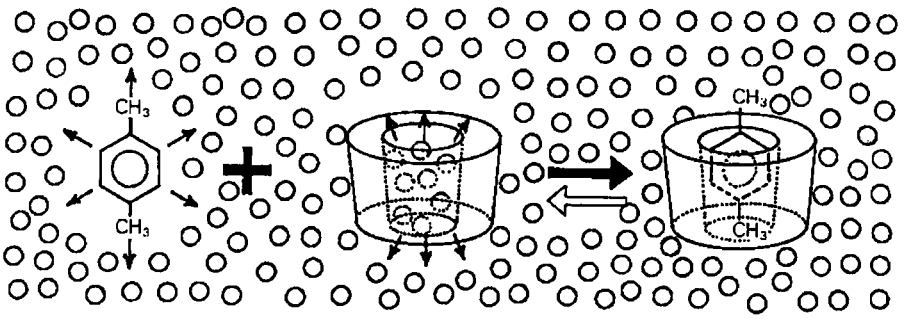

Figure 2.5 Schematic representation of CDs inclusion complex formation. *p*-Xylene is the guest molecule; the small circles represent the water molecules [2].

Formation of the inclusion complex is the result of equilibrium between the free guest and CDs molecules and the supramolecules of inclusion as expressed below:

free CDs + free guest $\Leftrightarrow$ CD/guest (inclusion complex)

The main driving force of complex formation is the release of enthalpy-rich water molecules from the cavity. After that, the more hydrophobic guest displaces the water molecules to attain apolar-apolar association and decreases ring stain, resulting in more stable compound [2].

Commonly, there are four interactions that help shift the equilibrium to form the inclusion complex:

- The displacement of polar water molecules from the apolar cavity.
- The increased number of the hydrogen bonds formed as the displaced water returns to the larger pools.
- A reduction of the repulsive interactions between the hydrophobic guest and the aqueous condition.
- An increment in the hydrophobic interactions when the guest inserts itself into the cavity of CDs.

The initial equilibrium occurs very rapid (often within minutes), while the final equilibrium can take much longer to reach. When the guest locates in CDs cavity, its conformation is adjusted to take maximum advantage of the weak van der Waals forces that exist. In addition, the guest molecule can enter CDs cavity either at the narrow size (primary hydroxyl groups) or at the wider size (secondary hydroxyl groups), depending on their respective sizes. (Figure 2.6)

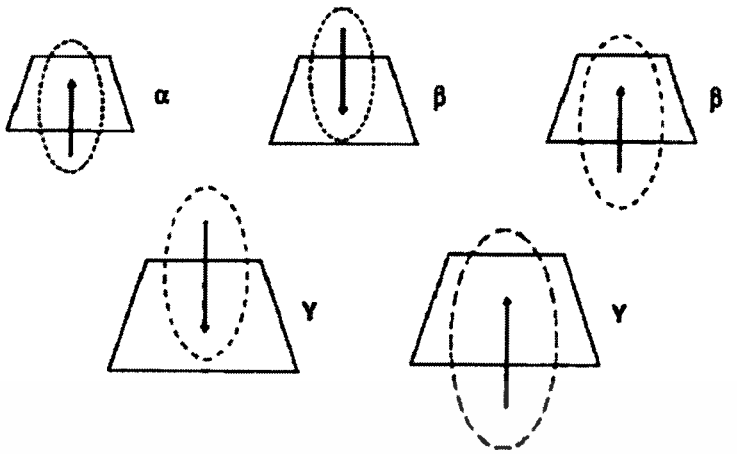

Figure 2.6 Influence of the guest and CDs cavity size on the inclusion mechanism [22].

Generally, one guest molecule can interact with one CDs (complex 1:1). However, depending on the respective size of the host and guest molecules, one guest molecule can also interact with two (or more) CDs molecules (complex 1:2), or two guest molecules can interact with one CDs (complex 2:1). The examples of 1:1 and 1:2 complex are shown in Figure 2.7.

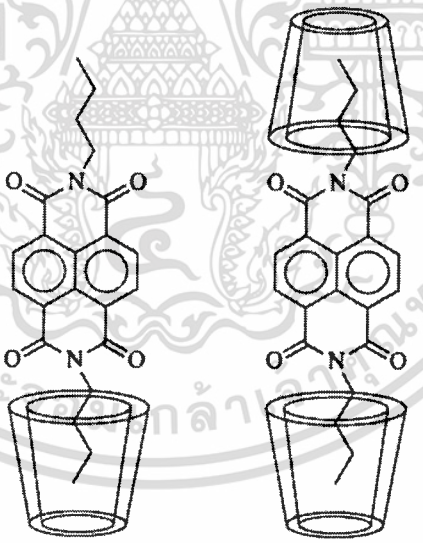

Figure 2.7 Examples of type 1:1 (left) and 1:2 (right) inclusion complexes [22].

Multiple inclusion equilibria can also coexist when using the asymmetric guest molecule, such as methyl orange, because the molecule can enter into the CDs cavity through different ways. Therefore, the orientational isomers so called inclumers are formed [9, 25]. The example of inclumers formation is illustrated in Figure 2.8.

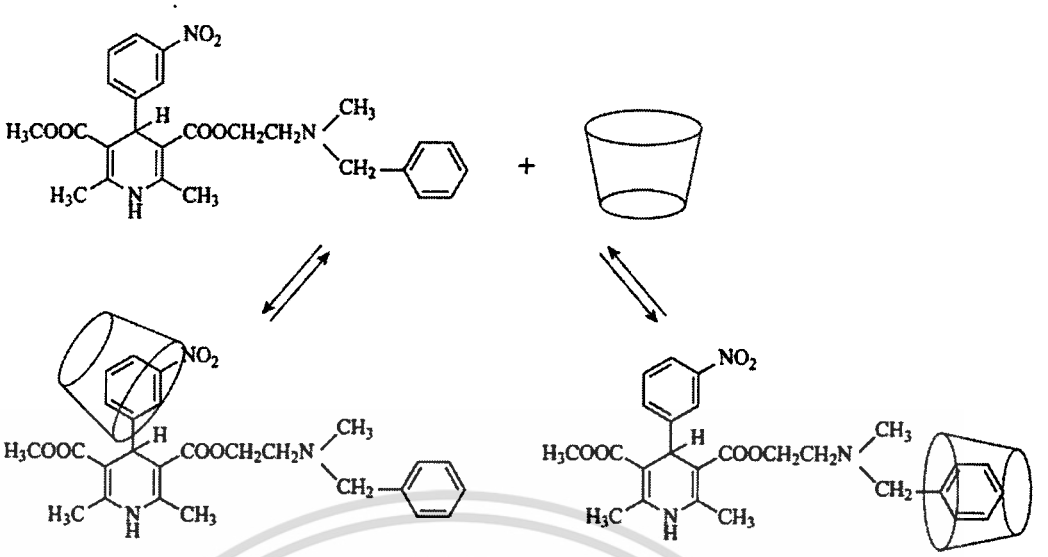

Figure 2.8 Example of coexistence of multiple inclusion equilibria in solution [22].

2.1.4.2 Preparation of inclusion complexes [1, 22]

The method used in preparing inclusion complexes between CDs and various guest molecules has a significant effect on the final product: yield, solubility, and stability of the complex. In addition, it has several factors to be considered prior to preparing the complexes:

- Solution dynamics

There is only the surface molecules of CDs available for complexation in the crystalline form. To obtain more available molecules for complexation, CDs crystalline is needed to be solubilized or dispersed into fine particles. In addition, solubility of both CDs and the guest are enhanced when heating, leading to an increase in the probability of complex formation.

- Temperature effects

As mentioned above, heating can increase the probability of complex formation due to more available molecules for complexation. However, a number of complexes are also destabilized at the same time. Consequently, temperature used in complexation process should be carefully considered.

- Use of solvents

In order to form inclusion complexes, guest molecules must be able to displace solvent in CDs cavity. Generally, water is the most popularly used as a solvent because it is very easily displaced. The solvent must be easily removed if solvent-free complexes are needed.

Nevertheless, some guests are not able to solubilize in water, making complexation either very slow or impossible. Therefore, an organic solvent is needed to overcome the issue. The solvent should not form complex with CDs and be easily removed by evaporation. Ethanol and diethyl ether are good examples for this case.

- Effect of water

It has already known that solubility of both CDs and the guest are enhanced when increasing water. However, when the amount of water is further increased, CDs and the guest are not easily in contact as they do in concentrated solution. Therefore, the amount of water should be optimized.

- Volatile guests

Volatile guests can be lost during complexation, especially when heat is applied. Thus, it can be minimized this problem by using sealing or refluxing.

Several techniques are used to prepare inclusion complex. The details are discussed below:

- Co-evaporation

This technique is most widely used in the laboratory. CDs and the guest (generally, in equimolar amounts) are mixed in water for several hours. After that, the solvent was removed, at an optimized temperature to decline dissociation of the complex, in hot air, vacuum oven, or under reduced pressure.

- Spray-drying and Freeze-drying

Spray-drying and freeze-drying techniques are derivative of the co-evaporation technique. The obtained products are easily solubilized by water because they are undergone amorphization during the drying process.

- Kneading

The guest is kneaded together with CDs. A small proportion of water, an aqueous solution of ethanol, acid, or base is then added to obtain a slurry. The product was left to equilibrate and then dried. Generally, owing to some crystals of CDs and the guest found in the product, its dissolution is only better than that of the corresponding physical mixture but slower than the spray-dried or the freeze-dried product.

- Sealed-heating

CDs, the guest, and additives, at the desired mole ratio, are placed in a glass container with a very small amount of water. The container is then sealed and kept in the oven at 75-90°C for 10-60 minutes or often 3 hours. The obtained product is also easily dissolved in water.

- Supercritical CO_2

Supercritical CO_2 has been widely used in CDs complex formation due to its safe, inexpensive, and non-flammable. The obtained product is less crystalline than physical mixtures.

- Microwave treatment

Microwave treatment makes it possible to obtain high temperature inside irradiated products. A mixture of the guest and CDs with little amount of solvent is subjected to microwave treatment, mostly at 60°C for 90 s. The obtained product shows unchanged solid state and very stable under ambient condition.

2.1.4.3 Characterization of inclusion complexes [22, 26]

Various methods can be used to characterize inclusion complexes. The details are discussed below:

- X-ray diffractometry

Powder x-ray diffractometry is used to measure the crystallinity of a product. Forming of inclusion complexes changes the x-ray diffractogram such as declination of crystallinity, appearance of new peaks, disappearance of the peaks, and peaks shift. A strong reduction or the appearance of the guest characteristic peaks can occur from strong guest-CDs interaction, inclusion complexation of the guest, or its molecular dispersion and the CDs.

- Differential scanning calorimetry

Differential scanning calorimetry can be used to analyze inclusion complexes because its melting, boiling, and sublimation points usually shift or disappear within the temperature at which CDs is decomposed.

- Ultraviolet spectroscopy

Generally, CDs do not show any significant UV absorbance. Therefore, the changes observed in a guest/CDs solution are resulted from perturbation of the chromophore electrons of the guest by its inclusion in CDs.

- Infrared spectroscopy

Infrared spectroscopy (IR) is one of the interesting methods which provides interesting information. The IR analysis can be carried out by KBr disk method, dispersing the samples in Nujol, and directly determining on the samples themselves. Unlike the physical mixture, the inclusion complex leads to significant changes in the characteristic bands of the guest such as strong reduction or complete disappearance of the characteristic bands, and a shift in C=O stretching.

- Proton nuclear magnetic resonance spectroscopy

Proton nuclear magnetic resonance spectroscopy (^{1}H-NMR) is a valuable method that can give the most accurate information about inclusion complex formation. Major changes of chemical shift values of the CDs protons, as shown in Figure 2.9, occur when inserting the guest molecule into the CDs cavity. The changes are specifically found at H_3 and H_5 located inside the cavity, or H_6 on the cavity rim.

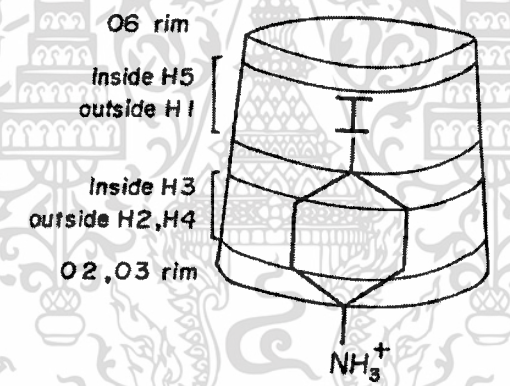

Figure 2.9 Structure of the 4-iodoaniline-α-CD crystalline complex, showing the relationship of the guest to the host hydrogen atoms. (The wider, secondary hydroxyl, end of the cavity is the 0(2), 0(3) end) [26].

2.1.5 Modified cyclodextrins [28]

To improve applications of CDs such as enhancing their solubility in desired solvents, CDs are needed to be modified by reacting at the hydroxyl groups. Examples of modified cyclodextrins are illustrated in Figure 2.10.

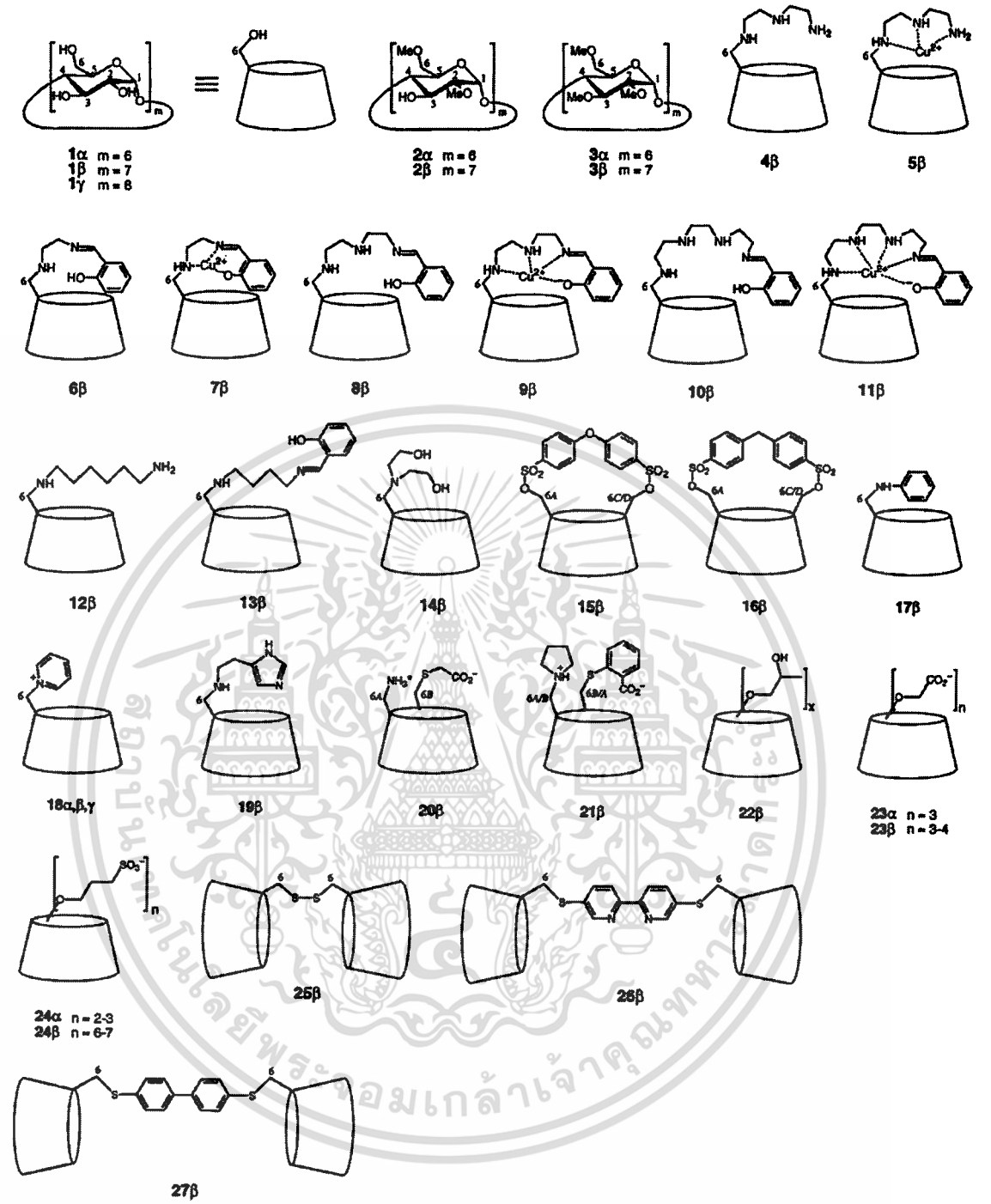

Figure 2.10 Natural and modified cyclodextrins [27].

Hydroxyl groups in CDs present at the 2-, 3-, and 6- position. Among these, those at the 6-position are the most basic, those at the 2-position are the most acidic, and those at the 3-position are the most inaccessible. Therefore, under normal condition, an electrophilic reagent attacks the 6-position. However, the more reactivity of the reagents, the less selectivity of the substitution. Thus, 2- and 3- positions are also substituted in the presence of reactive reagents.

Owing to the most acidic nature of the 2-position hydroxyl groups, they are firstly deprotonated. The oxyanion formed is more nucleophilic than the non-deprotonated hydroxyl group at the 6-position. However, this situation is complicated by proton transfers between these two positions which can lead to a mixture of modifications at the 2- and 6- positions.

If the electrophilic reagent can form a complex with CDs, then the orientation of the reagent within the complex should be considered as another factor. In case of very strong complex between reagent and CDs, then the major product formed will be controlled by the orientation of the reagent within the complex. On the contrary, if the complex is weak, then the product will be directed by the nucleophilicity of the hydroxyl groups.

Overview of the modification of CDs are shown in Figure 2.11.

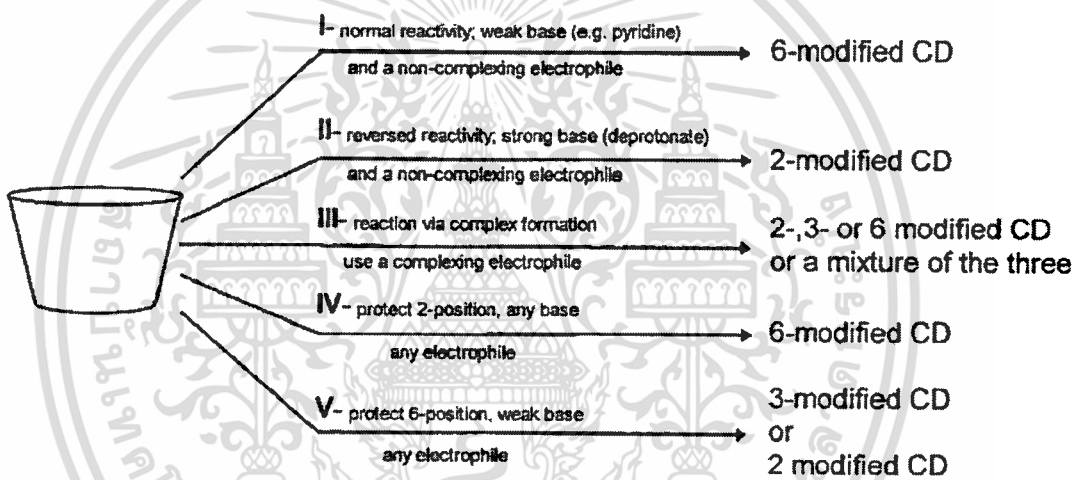

Figure 2.11 Overview of the modification of CDs [28].

2.1.5.1 Tosyl-modified β-cyclodextrin (TsCD) [17, 29-34]

Tosyl-modified β-cyclodextrin (TsCD) is one of the most important cyclodextrin derivatives because it can be converted into other functional groups such as amino, alkylamino, thioalkyl, halo, formyl groups and so on via nucleophilic addition reaction [17]. TsCD can be prepared by various methods as reviewed below:

Y. Liu et al. and P. R. Ashton et al. [29-30] prepared TsCD using pyridine as a solvent. Briefly, dried β-cyclodextrin was added into distilled pyridine. Subsequently, *p*-toluenesulfonyl chloride (TsCl) was added into the solution. The reaction mixture was stirred at room temperature for 24 h followed by pouring the resulting solution into water to obtain white precipitate. The precipitate was then recrystallized many rounds from a mixture of acetonitrile and methanol to give TsCD. However, this method has several drawbacks [28]. Specifically, the percent yield of the resulting product is low because the tosylate can exchange with chloride ions or can undergo

elimination reaction to obtain the 3,6 anhydro compound or an alkene. In addition, pyridine is a non-user-friendly solvent and it can form cyclodextrin-pyridine gel [31].

TsCD can also be prepared in alkaline condition in the presence of acetonitrile. D. Vizitiu et al. [32] prepared TsCD by dissolving β-cyclodextrin in 1% NaOH then dropwise added TsCl dissolved in acetonitrile into the β-cyclodextrin solution. The reaction mixture was stirred for 2 hours then filtered and acidified with 1 M HCl. The white solid (6.3%) was finally obtained after recystallization from water. S. Onozuka et al. [33] also prepared TsCD by dissolving β-cyclodextrin in 0.15 M NaOH and dissolving TsCl in minimum amount of acetonitrile. The TsCl solution was then dropped into the β-cyclodextrin solution. Finally, reaction was terminated by adding 1 M HCl and then purified using column chromatography. The results obtained from ^{1}H-NMR and paper chromatography showed that tosyl group was introduced at the C3-OH of β-cyclodextrin. They proposed that the mechanism occurred because the TsCl and CD can form inclusion complex at the ratio of 1:1, and the methyl group of the TsCl, as it is the hydrophobic part of the molecule, can locate near the C3-OH group of the CD as shown in Figure 2.12. The scale molecular model (CPK model) was used to confirm the mechanism. The result showed that the distance between S atom in the TsCl and the C3-O atom in the CD was shorter than the distance between S atom and the C2-O atom in the CD. Therefore, the monotosylation product is also formed on a specific secondary hydroxyl of β-cyclodextrin.

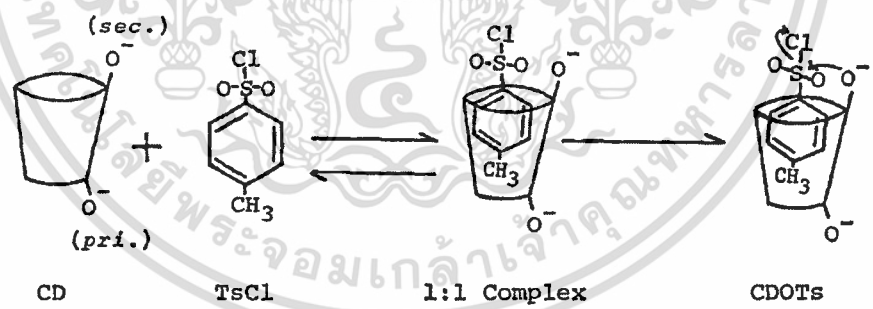

Figure 2.12 The proposed mechanism of the monotosylation of β-cyclodextrin with TsCl in alkaline solution [33].

An other method to prepare TsCD is using water as a solvent. This method was firstly reported by B. Brady et al. [34]. β-cyclodextrin hydrate and TsCl was reacted in the presence of 1.6% w/v NaOH for 5 hours at 0-5°C. After that, pH of the mixture was adjusted using HCl. The final product (25%) was obtained by recrystallizing from distilled water (3 times). The main advantages of this method are high percent yield and free from any solvents.

The B. Brady et al.'s method was adapted by P. Gonil et al. [17]. 10% w/v NaOH was used instead of 1.6% w/v NaOH. The ^{1}H-NMR spectra revealed that the degree of tosylation (DT) of the product (22%) was 1.76, which can be attribute to high NaOH concentration added. They inferred that tosylation of the CD was both occurred at C6-OH and C3-OH group. The reaction scheme is depicted in Figure 2.13.

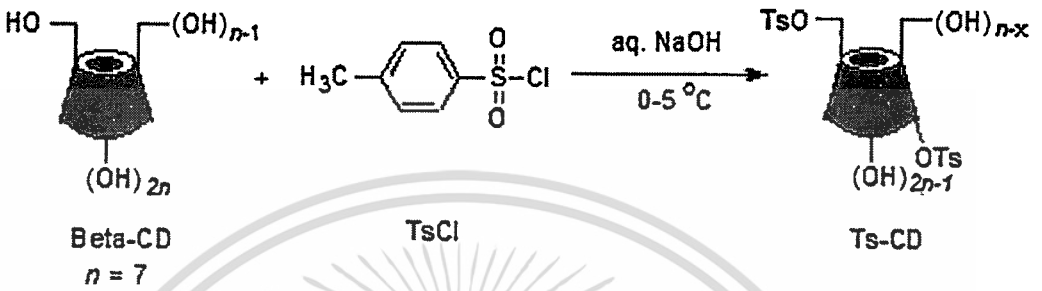

Figure 2.13 The reaction scheme for synthesis of TsCD [17].

In this research, TsCD was prepared by following P. Gonil et al.'s method with a modification.

2.2 Chitosan

2.2.1 Structure [11, 35-36]

Chitosan (CS) is a natural polymer derived from deacetylation reaction of chitin. Its structure has one amino group and two hydroxyl groups in the repeating glucosidic residue. Each unit is linked by (1→4)-β-glycosidic bonds, which is similar to cellulose. However, the hydroxyl group at C_2 is replaced by acetylamino or amino group, providing units so called *N*-acetyl-2-amino-2-deoxy-D-glucopyranose (*N*-acetylglucosamine, D- GlcNAc) and 2-amino-2-deoxy-D-glucopyranose (glucosamine, D-GlcN). The structure of chitin and chitosan is depicted in Figure 2.14. The degree of deacetylation (DD) of chitosan, giving indication of the number of amino groups along the chains, is calculated as the ratio of glucosamine unit to *N*-acetylglucosamine unit. To be named as chitosan, the degree of deacetylation has to over than 0.65.

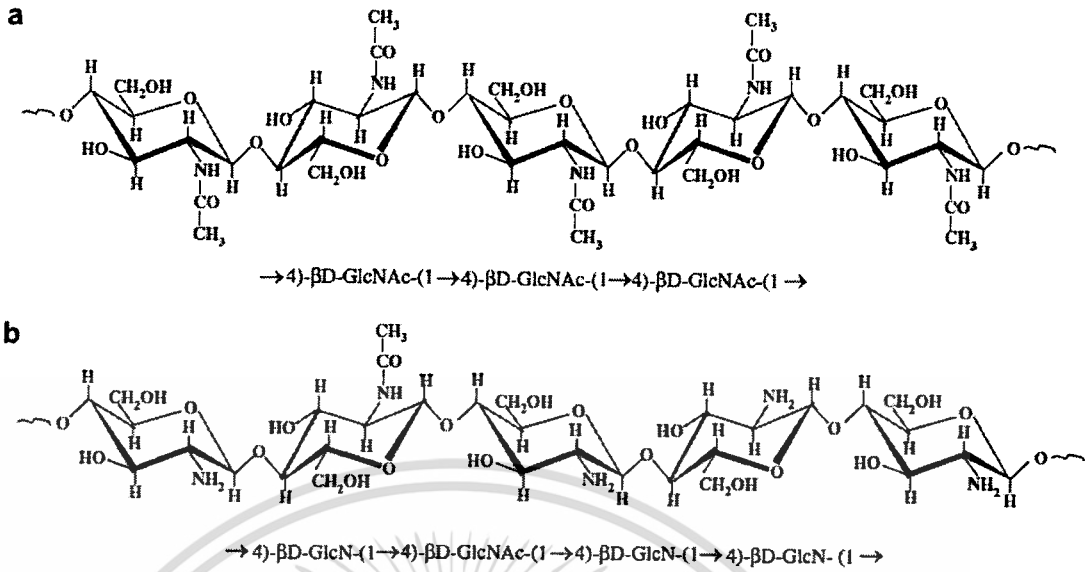

Figure 2.14 Primary structure of (a) chitin and (b) chitosan [36].

Regarding the structure of chitin and chitosan, they have many reaction sites for further modification such as hydroxyl group at C_6 and amino group at C_2. All possible reaction sites of chitin and chitosan are illustrated in Figure 2.15. Therefore, many reactions such as etherification [37], esterification [38], crosslinking [39], polymerization [40], carboxyalkylation [41], Michael addition [19-20] and etc. can be carried out to modify their structures.

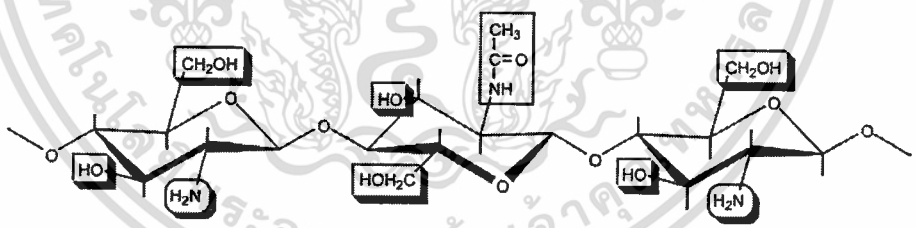

Figure 2.15 Illustration of the possible reaction sites in chitin and chitosan [11].

2.2.2 Production [35-36]

As discussed above, CS can be derived by deacetylation reaction of chitin. Chitin is a natural polymer obtained from crustacean shells (especially from shrimp, squid, shell, and crab) and fungi *mycelia*. To begin with, crustacean shell or fungi was demineralized to remove $CaCO_3$ by treating with HCl. After that, it was deprotenized by treating with NaOH. The resulting product was deacetylated using 40% NaOH at 120°C for 1-3 h to obtain 70% deacetylated chitosan. The simplified flowsheet for chitosan preparation is demonstrated in Figure 2.16.

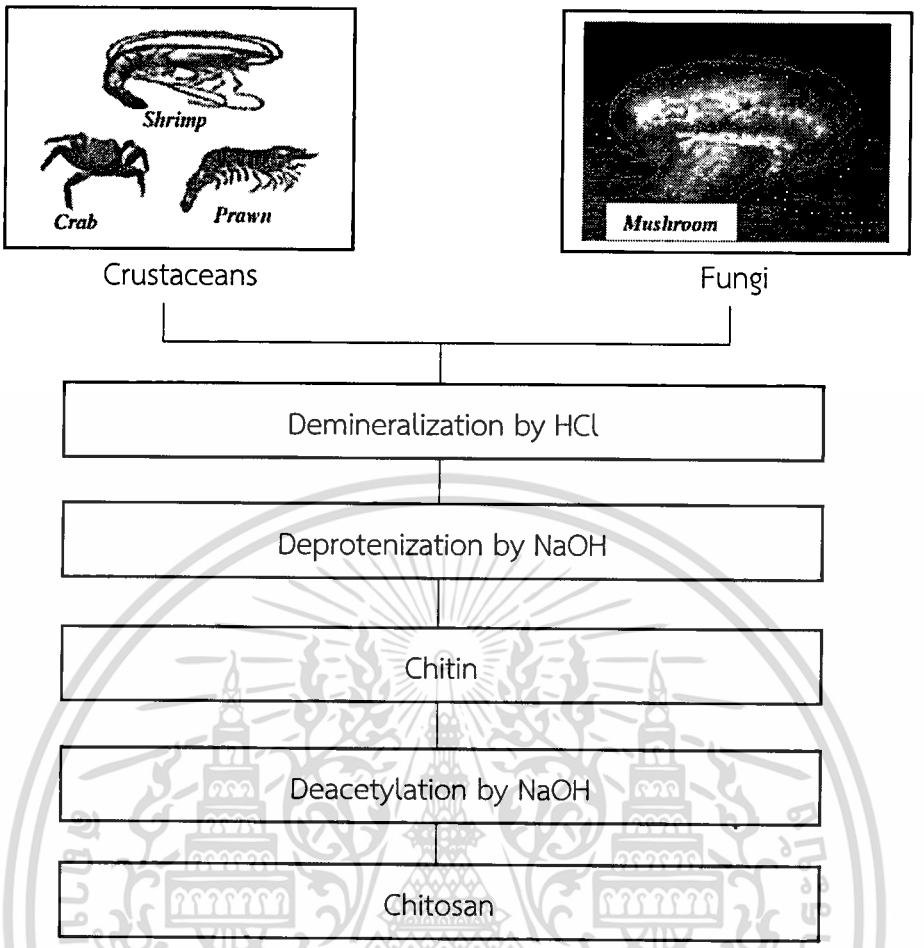

Figure 2.16 Production of chitin/chitosan [Modification from [36]].

2.2.3 Properties [10-11, 36, 42]

- Solubility [10-11, 42]

Chitosan is soluble in dilute acidic solution below pH 6.0 [42]. In acidic solution, amines in chitosan get protonated and turn to positive charge which can dissolve in water in form of a water-soluble cationic polyelectrolyte (Figure 2.17). The quaternary nitrogen salt is obtained by dissolving CS in acetic, formic, lactic, hydrochloric, nitric acid solutions. 1% w/v acetic acid (pH=4) is the most popular solvent for dissolving CS. However, CS cannot dissolve in either sulfuric or nitric acids and can be depolymerized when using concentrated acetic acid solutions as solvents at high temperature.

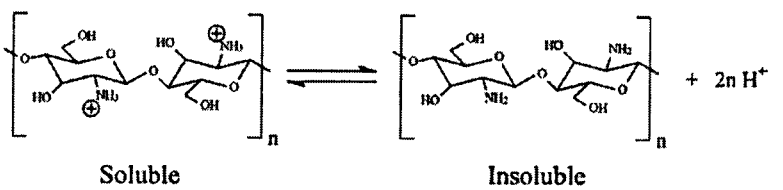

Figure 2.17 Structure of chitosan in protonated and deprotonated form [42].

When pH increases above 6, amines in CS become deprotonated and CS loses its charges and becomes insoluble. The soluble-insoluble transition takes place at its pK_a value around pH between 6 and 6.5. In fact, the solubility of CS is very hard to control owing to many parameters affecting its solubility such as the degree of deacetylation, the ionic concentration, the pH, the nature of acid used for protonation, the distribution of acetyl group along the chain, and the conditions of isolation and drying of the CS [10].

- Antimicrobial activities [36]

Chitosan has antimicrobial properties due to cationic charge of chitosan molecule. The cationic charge can bind onto anionic cell wall components (i.e., lipopolysaccharides and proteins), leading to gradual shrinkage of cell membrane and eventually death of the cell. It shows a broad-spectrum antimicrobial activity against gram-positive (such as *Bacillus subtilis*), gram-negative bacteria (such as *Escherichia coli*) and fungi.

2.2.4 Characterization [10, 35]

- Degree of deacetylation (DD)

The degree of deacetylation affects chitosan solubility and solution properties. Many techniques such as IR spectroscopy, pyrolysis gas chromatography, gel permeation chromatography and UV spectrophotometry, ^{1}H-NMR spectroscopy, ^{13}C solid state analysis, thermal analysis, acid hydrolysis and HPLC, and etc. are used for determining the DD of chitosan [35]. Among those techniques, ^{1}H-NMR is the most convenient technique for determining DD. Figure 2.18 shows the ^{1}H-NMR spectra of chitosan dissolved in D_2O containing DCl (pH about 4). The DD can calculated from the peak area at about 1.95 ppm of acetyl group against 4.79 ppm of the D-glucosamine residue and 4.50 ppm of the H-1 of the *N*-acetyl-D-glucosamine unit.

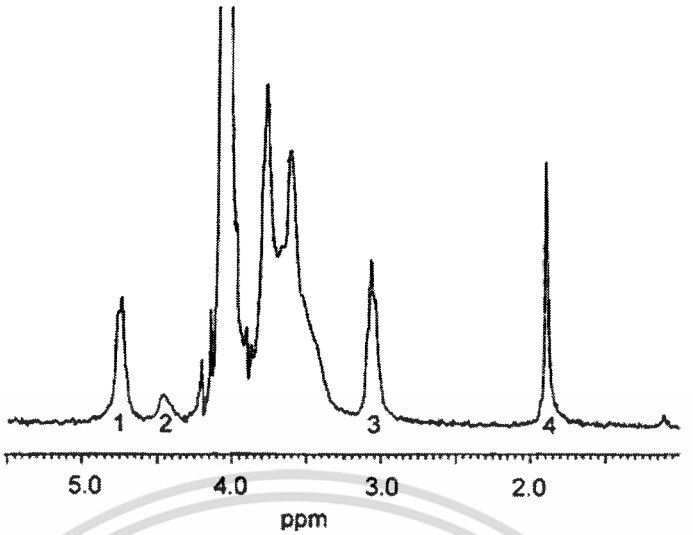

Figure 2.18 ^{1}H-NMR spectra of chitosan in D_2O, pH=4, T=85°C, conc. 5 g/L: (1) H-1 of glucosamine units, (2) H-1 of *N*-acetyl-glucosamine, (3) H-2, (4) protons of the acetyl group of *N*-acetyl-glucosamine [10].

- Molecular weight

Molecular weight and its distribution affect properties of chitosan. Size exclusion chromatography (SEC) with on-line viscometer and light scattering detectors is commonly used to determine average molecular weight (M_w) of chitosan. The intrinsic viscosity can be expressed as:

$$[\eta] = KM^{\alpha} \quad (2.1)$$

The constant α and K in Mark-Houwink equation are affected by types of tested solvent as described in Table 2.3. Generally, M_w of chitosan is in the range of $1x10^5$ to $5x10^5$ [35].

Table 2.3 Mark–Houwink parameters for chitosan in various solvents [Modification from [10]].

Solvent	K (mL/g)	α	T (°C)
0.1 M AcOH/0.2 M NaCl	1.81×10^{-3}	0.93	25
0.1 M AcOH/0.02 M NaCl	3.04×10^{-3}	1.26	25
0.2 M AcOH/0.1 M AcONa/4 M urea	8.93×10^{-2}	0.71	25
0.3 M AcOH/0.2 M AcONa (DD = 0.98)	8.2×10^{-2}	0.76	25
0.3 M AcOH/0.2 M AcONa (1>DD>0.97)	7.9×10^{-2}	0.796	25
0.02 M acetate buffer/0.1 M NaCl	8.43×10^{-2}	0.92	25

Where; AcOH is acetic acid and AcONa is sodium acetate.

2.2.5 Chitosan modification by Michael addition reaction [19-20, 43-49]

- General [43-44]

Michael addition reaction is the base-catalyzed nucleophilic addition of a carbanion such as enolate anion (Michael donor) to activated α,β-unsaturated carbonyl compound (Michael acceptor). The schematic representation of the Michael addition reaction is shown in Figure 2.19.

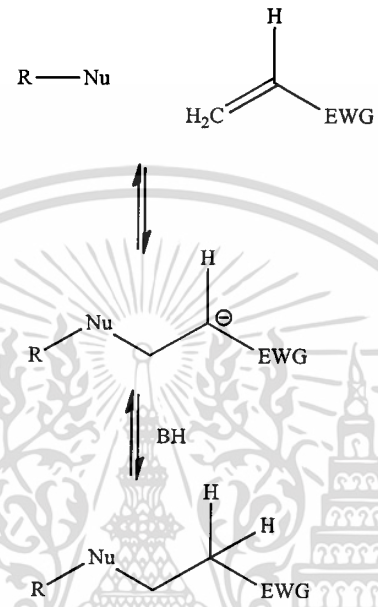

Figure 2.19 Schematic representation of the Michael addition reaction [43].

The general mechanism is presented in Figure 2.20. The acetoacetate is firstly deprotonated by the base, given an enolate anion (Michael donor). After that, the anion reacts in a 1,4-conjugate addition to the olefin of the acrylate (Michael acceptor). The carbonyl of the acrylate stabilizes the resulting anion until proton transfer takes place.

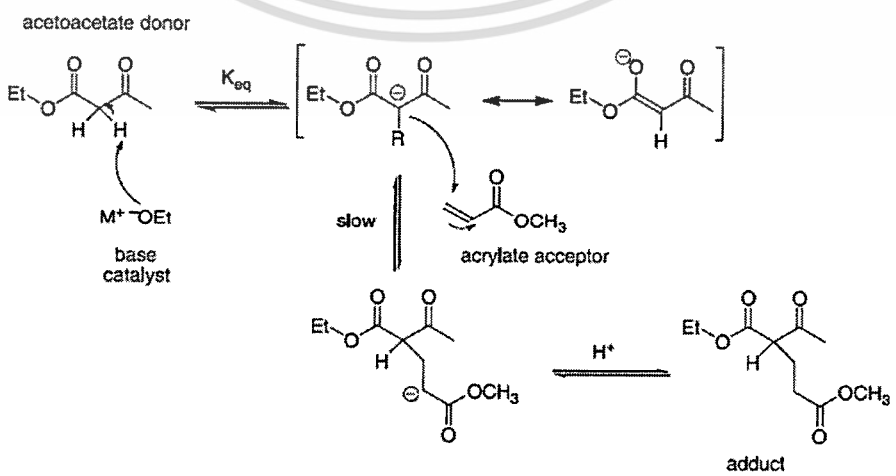

Figure 2.20 General carbon-Michael reaction mechanistic scheme [43].

- Acryl-modified chitosans [19-20, 45-49]

Owing to insolubility of chitosan in basic media, the Michael reaction between chitosan and various acryl agents is popularly prepared in acetic acid solution. Therefore, the methods for preparing acryl-modified chitosans are reviewed in detail below.

H. Sashiwa et al. [45] prepared *N*-carboxyethylchitosan from Michael addition reaction between ethyl acrylate and chitosan. Chitosan was firstly dissolved in a mixture of acetic acid and ethanol. Ethyl acrylate was then added into the solution. After that, the solution was stirred using various times and temperatures. The solubility results of *N*-carboxyethylchitosan indicated that the products could not dissolve in distilled water. Therefore, they were further reacted with various hydrophilic amines to obtain water-soluble products.

The previous research has several drawbacks. Organic solvents such as methanol are required to dissolve acrylic acid ester. In addition, a further reaction is needed to obtain water-soluble products. To overcome the mentioned issues, the same group [46] prepared *N*-carboxyethylchitosan by reaction between CS and acrylic acid (AA) using Michael addition reaction (Figure 2.21). AA was used in the research because it can act as proton donor to dissolve chitosan and the reagent for Michael reaction. The reaction was carried out at 50°C for 2 days. The solubility results indicated that the products were able to dissolve in aqueous media in a pH range from 1 to 13. The ^{1}H-NMR results indicated that the degree of substitution (DS) of the products increases when the degree of deacetylation (DD) of chitosan increases. This is because the number of reactive species (-NH_2) increases when increasing DD of chitosan.

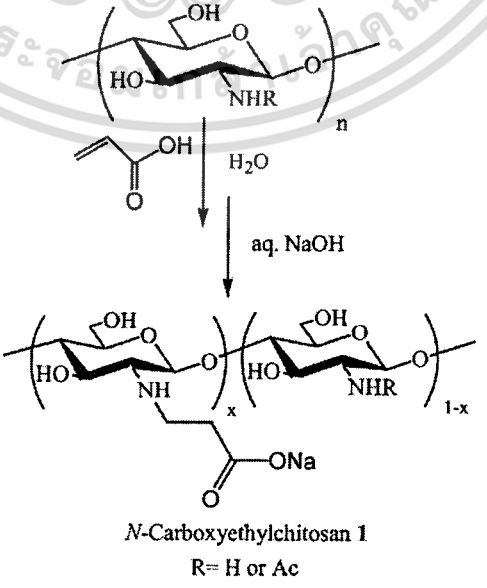

N-Carboxyethylchitosan 1
R= H or Ac

Figure 2.21 The reaction scheme for preparing *N*-carboxyethylchitosan [46].

H. Sashiwa et al. [47] also prepared acryl-modified chitosans using various acryl agents as demonstrated in Figure 2.22. The results showed that DS of products prepared from acrylic acid esters (1-4) were dramatically higher than those for acrylamide (5) or acrylonitrile (6) due to higher reactivity of esters in the reaction. Therefore, those products were soluble in distilled water.

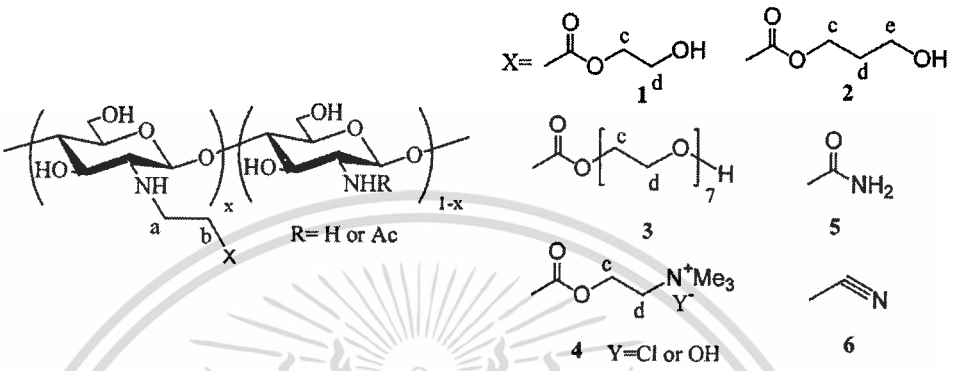

Figure 2.22 Various acryl agents used in preparing acryl-modified chitosans [47].

K. Wang et al. [48] prepared glucosyloxyethyl acrylate-modified chitosan by reaction between glucosyloxyethyl acrylate (GEA) and chitosan. The reaction scheme is illustrated in Figure 2.23. Data from elemental analysis indicated that DS of the product was 0.14. TGA and DSC results suggested that the product was less thermal stable than chitosan. XRD data revealed that crystallinity of the product was lower than chitosan because of GEA incorporated into the chain.

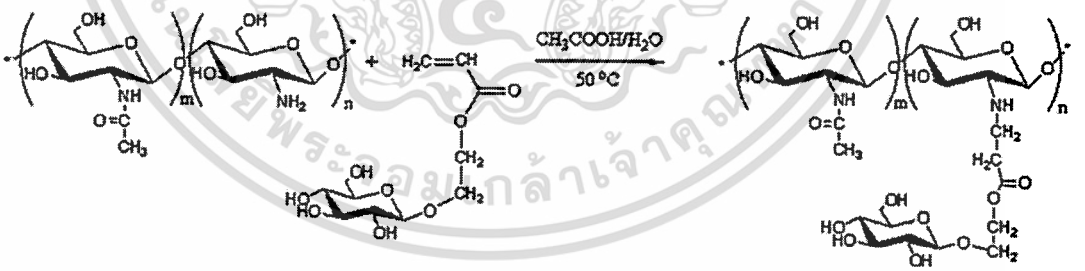

Figure 2.23 Synthesis of CS–GEA through Michael addition reaction of CS and GEA [48].

X. Gao et al. [49] prepared (methacryloyloxy) ethyl carboxyethyl chitosan for using as photopolymerized hydrogels via Michael addition reaction. The reaction was carried out for 2 days at 60°C. Chitosan and ethylene glycol acrylate methacrylate (EGAMA) were used to prepare the products. NMR results showed DS of the products varied from 0.1 to 0.35, depending on mole ratio between CS and GEAMA.

G. Ma et al. [19] prepared *N*-alkylated chitosan from Michael addition reaction between chitosan and hydroxyethylacrylate (HEA) with varying mole ratio, reaction temperature, and reaction time. The solubility test indicated that the *N*-alkylated chitosan could dissolve in distilled water. This is because the random distribution of HEA residue disturbs the formation of ordered structure and the hydrophilic behavior of HEA. ^{1}H-NMR results revealed that DS was from 0.18 to 1.2. The DSC results indicated that thermal stability of the *N*-alkylated chitosan was lower than pristine chitosan and they decomposed around 226°C for those with DS higher than 1.05. The XRD results showed that crystallinity of the *N*-alkylated chitosan was significantly reduced due to the presence of bulky HEA group that might hinder the formation of hydrogen bonds. All in all, the antimicrobial activity of the *N*-alkylated chitosan was lower than that of chitosan, but it is still applicable.

P. Treenate et al. [20] prepared hydroxyethylacrylchitosan (HC) by following G. Ma et al.'s method with slightly modification. The proposed route of HC synthesis is depicted in Figure 2.24. They prepared the HC using the mole ratio between CS to HEA at 1:6. The reaction was carried out at 60°C for 48 h. The solubility test showed that HC completely dissolved in distilled water at 70°C. The average molecular weight of HC obtain from GPC was declined by 13-fold compared with unreacted chitosan because CS chain was able to be hydrolyzed by acetic acid during the reaction. For other results such as ^{1}H-NMR and XRD, they were close to G. Ma et al.'s.

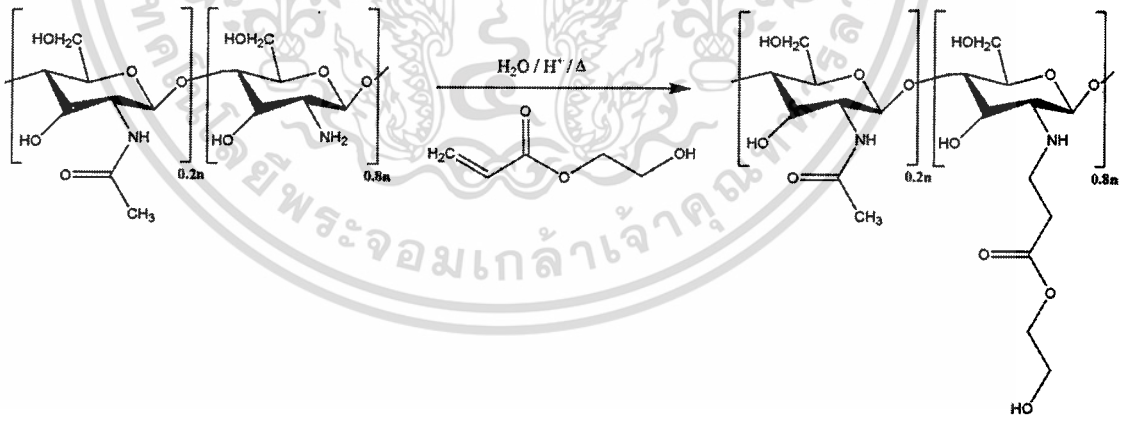

Figure 2.24 Proposed route of HC synthesis [20].

In this work, various acryl agents were applied to react with CS to prepare hydroxyalkylacrylchitosans which can be further used for reacting with TsCD to obtain β-cyclodextrin-modified hydroxyalkylacrylchitosans.

2.2.6 β-Cyclodextrin-modified chitosans [13-15, 17, 50-56]

Cyclodextrin-modified chitosans (CS-g-CDs) are developed in order to combine unique characteristics of chitosan with the potential of cyclodextrin to form non-covalent inclusion complexes which can be used in many applications such a drug delivery, cosmetics, and analytical chemistry. The schematic representation of cyclodextrin-modified chitosans is illustrated in Figure 2.25.

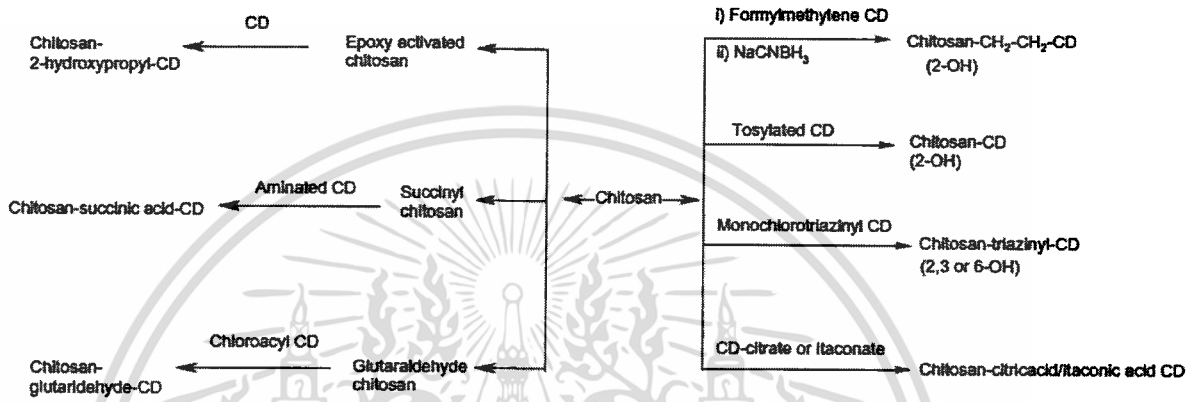

Figure 2.25 β-Cyclodextrin-modified chitosans: (1) by the reductive amination using formylmethylene CD, (2) by using tosylated CD, (3) by the nucleophilic substitution reaction using monochlorotriazinyl derivative of CD, (4) via epoxy-activated chitosan, (5) by using redox aminated CD (mono-6-amino-mono-6-deoxy-β-cyclodextrin), (6) by the condensation of CD-citrate or itaconate with chitosan, (7) cross-linking of CD and chitosan by glutaraldehyde [50].

X. Zhang et al. [51] prepared CS-g-CD by the reaction between epoxy-activated chitosan (EACTS) and β-cyclodextrin as described in Figure 2.26. EACTS was swelled in 0.1 M NaOH. After that, the solution of β-cyclodextrin in 0.1 M NaOH was slowly added. The mixture was stirred for 4 h at 60°C followed by filtering, washing with distilled water, and drying. The apparent amount of grafting calculated by data obtained from spectrometer was 25.8 μmol/g.

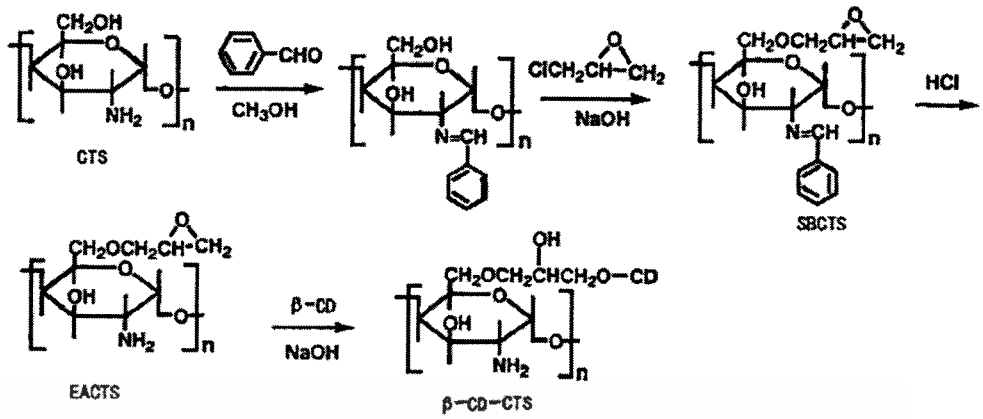

Figure 2.26 CS-g-CD prepared by reaction between CS and β-CD [51].

R. Auzely-Velty and M. Rinaudo [52] stated the preparation of CS-g-CD as followed. β-CD derivative possessing a reducing sugar was prepared followed by its reductive amination. The reaction scheme is shown in Figure 2.27. The results revealed that CS-g-CD was able to be prepared by reductive amination method.

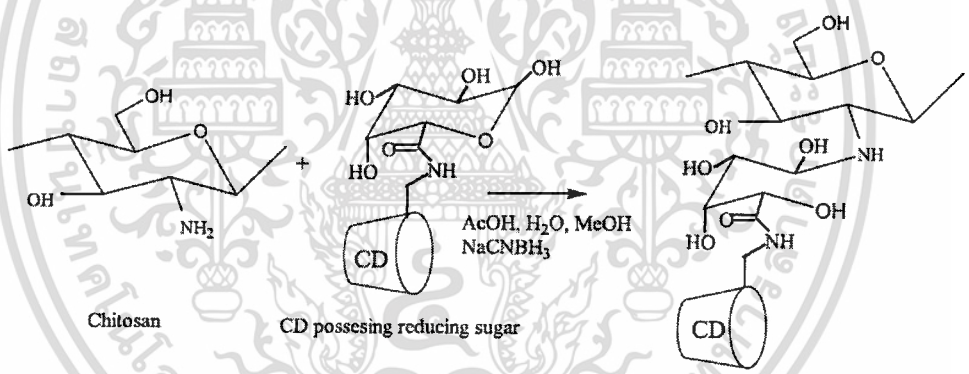

Figure 2.27 CS-g-CD prepared by reductive amination reaction [13].

B. Martel et al. [53] prepared CS-g-CD using monochlorotriazinyl derivative of β-CD (βW7MCT) as depicted in Figure 2.28. The solubility test showed that all products were not soluble in water and numerous organic solvents, but did swell in water. This is because βW7MCT contained an average of 2.8 monochlorotriazinyl groups per β-CD unit. One CD unit could react with several amino sites at the same time, therefore three-dimensional network was obtained. This crosslinking reaction explained the insolubility of the products.

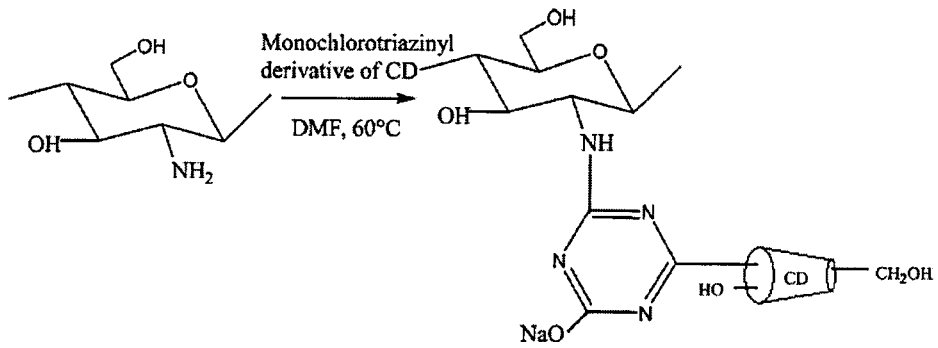

Figure 2.28 Reaction scheme for preparing CS-g-CD using monochlorotriazinyl derivative of β-CD [13].

M. Prabaharen and R. Jayakumar [54] prepared CS-g-CD using carbodiimide chemistry. The reaction scheme is depicted in Figure 2.29. 1 mmol of carboxymethyl β-cyclodextrin (CmCD) was firstly activated with 1 mmol of 1-ethyl-3-(3-dimethylaminopropyl)carbodiimide (EDC) and 1 mmol of *N*-hydroxysuccinimide (NHS) for 30 minutes. After that, 1 mmol of CS dissolved in 1% v/v acetic acid was dropwise added. The reaction was carried out at room temperature with stirring for 8 h followed by dialysis against distilled water for 3 days and lyophilization. The IR result confirmed that β-cyclodextrin was successfully grafted onto CS chain. DS calculated from integration of ^{1}H-NMR spectra was 43%. The product was further used as scaffold for studying controlled drug release.

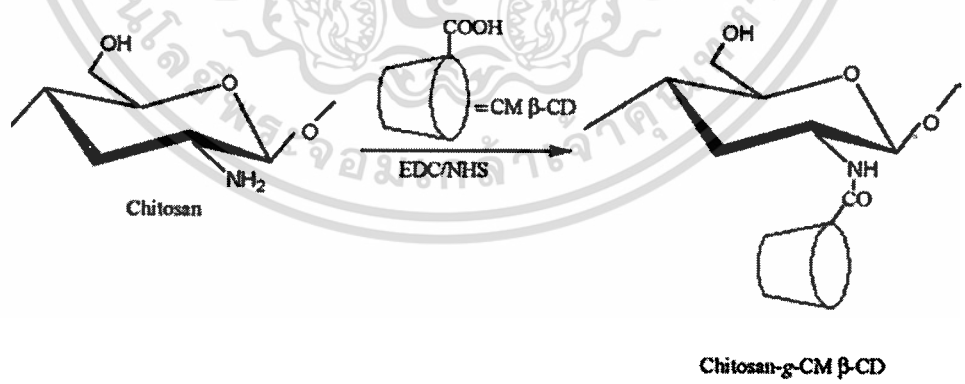

Figure 2.29 CS-g-CD prepared by reaction between CS and CmCD [54].

N. Aoki et al. [15] also prepared CS-g-CD using carbodiimide chemistry. Chitosan was succinylated using succinic anhydride. The mixture was vigorously stirred for 5 days at room temperature followed by dialysis and evaporation. Succinylated chitosan was then reacted with EDC and mono-6-amino-mono-6-deoxy-β-cyclodextrin (ACD). The reaction was carried out for 48 h. After that, pH of the mixture was adjusted to 2 by HCl. The CS-g-CD was obtained after dialysis and freeze-drying. The reaction scheme is shown in Figure 2.30. DS of the CS-g-CD was 0.16. (CD content was 45 wt%) The CS-g-CD was then used to adsorb *p*-nonylphenol and bisphenol A.

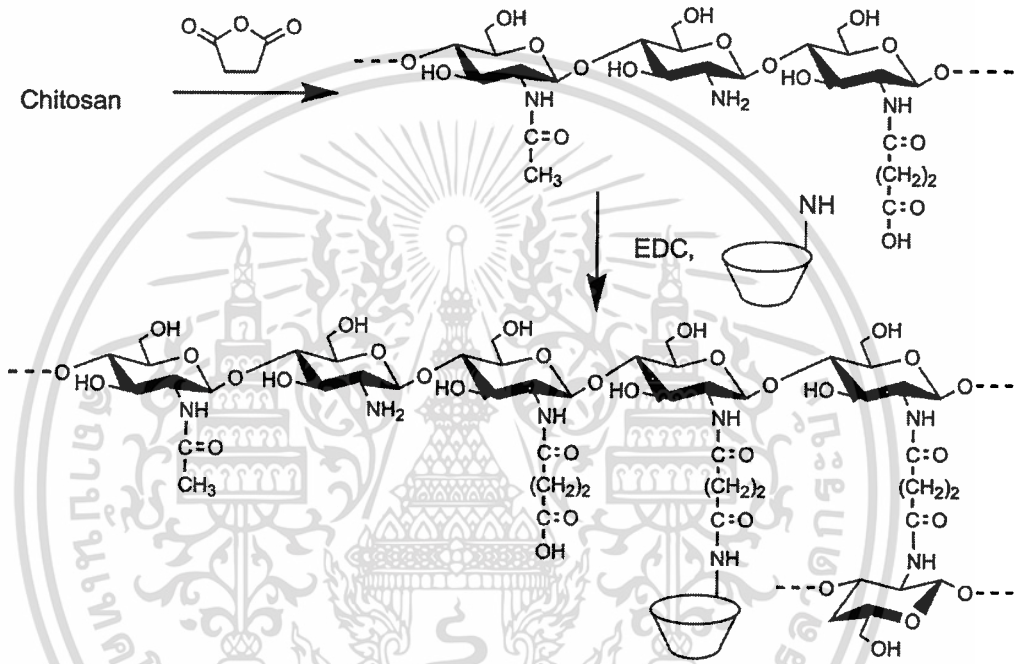

Figure 2.30 CS-g-CD from succinylated chitosan [15].

K. El-Tahlawy et al. [55] prepared CS-g-CD from the reaction between β-cyclodextrin citrate (β-CD citrate) and chitosan. The β-CD citrate was prepared by reacting β-cyclodextrin with citric acid (CA) at different temperatures. Thereafter, a defined volume of water containing different β-CD citrate concentrations was introduced into a solution containing chitosan dissolved in different formic acid concentrations. The mixture was stirred for 3 h at different reaction temperatures (80-140°C). After that, the products were precipitated by adding 0.2 N NaOH followed by washing with distilled water and acetone. The products were then dried in an oven at 60°C for 24 h. Grafting efficiency of the products was obtained by determining the nitrogen percentage of chitosan before and after modification. The results suggested that the molecular weight of chitosan, reaction temperature, and formic acid concentration were the major factors affecting the grafting efficiency of the products.

TsCD is also used to prepare CS-g-CD. The reaction between CS and TsCD is nucleophilic addition reaction. S. Chen and Y. Wang [14] prepared CS-g-CD by the reaction between TsCD and CS. Briefly, 3 g of chitosan was swelled in 150 mL of DMF. Subsequently, 0.5 g of TsCD in 20 mL of DMF was slowly dropped into the chitosan solution. The mixture was stirred for 48 h at 50°C followed by filtering, washing, and drying. ^{13}C NMR spectra of CS-g-CD showed the characteristic peak at 78.43 ppm, which is the 2-position carbon atom in the substituted glucopyranose unit of β-cyclodextrin. IR spectra of the product showed α-pyanyl vibration of β-cyclodextrin at 848.6 cm^{-1}. Data obtained from XRD indicated that crystallinity of the product reduced significantly because of β-cyclodextrin grafted onto chitosan chain. Hence, it can conclude that β-cyclodextrin was successfully grafted onto chitosan skeleton.

P. Gonil et al. [17] also prepared CS-g-CD using TsCD. 1 g of chitosan was dissolved in 80 mL of 1% w/v acetic acid. Thereafter, TsCD in 40 mL of DMF was added into the solution. The mixture was refluxed at 100°C for 24 h followed by dialysis against distilled water for 3 days and lyophilization. ^{1}H-NMR data indicated that DS of the products was in the range of 5±2% to 23±2%. The DS increased when increasing TsCD in the reaction. The reaction scheme for preparing CS-g-CD by P. Gonil et al.'s method is presented In Figure 2.31.

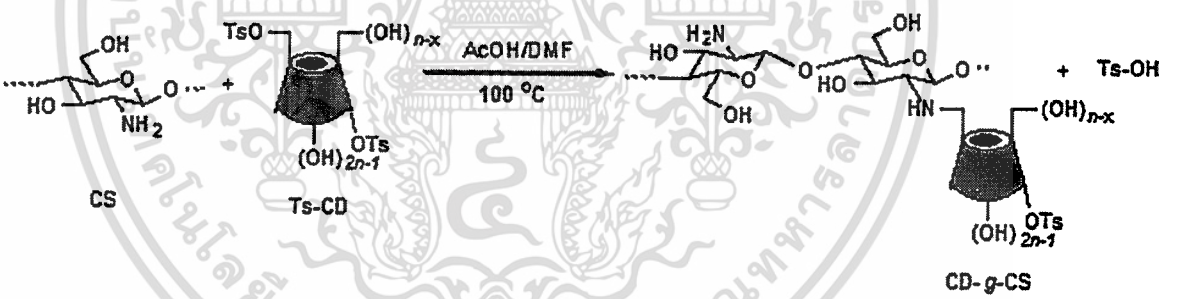

Figure 2.31 The reaction scheme for preparing CS-g-CD by Gonil P. et al.'s method [17].

Z. Yuan et al. [56] prepared CS-g-CD by following P. Gonil et al. with slightly modification. They refluxed the mixture of CS and TsCD at 100°C for 16 h. The characterization results were similar to P. Gonil et al.

In this research, β-cyclodextrin-modified hydroxyalkylacrylchitosans were prepared by nucleophilic addition reaction between hydroxyalkylacrylchitosans and TsCD.

2.3 Methyl orange [3, 8-9, 57]

Methyl orange (*p*-sulfobenzeneazo-4-dimethylaniline sodium salt, MO) is one of the azo compounds. It was prepared by a reaction between sulfanilic acid and *N.N*-dimethylaniline. The preparation scheme is illustrated in Figure 2.32.

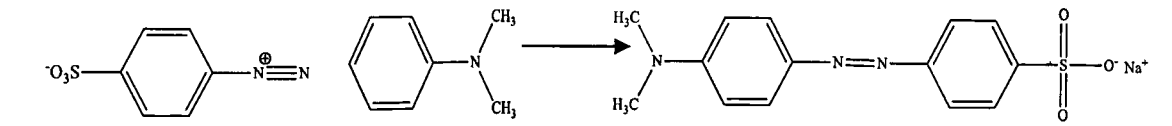

Diazotized sulfanilic acid
4-Diazobenzenesulfonic acid

***N,N*-Dimethylaniline**
MW 121.18
bp 194°C

Methyl orange
4-[4-(Dimethylamino) phenylazo]benzenesulfonic acid, sodium salt
MW 327.34 λ_{max} 507 nm

Figure 2.32 The preparation scheme of MO [57].

Briefly, sulfanilic acid is dissolved in sodium carbonate solution followed by adding sodium nitrite. The mixture is cooled down to 0-5°C and then add concentrated HCl. In a minute or two, a powdery white precipitate of the diazonium salt should form. The diazotized product is pure enough for using in a further step. After that, *N,N*-dimethylaniline in glacial acetic acid is added to the diazotized product. The red-colored precipitate is occurred after stirring the mixture for a few minutes. Finally, NaOH solution is added to the mixture to obtain the orange sodium salt. The crude product can be recrystallized from water to obtain the pure product.

In addition to its application in textiles, MO can be applied as an acid-base indicator. It changes color of the solution to red when pH is lower than 3.2 and yellow when pH is upper than 4.4 (Figure 2.33).

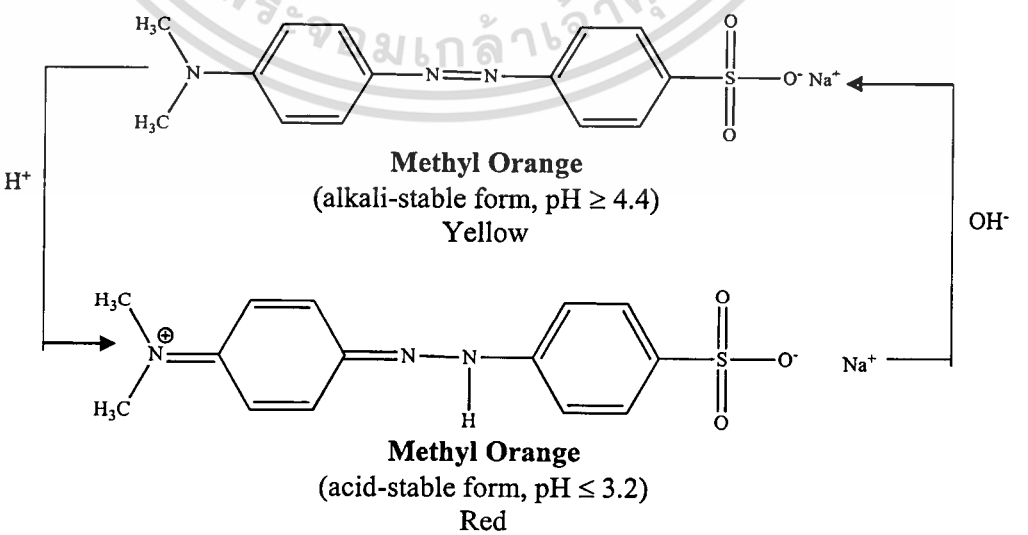

Figure 2.33 Alkali- and acid-stable form of MO [57].

Acid-stable form of methyl orange can tautomerize into 2 forms: ammonium tautomer (am) and azonium tautomer (az). The structural formulae of each tautomer are depicted in Figure 2.34.

.

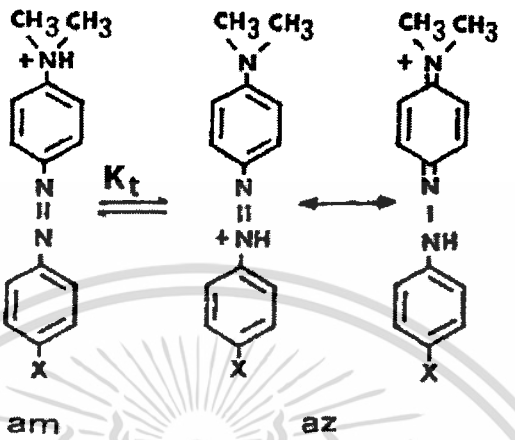

Figure 2.34 Structural formulae of the ammonium tautomer (am) and the azonium tautomer (az) of the monoprotonated forms of methyl orange (X = SO_3^-) and methyl yellow (X = H) [8].

Several researches have been aimed to prepare inclusion complexes between cyclodextrins and methyl orange as reviewed below:

M. K. Tawarah [8] studied inclusion complexes between cyclodextrins and methyl orange. He prepared acidic solution containing methyl orange and cyclodextrin. UV-Vis spectra of the resulting solutions were measured at 300-600 nm in various temperatures. He presented that the inclusion complexes of the ammonium tautomer are more stable than those of the azonium tautomer. In addition, unlike α- and β-cyclodextrin, measurable changes in the absorbance were not observed when complexing methyl orange with γ-cyclodextrin.

M. Kompany-Zareh et al. [9] studied orientational isomers formed by inclusion of methyl orange and β-cyclodextrin. They prepared inclusion complexes between methyl orange and β-cyclodextrin in acidic and basic media. After that, thermodynamic of the complexes was determined using data obtained from titrations. They presented that the inclusion complex prepared in basic condition leads to two orientational isomer (inclumers). On the contrary, in acidic condition, only ammonium tautomer of methyl orange can form a stable complex with β-cyclodextrin. The model of inclusion complexation between methyl orange and β-cyclodextrin in acidic and basic condition is shown in Figure 2.35.

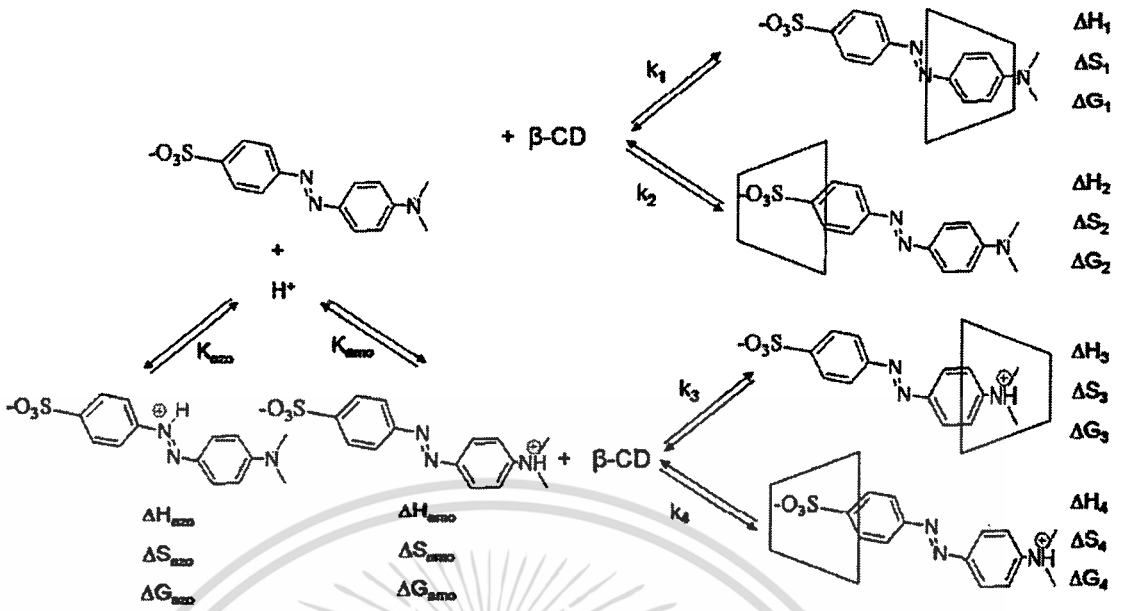

Figure 2.35 Inclusion of protonated and deprotonated methyl orange into cyclodextrin nanocavity [9].

β-Cyclodextrin-modified chitosan can be used to complex with methyl orange. P. Zhao et al. [3] prepared β-cyclodextrin-modified chitosan microspheres. Briefly, CS was reacted with PEG-2000 and formaldehyde to obtain cross-linked CS microspheres. β-cyclodextrin and epoxy chloropropane were then added to the microsphere suspensions follow by washing and drying. β-cyclodextrin-modified chitosan microspheres were used as an absorbent to remove methyl orange from water. The absorption equilibrium was reached within a contact time of 120 min, while the result from thermodynamic calculation indicates that adsorption of MO on the surface of β-cyclodextrin-modified chitosan microspheres was a spontaneous adsorption process. Therefore, the microspheres can be effectively applied to remove MO from wastewater.

In this work, β-cyclodextrin-modified hydroxyalkylacrylchitosans were synthesized and used to prepare inclusion complexes with methyl orange.

Chapter 3
Research methodology

3.1 Materials

- Chitosan (CS), Eland Co., Ltd., Analytical grade
- 2-Hydroxyethylacrylate (HEA), Thai Mitsui Specialty Chemicals Co., Ltd., Commercial grade
- 2-Hydroxypropylacrylate (HPA), Thai Mitsui Specialty Chemicals Co., Ltd., Commercial grade
- 4-Hydroxybutylacrylate (HBA), Thai Mitsui Specialty Chemicals Co., Ltd., Commercial grade
- Acetone (CH_3COCH_3), Zen Point, Commercial grade
- Isopropanol (i-PrOH), Zen Point, Commercial grade
- Acetic acid (AcOH), Carlo-Erba, Analytical grade
- Sodium hydroxide (NaOH), Laboratory Reagents & Fine Chemicals, Analytical grade
- β-Cyclodextrin (CD) , Wako chemical, Analytical grade
- *p*-Toluenesulfonyl chloride (TsCl), Sigma-Aldrich, Analytical grade
- Celite, Sigma-Aldrich, Analytical grade
- Hydrochloric acid (HCl), Carlo-Erba, Analytical grade
- Methyl orange (MO), Labchem, Analytical grade
- *N,N*-Dimethylformamide (DMF), Carlo-Erba, Analytical grade
- Potassium bromide (KBr) , Carlo-Erba, Spectroscopic grade
- Dimethylsulfoxide (DMSO), Carlo-Erba, Analytical grade
- Ethanol (EtOH), Carlo-Erba, Analytical grade
- Dichloromethane (DCM) , Zen Point, Commercial grade
- Tetrahydrofuran (THF), Fischer Scientific, Analytical grade
- Diiodomethane, Sigma-Aldrich, Analytical grade

3.2 Apparatus

- Fourier transform infrared spectrophotometer (FT-IR), Perkin Elmer Inc., Spectrum GX
- Fourier transform nuclear magnetic resonance spectrometer (FT-NMR), Bruker AG, NMR 300 Ultra Shield
- Nuclear magnetic resonance spectrometer (NMR), Bruker AG, Avance III HD (CU, Thailand)

- Thermogravimetric analyzer (TGA) , Rigaku, Thermo plus EVO 2 TG 8121 (JAIST, Japan)
- Gel permeation chromatography (GPC), Waters, Waters 600E (MTEC, Thailand)
- UV-Vis spectrophotometer, BECTHAI Bangkok Equipment & Chemical Co., Ltd., Model Genesys los UV-Vis
- UV-Vis spectrophotometer, Perkin Elmer Inc., lambda 25 (JAIST, Japan)
- X-ray diffractometer (XRD), Rigaku, Smartlab (JAIST, Japan)
- Dynamic mechanical analyzer (DMA), UBM rheogel, E4000 (JAIST, Japan)
- Humidity controlled chamber, Yamato, IG 420 (JAIST, Japan)
- Karl Fischer titrator, Mettler Toledo, 860 KF Thermoprop (JAIST, Japan)
- Abbe refractometer, Atago, DR-A1 (JAIST, Japan)
- Centrifuge, Hettich Zen Zentrifugation, Universal 320
- pH meter, DKK-TOA Co., HM-20P
- Gallenkamp melting point test apparatus, Sanyo
- Micrometer, Mitutoyo, PK-0505SUE
- Petri dish, Hycon, K1004
- Hotplate, IKA HS-5
- Thermostat, IKA, Euro-ST B
- Balance, Denver Instrument, TC-254
- Hydraulic compression machine, Sang Thai Intertrade Co.
- Dessicator, Thai Pure Science Company
- Oven, Fisher Scientific, Isotemp
- Glass microfiber filter, GE healthcare, GF/C™
- Magnetic bar
- Glassware

3.3 Experiment

3.3.1 Preparation and characterization of β-cyclodextrin modified hydroxyalkylacrylchitosans (HAACSs-g-CDs) as host polymers

Host polymers in this research are HAACSs-g-CDs. To obtain the host polymers, HAACSs were firstly synthesized by Michael addition reaction between different hydroxyalkylacrylates (HEA, HPA, and HBA) and CS. Structures of hydroxyalkylacrylates used in this research are illustrated in Figure 3.1. Thereafter, different HAACSs were then reacted with TsCD, which was synthesized by nucleophilic addition reaction between TsCl and CD, to obtain HAACSs-g-CDs. In addition, mole ratio between TsCD and HBACS was also varied. Methods for preparation and characterization of each product are described in section 3.3.1.1-3.3.1.4.

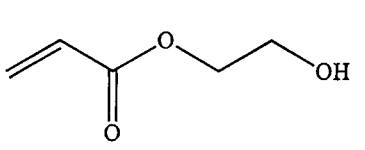

2-Hydroxyethylacrylate (HEA)

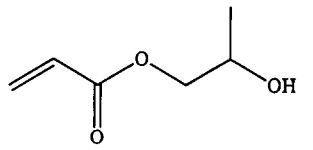

2-Hydroxypropylacrylate (HPA)

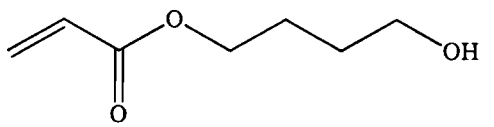

4-Hydroxybutylacrylate (HBA)

Figure 3.1 Structures of hydroxyalkylacrylates used in the research.

3.3.1.1 Preparation of hydroxyalkylacrylchitosans (HAACSs)

Hydroxyalkylacrylchitosans were prepared by Michael addition reaction by partially following the procedure of P. Treenate et al. and G. Ma et al. [19-20]. In detail, 6 g (36.59 mmol) of CS was dissolved in 600 mL of 1% w/v acetic acid. Different hydroxyalkylacrylates (206.87 mmol) were then added as followed in Table 3.1. The reaction was carried out with continuous stirring at 60°C for 2 days. After that, pH of the solution was adjusted to 7 by adding 10% w/v NaOH and then precipitated by dropping the solution into precipitating solvent. The precipitate was washed with plenty of precipitating solvent as described in Table 3.1 followed by drying at 60°C overnight in an oven to obtain HAACSs.

Table 3.1 Chemical ingredients for synthesis of HAACSs.

Formula	Chitosan		Hydroxyalkylacrylates			Precipitating solvent
	mmol	Weight (g)	Type	mmol	Weight (g)	
HEACS	36.59	6	HEA	206.87	24.02	Acetone
HPACS			HPA		26.92	Isopropanol
HBACS			HBA		29.82	Isopropanol

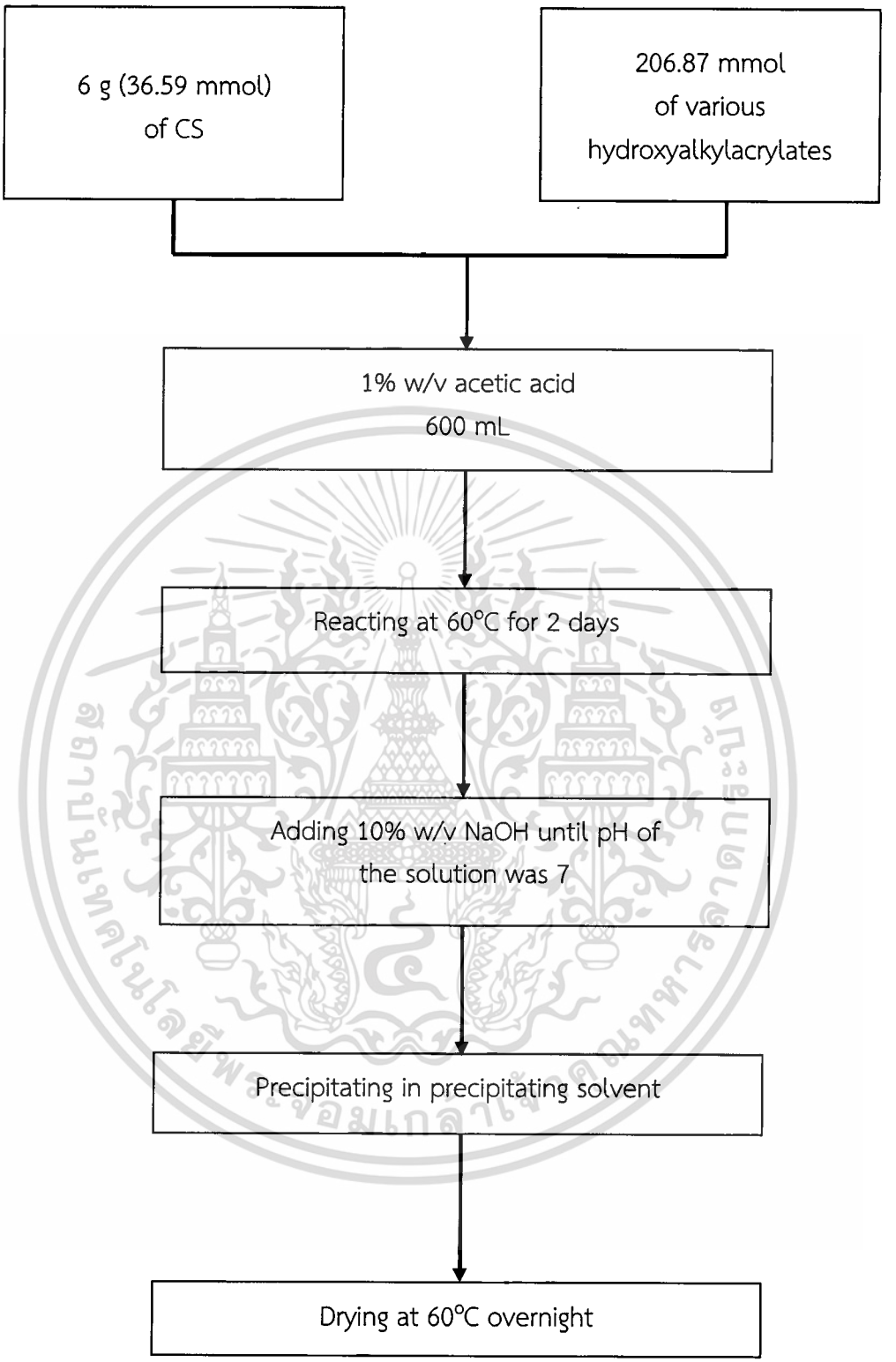

Figure 3.2 Schematic of preparation of HAACSs.

3.3.1.2 Preparation of tosyl-modified β-cyclodextrin (TsCD)

Tosyl-modified β-cyclodextrin (TsCD) was synthesized by modifications of P. Gonil et al.'s method [17] and B. Brady et al.'s method [34]. β-Cyclodextrin (10 g, 8.81 mmol) was dissolved in 140 mL of 10% w/v NaOH then stored overnight in a refrigerator. TsCl (4 g, 20.98 mmol) was added into the solution and then stirred vigorously at 0-5°C for 2 hours. Afterwards, TsCl (6 g, 31.47 mmol) was another added and then stirred at the same temperature for further 3 hours. The reaction mixture was filtered through Celite on a sintered glass funnel to remove unreacted TsCl. Concentrated HCl was dropwise added into the filtrate at 0-5°C until obtaining a white solid of TsCD, then kept the filtrate in a refrigerator overnight. The filtrate was centrifuged, washed several times with acetone and dried overnight in an oven at 50°C to obtain TsCD.

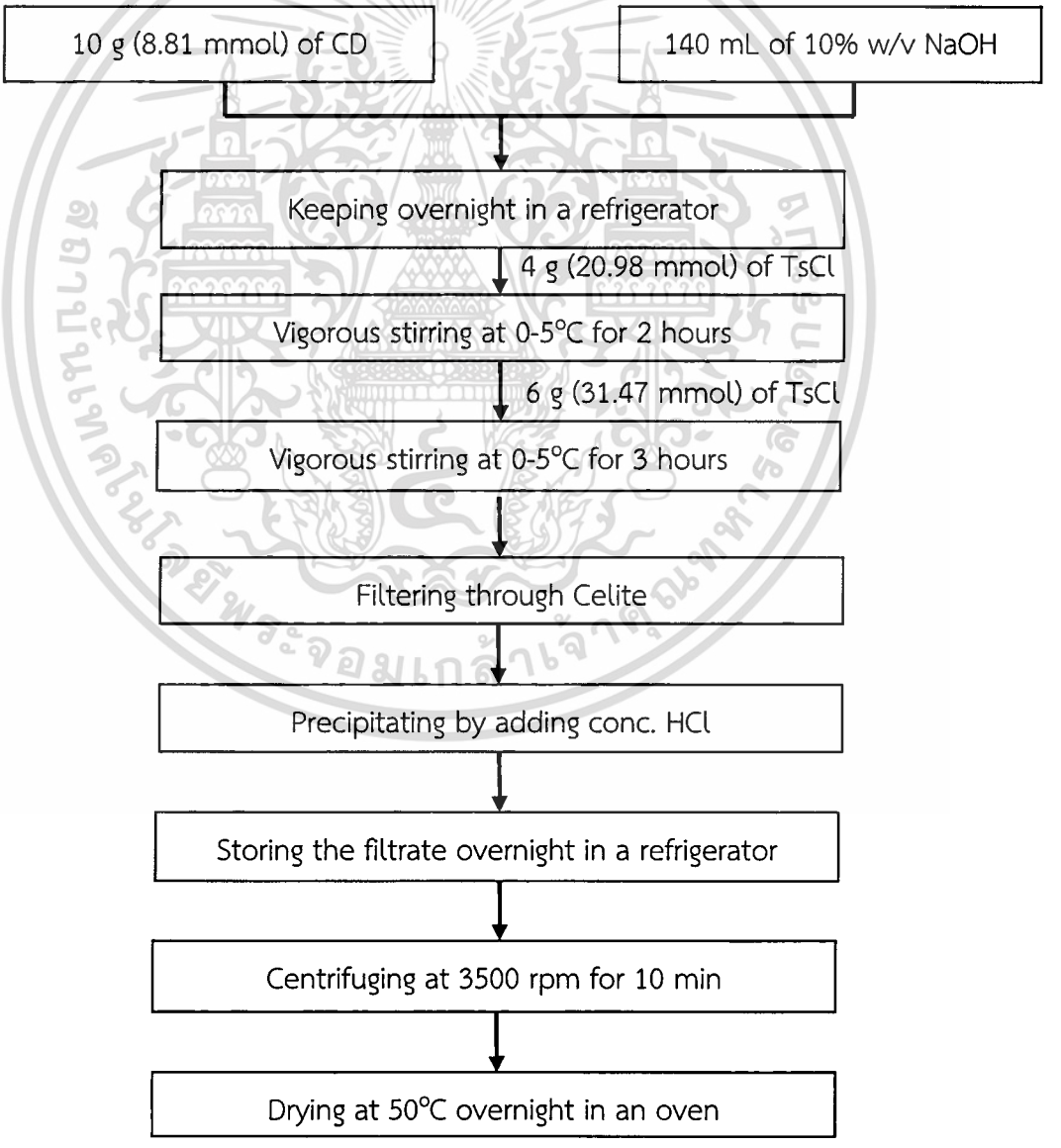

Figure 3.3 Schematic of preparation of TsCD.

3.3.1.3 Preparation of β-cyclodextrin modified different hydroxyalkylacrylchitosans (HAACSs-g-CDs)

0.5 g of HEACS, HPACS, or HBACS was firstly dissolved in 40 mL of distilled water to prepare HAACSs aqueous solution. Various amounts of TsCD as shown in Table 3.2 and 20 mL of DMF were then added into the solution. The solution was reacted under stirring at 60°C for 6 hours and then precipitated by dropping the solution into acetone. The precipitate was stored in a refrigerator overnight. Subsequently, the precipitate was centrifuged at 3500 rpm for 10 minutes then discarded the supernatant. The precipitate was then centrifuged at the same condition for 2 rounds using DMF and acetone as washing solvent, respectively. Thereafter, the precipitate was collected by filtration followed by drying in an oven at 60°C overnight.

Table 3.2 Chemical ingredients for synthesis of HAACSs-g-CDs.

Formula	Type of HAACS	Weight (g)		mmol*		Mole ratio	
		HAACS	TsCD	HAACS	TsCD	HAACS	TsCD
TE-1	HEACS	0.5	0.77	1.82	0.53	3.43	1
TP-1	HPACS		0.73	1.87	0.51	3.67	
TB-1	HBACS		0.71	1.67	0.49	3.41	
TB-2	HBACS		1.06		0.73	2.29	
TB-3	HBACS		2.11		1.46	1.14	

* Calculating by using molecular weight depended on DS obtaining from ^{1}H-NMR spectra.

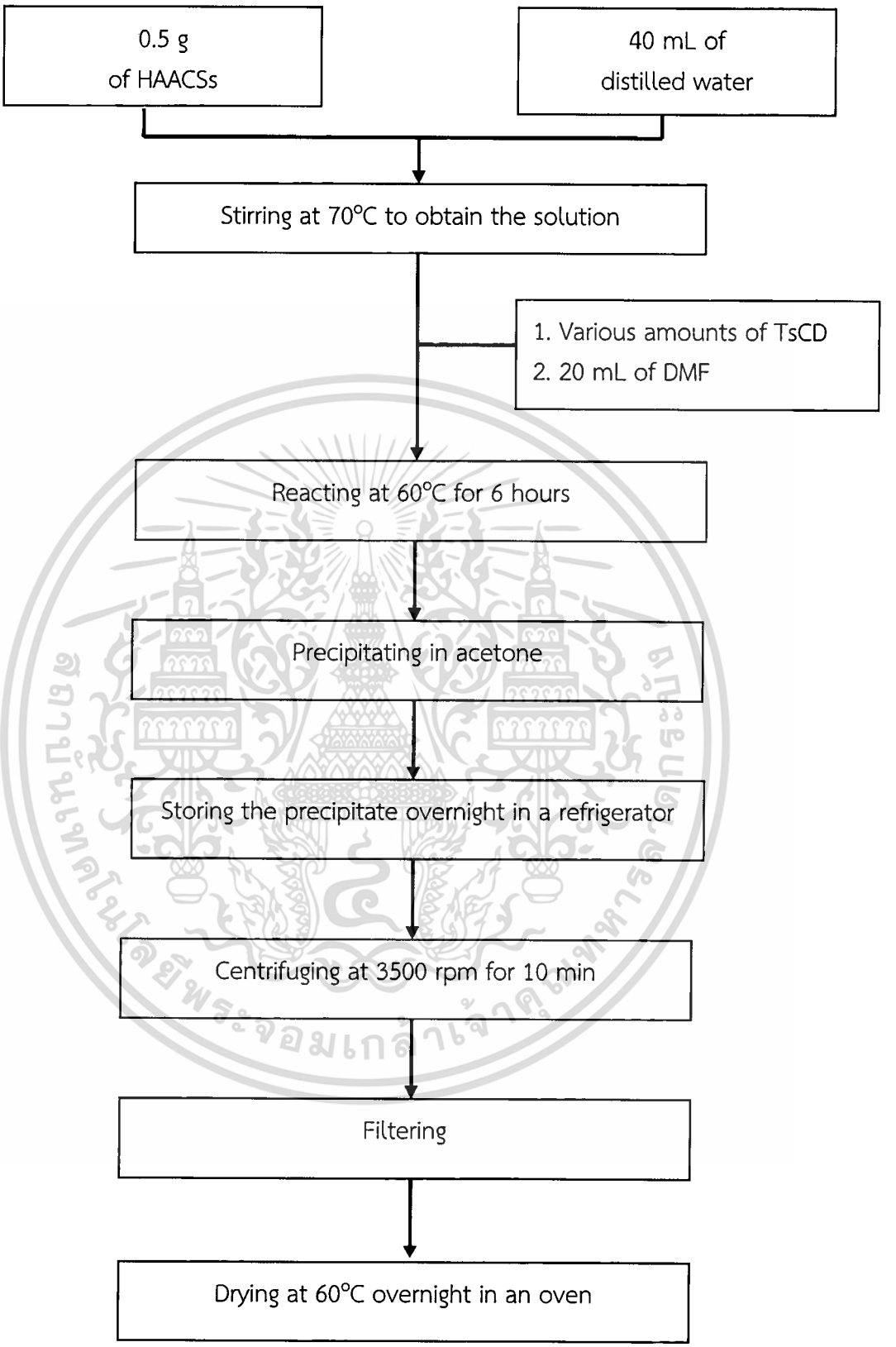

Figure 3.4 Schematic of preparation of HAACSs-g-CDs.

3.3.1.4 Characterization of HAACSs, TsCD, and HAACSs-g-CDs

HAACSs, TsCD, and HAACSs-g-CDs were characterized in terms of solubility, structure, molecular weight, and thermal properties. The details are presented below.

- Solubility test

Solubility of compounds was evaluated in different solvents and temperatures as depicted in Table 3.3.

Table 3.3 Conditions for testing solubility of the compounds.

Compound	Condition
HAACSs and HAACSs-g-CDs	Testing at a concentration of 1% w/v in distilled water at 70°C
CD, TsOH, and TsCD	Testing at a concentration of 1% w/v at ambient temperature using following solvents: - H_2O - DMSO - DMF - Acetone - Ethanol - THF - Isopropanol - Dichloromethane

- Structure

Structure of the compounds was characterized by various techniques as discussed below:

IR spectroscopy

FTIR spectra of the compounds were obtained by preparing the samples as KBr pellets then recorded the spectra over a range of 400-4000 cm^{-1} using 8 scans with a resolution of 4.0 cm^{-1}.

^{1}H-NMR spectroscopy

^{1}H-NMR spectra of the compounds were recorded by using tetramethylsilane (TMS) as an internal standard.

HAACSs were dissolved in D_2O. Structures of HAACSs are shown in Figure 3.5.

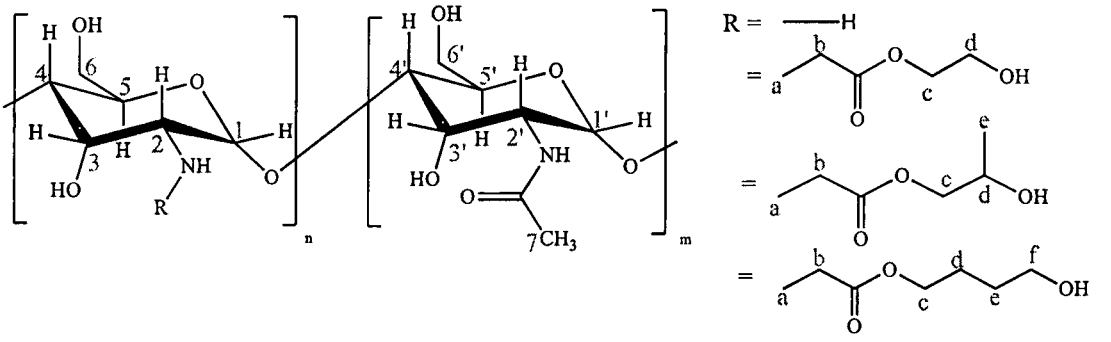

Figure 3.5 Structures of HAACSs.

. Degree of substitution percentage (%DS) of HAACSs can be calculated using equation 3.1-3.2.

$$\%DS\ (HEACS) = \frac{H_b/2}{H_{(2,2')}} x100 \quad (3.1)$$

$$\%DS\ (HPACS, HBACS) = \frac{H_a/2}{H_{(2,2')}} x100 \quad (3.2)$$

Where H_a is the integral area of HPA or HBA moiety protons (-NH-CH_2-) at δ = 3.05 ppm, H_b is the integral area of HEA moiety protons (-CH_2-CO-) at δ = 2.35 ppm, and $H_{(2,2')}$ is the integral area of CS proton at δ = 2.73 ppm.

TsCD was dissolved in DMSO-d_6. Structure of TsCD is depicted in Figure 3.6.

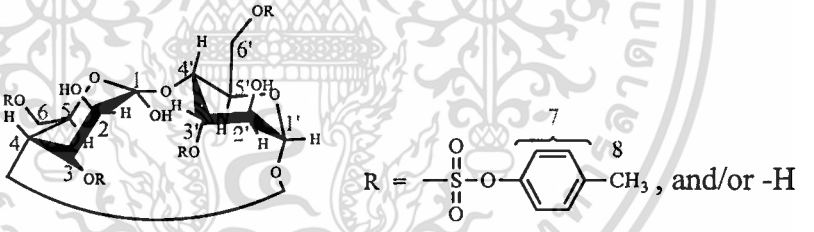

Figure 3.6 Structure of TsCD.

%DT of TsCD can be calculated using equation 3.3.

$$\%DT\ (TsCD) = \frac{H_{Ar}/4}{(H_1+H_{1'})/7} x100 \quad (3.3)$$

Where H_{Ar} is the integral area of aromatic protons from tosyl group at δ = 7.72 and 7.40 ppm, while H_1 and $H_{1'}$ are the integral area of H_1 protons of CD at δ = 4.85 and 4.75 ppm.

HAACSs-g-CDs were dissolved in D_2O. Structures of HAACSs-g-CDs are presented in Figure 3.7.

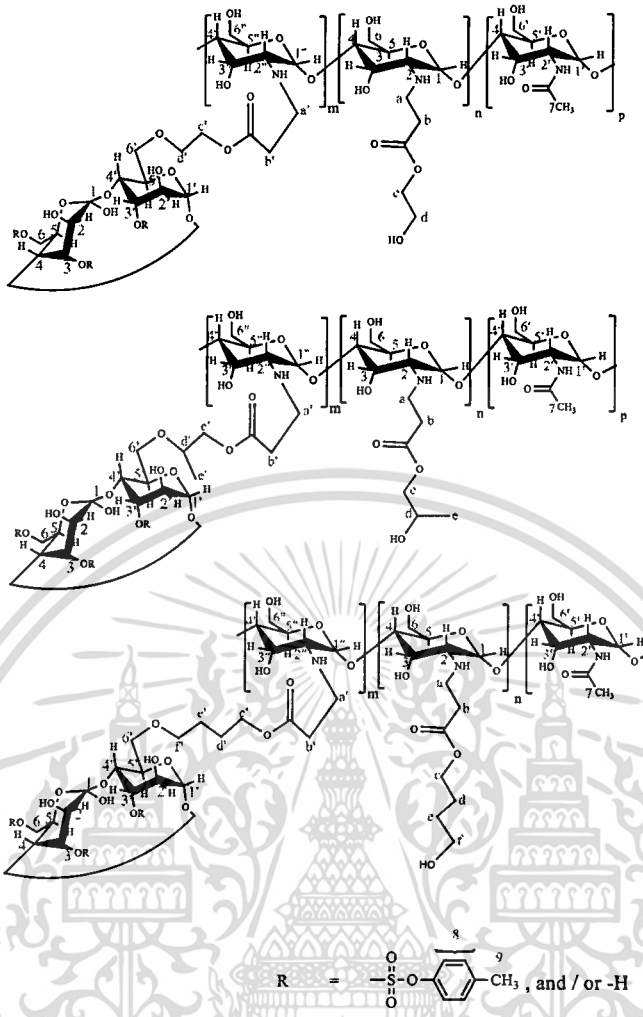

Figure 3.7 Structures of HAACSs-g-CDs.

%DS of HAACSs-g-CDs can be calculated using equation 3.4-3.5.

$$\%DS\ (TE\text{-}1) = \frac{H_{1CD}/7}{H_{(2,2')[\%DS=100]}} x100 \quad (3.4)$$

$$\%DS\ (TP\text{-}1, TB\text{-}1\text{-}3) = \frac{H_{1CD}/7}{H_a/2[\%DS=100]} x100 \quad (3.5)$$

Where H_{1CD} is the integral area of cyclodextrin (H_1) proton at δ = 4.94 ppm, $H_{(2,2')}$ is the integral area of CS proton at δ = 2.73 ppm, and H_a is the integral area of HPA or HBA moiety protons (-NH-C*H*$_2$-) at δ = 3.05 ppm.

UV-Vis spectroscopy

UV-Vis spectra of CD, TsCD and TsOH were recorded by scanning wavelength from 190 to 800 nm using quartz cell with optical path length of 1.00 cm. All samples were dissolved in distilled water at a concentration of 0.001% w/v.

- Average molecular weight

The weight average molecular weight (M_w), number average molecular weight (M_n), and polydispersive index (PDI, M_w/M_n) of CS, HAACSs, and HAACSs-g-CDs were determined by gel permeation chromatography (GPC) using pullulans as a standard. Samples were dissolved in eluent (0.1 M NaCl for HAACSs and HAACSs-g-CDs and acetate buffer pH 4 for CS) and then filtered through nylon syringe filter (pore size 0.45 μm) before injection.

- Thermal properties

Thermal properties of CD and TsCD were evaluated using Gallenkamp melting point test apparatus and TGA as described below:

Melting point test

Melting point of samples were obtained by Gallenkamp melting point test apparatus. Samples were added into capillary tube and then heated until physical changes presented.

Thermogravimetric analysis (TGA)

TGA thermograms of the compounds were obtained by heating samples from 30 to 500°C at a rate of 10°C/min under nitrogen purse.

3.3.2 Preparation and characterization of inclusion complex solutions

Inclusion complexes between CD, TE-1, TB-1 and MO were prepared. Thereafter, their complexes were characterized by UV-VIS spectroscopy.

3.3.2.1 Preparation of MO and CDMO solutions

- MO solutions

0.001% w/v MO solution was prepared from 0.1% w/v MO solution. After that, pH of the solution was adjusted to 1, 4, 6 and 10 using a drop of concentrated HCl, glacial acetic acid, and 30% w/v NaOH.

- CDMO solutions

The formulations of CDMO solutions are summarized in Table 3.4. In terms of CDMO-1, 0.05 g (0.044 mmol) of CD and 0.015 g (0.046 mmol) of MO were dissolved in 50 mL of distilled water followed by diluting to obtain 0.001% w/v of MO and adjusting pH to 1, 4, 6 and 10 by a drop of concentrated HCl, glacial acetic acid, and 30% w/v NaOH. For CDMO-2 and CDMO-3, 0.05 g (0.044 mmol) and 0.5 g (0.44 mmol) of CD were added into 0.001% w/v MO solution, respectively.

Table 3.4 The formulations of CDMO solutions.

Formula	mmol		mole ratio	
	CD	MO	CD	MO
CDMO-1	1.47×10^{-3}	1.53×10^{-3}	1	1.04
CDMO-2	0.044			0.035
CDMO-3	0.44			0.0035

3.3.2.2 Preparation of TE-1MO and TB-1MO solutions

- TE-1MO solutions

Different amounts of TE-1 were dissolved in 25 mL of distilled water. After measuring, 5 mL of 0.002% w/v MO was added into the solutions until total volume reached 50 mL. The experiment was done in both pH 4 and pH 6. For pH 4 condition, pH of TE-1 and MO solutions were adjusted by a drop of glacial acetic acid before mixing altogether. The formulations of TE-1MO solutions are presented in Table 3.5.

- TB-1MO solutions

Various amounts of TB-1 were dissolved in 25 mL of distilled water. 5 mL of 0.002% w/v MO was then added into the solutions until total volume became 50 mL. The experiment was carried out in both pH 4 and pH 6. In case of pH 4 condition, pH of TB-1 and MO solutions were adjusted by a drop of glacial acetic acid prior to mixing altogether. The formulations of TE-1MO solutions are depicted in Table 3.6.

Table 3.5 The formulations of TE-1MO solutions.

Series	V_{total} (mL)	V_{MO} (mL)	g_{TE-1}	mmol			Mole ratio	
				TE-1	CD	MO	CD	MO
A	25	0	0.05	0.122	0.0146	-	-	-
	30	5				$3.06x10^{-4}$	1	0.021
	35	10				$6.12x10^{-4}$		0.042
	40	15				$9.17x10^{-4}$		0.063
	45	20				$1.22x10^{-3}$		0.084
	50	25				$1.53x10^{-3}$		0.10
B	25	0	0.004	$9.76x10^{-3}$	$1.17x10^{-3}$	-	-	-
	30	5				$3.06x10^{-4}$	1	0.26
	35	10				$6.12x10^{-4}$		0.52
	40	15				$9.17x10^{-4}$		0.78
	45	20				$1.22x10^{-3}$		1.04
	50	25				$1.53x10^{-3}$		1.31
	50	-	0.0025	$6.10x10^{-3}$	$7.32x10^{-4}$	$1.53x10^{-3}$	1	2.09

Table 3.6 The formulations of TB-1MO solutions.

Series	V_{total} (mL)	V_{MO} (mL)	g_{TB-1}	mmol			Mole ratio	
				TB-1	CD	MO	CD	MO
A	25	0	0.05	0.145	5.80×10^{-3}	-	-	-
	30	5				3.06×10^{-4}	1	0.053
	35	10				6.12×10^{-4}		0.11
	40	15				9.17×10^{-4}		0.16
	45	20				1.22×10^{-3}		0.21
	50	25				1.53×10^{-3}		0.26
B	25	0	0.008	0.023	9.28×10^{-4}	-	-	
	30	5				3.06×10^{-4}	1	0.33
	35	10				6.12×10^{-4}		0.66
	40	15				9.17×10^{-4}		0.99
	45	20				1.22×10^{-3}		1.31
	50	25				1.53×10^{-3}		1.65
	50	-	0.0025	7.23×10^{-3}	2.89×10^{-4}	1.53×10^{-3}	1	5.29

3.2.2.3 Characterization of inclusion complex solutions

λ_{max} of inclusion complex solutions were determined by UV-Vis spectroscopy. The spectra were recorded by scanning wavelength from 190 to 800 nm using quartz cell with optical path length of 1.00 cm.

3.3.3 Preparation and characterization of films

Films from CS, HAACSs, TB-1, and inclusion complex between TB-1 and various amounts of MO were prepared using solution casting method. The methods for preparation and characterization of the films are shown below.

3.3.3.1 Preparation of films

3.3.3.1.1 Preparation of CS, HAACSs and TB-1 films

HAACSs and TB-1 were dissolved in distilled water at 70°C and CS was dissolved in 1% w/v acetic acid at ambient temperature. After that, the solution was poured into a Petri dish and then dried at 40°C.

3.3.3.1.2 Preparation of MO-incorporated TB-1 films

MO as a guest was added into TB-1 film to study effect of inclusion complex affecting films properties. TB-1 was dissolved in distilled water at 70°C. After cooling to room temperature, various amounts of MO were added into the solution. The solution was then stirred for another 2 hours at 40°C followed by pouring into a Petri dish and drying at 40°C in an oven. The formulations of the films are summarized in Table 3.7.

Table 3.7 The formulations of MO-incorporated TB-1 films.

Formula	Weight (g)		mmol		Mole ratio	
	TB-1	MO	CD	MO	CD	MO
TB-1MO0.01	1	0.01	0.116	0.0306	1	0.26
TB-1MO0.04		0.04		0.122		1.05
TB-1MO0.1		0.1		0.306		2.64

3.3.3.2 Characterization of films

The films were characterized by various methods as shown below:

- **Refractive indexes**

Refractive index of the films was determined by Abbe refractometer. The samples (2x1 cm^2) were placed into the machine. Diiodomethane acting as a contact solvent was then dropped into the samples until observing phase contrast. The photo of the machine is presented in Figure 3.8.

Figure 3.8 Abbe refractometer.

- **Crystallinity**

Crystallinity of the films was determined by wide-angle X-ray scattering (WAXS) technique. The samples (2x2 cm^2) were scanned from 2θ = 5° to 40° at a rate of 4°/min.

- **Structure**

Structure of MO-incorporated films was determined by IR spectroscopy. The dried films were mixed with KBr to obtain KBr pellet. After that, the spectra were recorded over a range of 400-4000 cm^{-1} using 8 scans with a resolution of 4.0 cm^{-1}.

- **Light transmittance**

Light transmittance of the films was determined by UV-Vis spectroscopy. The films (2x1 cm^2) were placed into the machine and then scanned in a range of 200-700 nm.

- **Thermal properties**

Thermal properties of the films were determined by TGA and DMA as described below:

TGA

To obtain TGA thermograms, the dried samples (5 mg) were heated from 30 to 500°C at a rate of 10°C/min under nitrogen purse.

Dynamic mechanical analysis (DMA)

All samples (2x0.5 cm^2) were kept in a humidity controlled chamber prior to carrying out the experiment. The experiment was conducted using tension mode at a frequency of 1 Hz and heated from -50 to 200°C at a heating rate of 2°C/min.

Chapter 4
Results and discussion

This research studied on the inclusion complexes between β-cyclodextrin-modified hydroxyalkylacrylchitosans (HAACSs-g-CDs) and methyl orange (MO). To prepare HAACSs-g-CDs as host polymers, hydroxyalkylacrylchitosans (HAACSs) were firstly synthesized via Michael addition reaction between chitosan (CS) and different hydroxyalkylacrylates and then they were reacted with tosyl-modified β-cyclodextrin (TsCD) prepared by the reaction between β-cyclodextrin (CD) and tosyl chloride (TsCl). The products from each reaction were then characterized and tested in terms of their solubility, structure, and molecular weight. After that, inclusion complex solutions were prepared using HAACSs-g-CDs and MO with varying mole ratio and then they were characterized by UV-Vis spectroscopy. Subsequently, solution-casted films from CS, HAACSs, β-cyclodextrin-modified hydroxybutylacrylchitosan (TB-1), and inclusion complexes between TB-1 and MO with different amounts of MO were prepared. Photo, crystallographic, and thermal properties of the films were then determined. The results were collected and discussed in details as below:

4.1 Synthesis and characterization of HAACSs

The HAACSs were prepared by Michael addition reaction between CS and different hydroxyalkylacrylates i.e., 2-hydroxyethylacrylate (2-HEA) to yield hydroxyethylacrylchitosan (HEACS), 2-hydroxypropylacrylate (2-HPA) to yield hydroxypropylacrylchitosan (HPACS), and 4-hydroxybutylacrylate (4-HBA) to yield hydroxybutylacrylchitosan (HBACS). Mole ratio between CS and hydroxyalkylacrylates used in the reaction was 1:6. The reactions are shown in Figure 4.1. In addition, their percent yields and solubility results are summarized in Table 4.1.

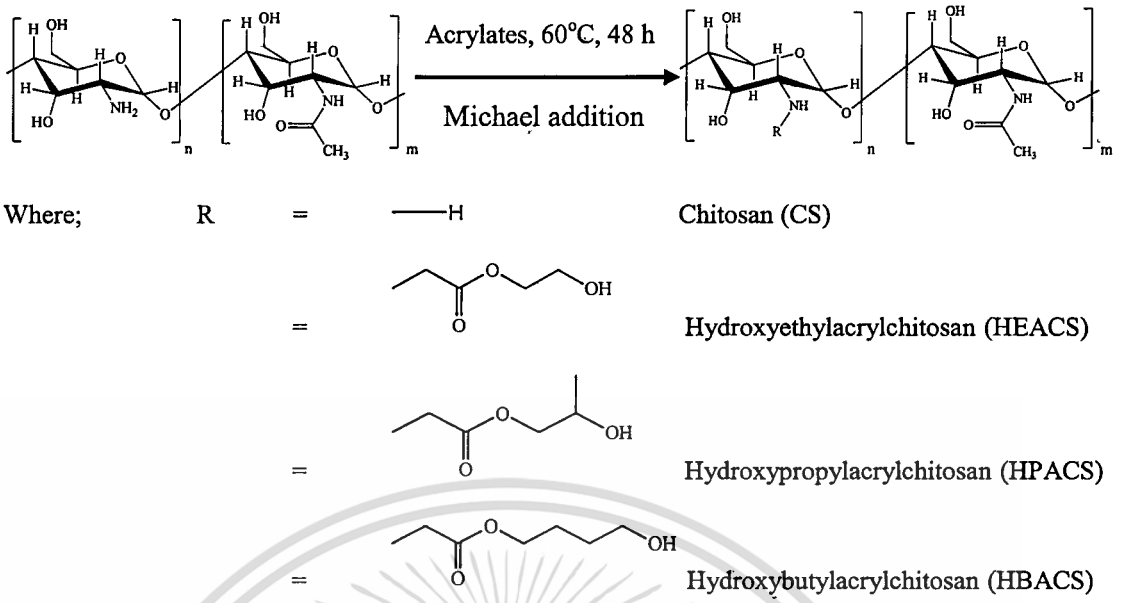

Figure 4.1 Synthetic schemes of HAACSs.

Table **4.1** The percent yields and solubility results of HAACSs.

Formula	Precipitating solvent	%Yield*	Time used for completely dissolved at 70°C (1%w/v)
HEACS	Acetone	93	3 days
HPACS	i-PrOH	70	2 days
HBACS	i-PrOH	87	1 day

* Methods for calculating %yield of HAACSs were shown in Appendix B.

4.1.1 Solubility results

Water solubility tests of HAACSs in distilled water were carried out at 70°C using a concentration of 1% w/v. The resulting solutions were filtered through a syringe filter (pore size 0.45 μm) to ensure that the solutions were dissolved completely. The solubility results of HAACSs are depicted in Table 4.1.

From the results, they showed that all HAACSs could dissolve in distilled water. This is owing to hydrophilicity of hydroxyalkylacrylates moieties. In addition, the hydroxyalkylacrylates moieties can disturb the formation of the ordered structure and the hydrogen bonds in the molecules [19]. For HBACS, it used the least time to dissolve completely in distilled water comparing with others. This is because of its longest alkyl chain.

4.1.2 FTIR spectra

FTIR spectra of CS and HAACSs are shown in Figure 4.2. For CS spectrum, the broad peak at about 3373 cm^{-1} assigned to –NH and –OH stretching vibration. The peak at 2917 cm^{-1} attributed to –CH- stretching vibration. The peaks at 1654, 1596, and 1423 cm^{-1} were involved with amide vibration, amine ($-NH_2$) vibration, and CH_2 bending, respectively. The absorption band at 1152 cm^{-1} was the asymmetric stretching of the C-O-C bridge, and the bands at 1080 and 1028 cm^{-1} assigned to the C-O stretching vibration [19, 58]. In addition, the peak at 897 cm^{-1} corresponded to β-pyranyl vibration [56]. For HAACSs spectra, the additional peaks from C=O stretching of the hydroxyalkylacrylates moieties and asymmetric and symmetric stretching of the carboxylate (COO^-) groups were observed [20]. Their additional peaks are summarized in Table 4.2.

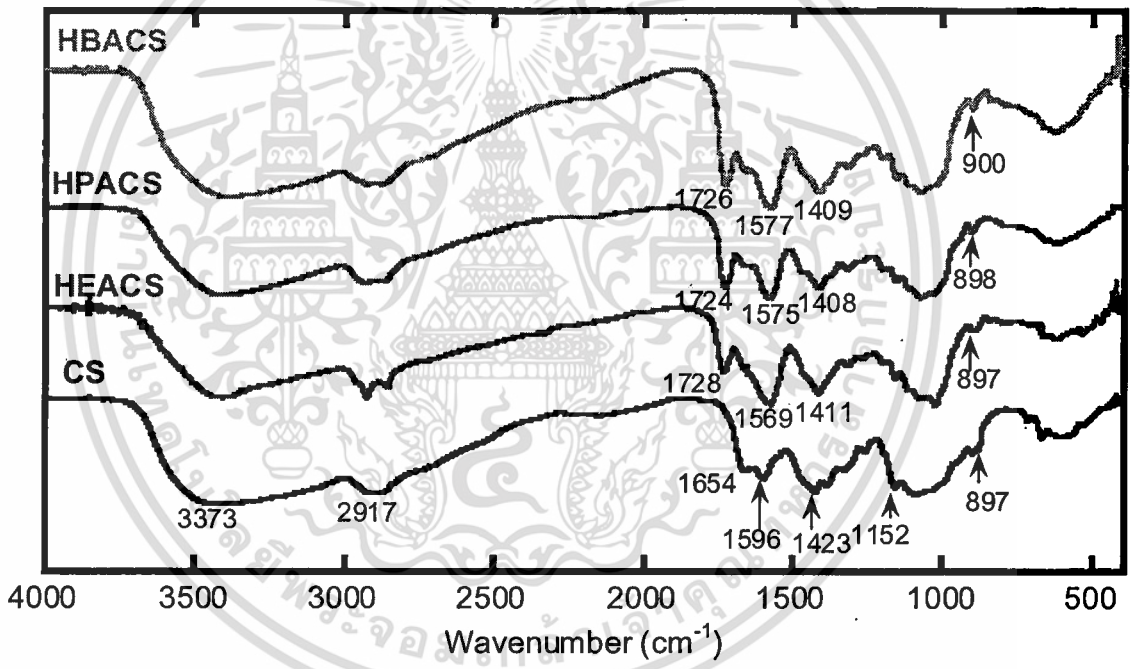

Figure 4.2 FTIR spectra of CS and HAACSs.

Table 4.2 The C=O stretching and COO^- stretching of HAACSs.

Formula	$\nu_{C=O}$ (cm^{-1})	ν_{COO^-} (cm^{-1})	
		Asymmetric	Symmetric
HEACS	1728	1569	1411
HPACS	1724	1575	1408
HBACS	1726	1577	1409

These additional peaks found in HAACSs spectra were the first evidence suggesting that HAACSs were successfully prepared. To confirm the results and obtain more details about structures, ^{1}H-NMR experiment was conducted. The spectra are shown and discussed in next section.

4.1.3 ^{1}H-NMR spectra

^{1}H-NMR spectroscopy was used to confirm the FTIR results and investigate more details about structures. The ^{1}H-NMR spectra of HAACSs are shown in Figure 4.3. In ^{1}H-NMR spectrum of HEACS, it showed signals at δ = 4.45 ($H_{1,1'}$), δ = 3.85 - 3.51 ($H_{3,3'}$, $H_{4,4'}$, $H_{5,5'}$, $H_{6,6'}$, H_c, H_d), δ = 3.07 (H_a), δ = 2.73 ($H_{2,2'}$), δ = 2.35 (H_b), and δ = 1.94 ppm (H_7) [20]. For HPACS spectrum, it showed signals at δ = 4.45 ($H_{1,1'}$), δ = 3.80 - 3.50 ($H_{3,3'}$, $H_{4,4'}$, $H_{5,5'}$, $H_{6,6'}$, H_c, H_d), δ = 3.05 (H_a), δ = 2.73 ($H_{2,2'}$), δ = 2.35 (H_b), δ = 1.94 (H_7), and δ = 1.45 ppm (H_e). In ^{1}H-NMR spectrum of HBACS, it showed signals at δ = 4.45 ($H_{1,1'}$), δ = 3.85 - 3.51 ($H_{3,3'}$, $H_{4,4'}$, $H_{5,5'}$, $H_{6,6'}$, H_c, H_f), δ = 3.05 (H_a), δ = 2.69 ($H_{2,2'}$), δ = 2.34 (H_b), δ = 1.94 (H_7), and δ = 1.02 ppm ($H_{d,e}$).

From the spectra, it was recommended that hydroxyalkylacrylates were successfully grafted onto CS skeletons due to the presence of additional signals attributed to hydroxyalkylacrylates side chains (H_{a-d} for HEACS, H_{a-e} for HPACS, and H_{a-f} for HBACS). This results supported the results obtained from FTIR spectra. Therefore, it could be suggested that HAACSs were successfully synthesized.

Table 4.3 shows the %DS and average molecular weight per repeating unit of HAACSs. The %DS of HAACSs was calculated using equation 3.1-3.2. The methods for calculating the %DS and average molecular weight per repeating unit of HAACSs are depicted in Appendix B.

Table 4.3 The %DS and average molecular weight per repeating unit of HAACSs.

Formula	%DS	Average molecular weight per repeating unit
HEACS	97	276
HPACS	80	267
HBACS	95	300

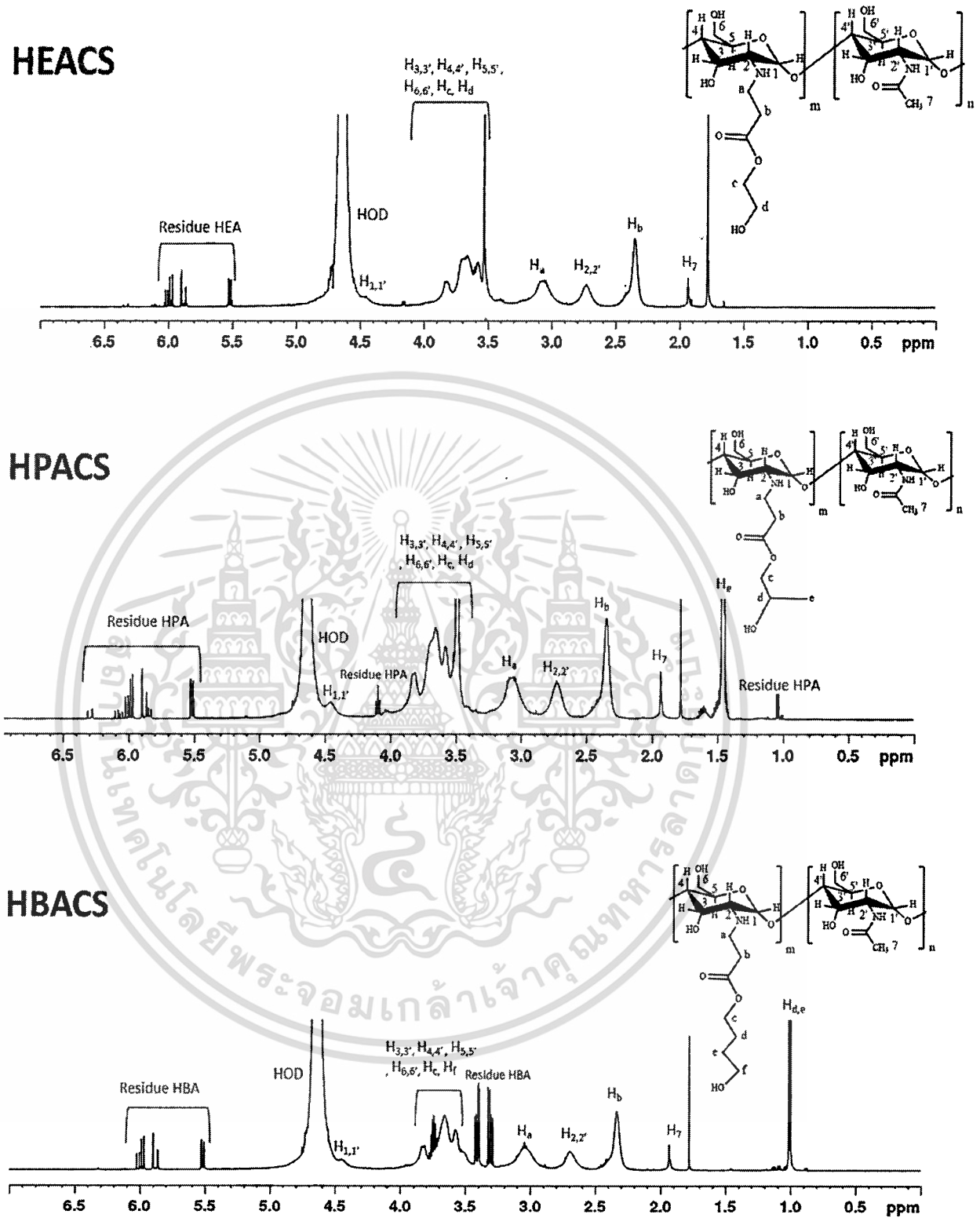

Figure 4.3 ^{1}H-NMR spectra of HAACSs.

In addition to all spectra, the residue hydroxyalkylacrylates in the reaction were found. This is because hydroxyalkylacrylates could not be completely removed after the reaction due to their high amount. Therefore, the further purification step such as dialysis should be performed in order to decrease unreacted hydroxyalkylacrylates remaining in the products.

4.1.4 GPC results

The weight average molecular weight (M_w), number average molecular weight (M_n), and polydispersive index (PDI, M_w/M_n) of CS and HAACSs were determined by GPC. The results are depicted in Table 4.4. In addition, the GPC chromatograms of CS and HAACSs are presented in Appendix C.

Table 4.4 The M_n, M_w, and PDI of CS and HAACSs.

Formula	M_n	M_w	PDI	Eluent
CS	83,000	270,000	3.30	Acetate buffer pH 4
HEACS	22,700	69,200	3.04	0.1 M NaCl
HPACS	23,600	69,900	2.96	
HBACS	33,900	90,000	2.66	

From the results, they showed that the molecular weight of all HAACSs was lower than unmodified chitosan. This could be ascribed to acid hydrolysis occurring during the time of Michael addition reaction [20].

4.2 Characterization and properties of HAACSs films

HAACSs films were prepared by solution casting method using distilled water as a solvent. The CS film was also prepared as a reference by dissolving CS in 1% w/v acetic acid. Subsequently, the yellowish-transparent films were characterized by various techniques. The appearance and the average thickness of the films are presented in Figure 4.4 and Table 4.5, respectively.

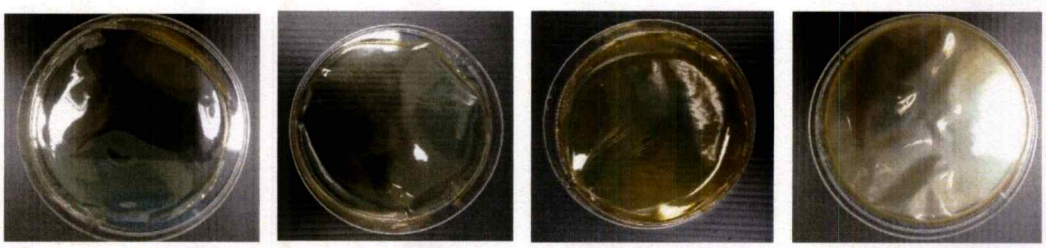

Figure 4.4 The appearance of CS and HAACSs films.

Table 4.5 The average thickness of CS and HAACSs films.

Formula	Average thickness (μm)
CS	148±14
HEACS	122±16
HPACS	112±19
HBACS	130±17

4.2.1 Light transmittance

The light transmittance of the CS and HAACSs films were determined by UV-Vis spectroscopy. Figure 4.5 shows the light transmittance curves of the films at wavelengths of 200-700 nm. From the curves, it could be seen that all films were transparent in visible region (400-700 nm). However, they could absorb most energy in UV region (200-400 nm for this experiment). Therefore, it could be suggested that these films can be used in transparency-concerned applications such as a packaging film or wound dressing.

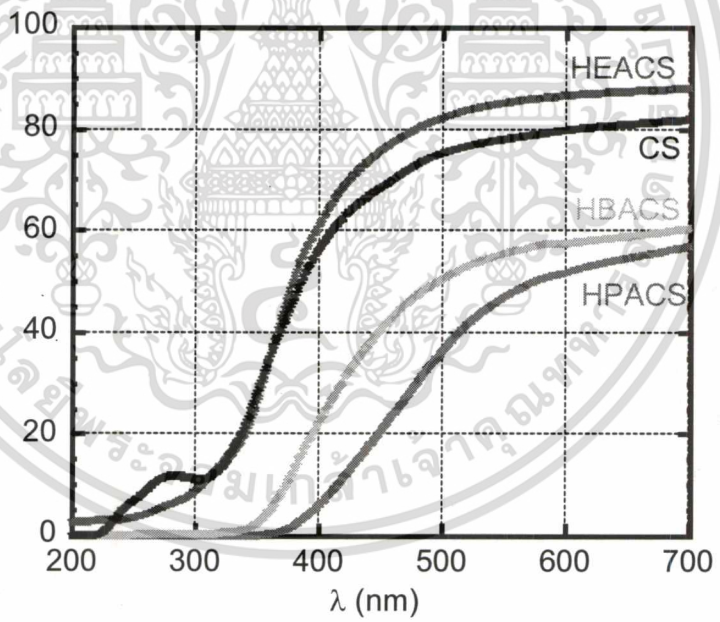

Figure 4.5 Light transmittance curves of CS and HAACSs films.

4.2.2 Refractive indexes

The optical properties of solvent-cast polymer films are important in optoelectronic systems and devices. The properties of the films are generally controlled by the intrinsic optical anisotropy of the polymer chain and by the orientation induced during casting [59]. Consequently, refractive index, a one of the optical properties, of CS and HAACSs films was determined using Abbe refractometer at a wavelength of 589 nm. The results are depicted in Figure 4.6.

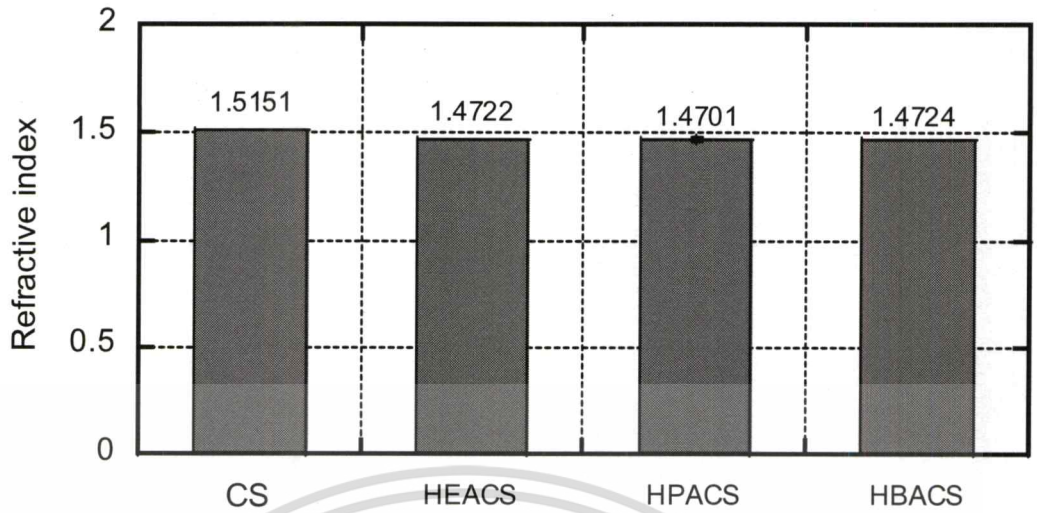

Figure 4.6 Refractive indexes of CS and HAACSs films at 589 nm.

From the results, it could be obviously seen that refractive index of CS film was higher than those of HAACSs films. However, there was no significant difference in refractive index found in HAACSs species. The refractive index of CS film in this experiment was 1.5151, which slightly higher than the result obtained from Ellipsometry reported by H. Jiang et al. at 1.500 [60]. The phenomenon that the refractive indexes of HAACSs films were lower than CS film could be described that grafting hydroxyalkylacrylates can increase molar volume of the molecules. The relationship between molar volume and refractive index can be expressed by Lorentz-Lorenz theoretical models as depicted in equation 4.1: [61]

$$\frac{n^2-1}{n^2+2} = \frac{4\pi N_A \alpha}{3V} \qquad (4.1)$$

In which n is the refractive index, N_A is the Avogadro's number, α is the polarizability (cm^3), and V is the molar volume (cm^3/mol). Therefore, refractive index decreases when increasing molar volume.

In addition, the results were in the same trend as C. Yang and S. Jenekhe's work [61] who reported that refractive index of polymethylphenyleneimine (PMPI) reduced by 0.13 from polyphyneleneimine (PPI). They presented that the reduction in the refractive index of PMPI comparing with PPI was owing to the increment in molar volume by the presence of methyl groups substituted.

4.2.3 WAXS patterns

Crystallinity of CS and HAACSs films were determined by WAXS. The WAXS patterns of CS and HAACSs films are presented in Figure 4.7.

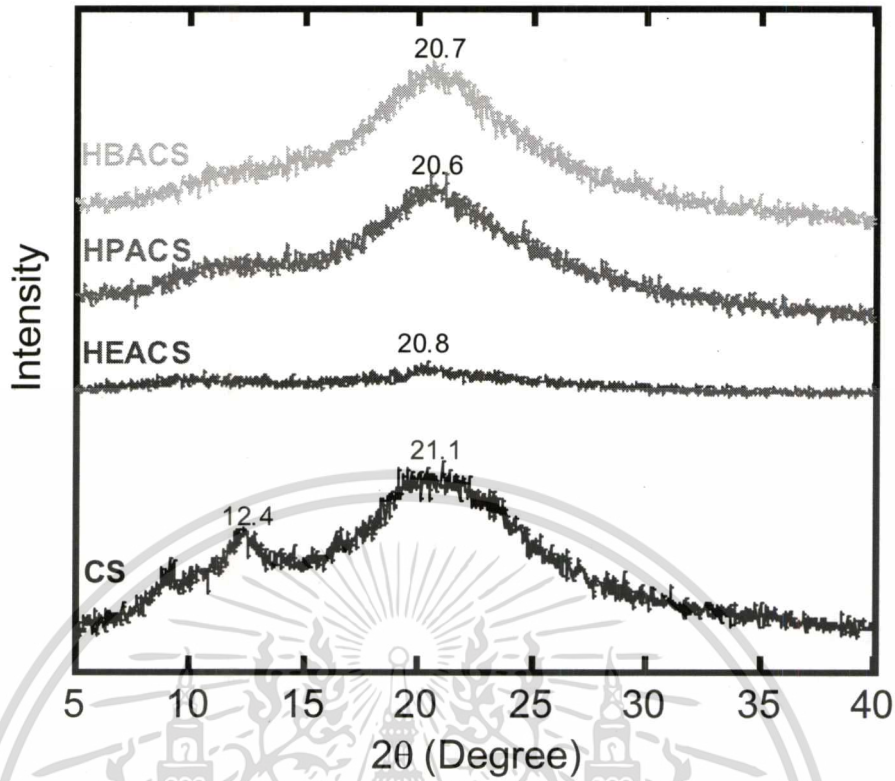

Figure 4.7 WAXS patterns of CS and HAACSs films.

In WAXS pattern of CS film, the peak at $2\theta = 12.4^{\circ}$ corresponded to crystal form I which having more extended chain and the peak at $2\theta = 21.1^{\circ}$ assigned to crystal form II which is the constrained chain conformation [62]. Unlike CS film, the WAXS patterns of HEACS, HPACS and HBACS films showed only one significant peak at $2\theta = 20.8^{\circ}$, 20.6° and 20.7°, respectively. This could be interpreted that grafting hydroxyalkylacrylates onto CS can disrupt the formation of intra- and inter-molecular hydrogen bonds [19].

4.2.4 TGA thermograms

Thermal behavior of CS and HAACSs films was investigated by TGA. The dried films (5 mg) were heated from 30 to 500°C at a heating rate of 10°C/min. Figure 4.8 shows TGA thermograms of the films and Table 4.6 shows T_{90} and T_{50} obtained from the thermograms. From CS thermogram (a), it showed two weight loss stages. The change in weight loss at a lower temperature (ca. 75 to 120°C) corresponded to dehydration of bound water and the change at higher temperature (ca. 200 to 400°C) attributed to the degradation of CS molecules [63].

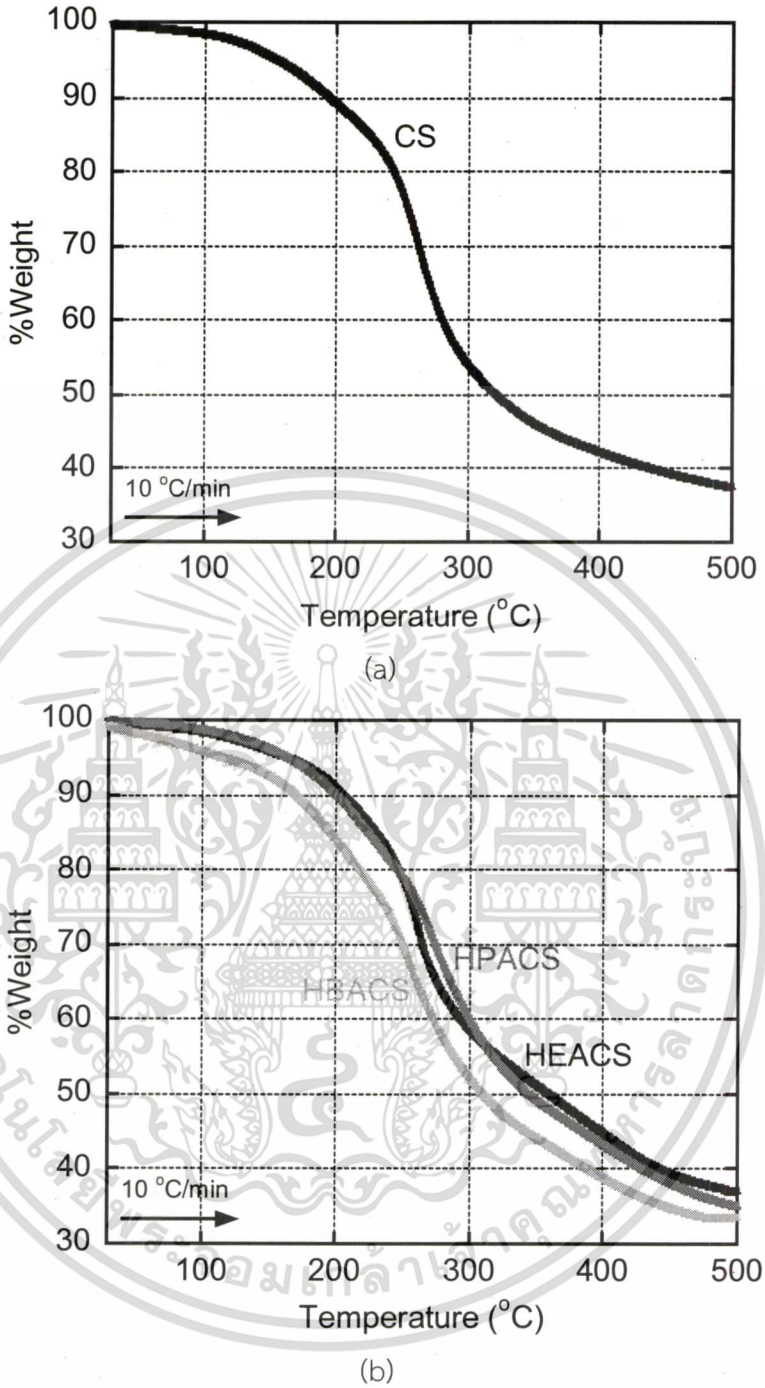

Figure 4.8 TGA thermograms of CS (a) and HAACSs (b) films.

The thermograms of HAACSs films (b) also showed two weight loss stages due to the loss of bound water at a lower temperature zone (ca. 75 to 130°C) and the molecular decomposition at a higher temperature zone (ca. 200 to 400°C). From the results, HBACS had the lowest T_{90} and T_{50} among all HAACSs because of its longest alkyl chain moiety. However, the T_{90} and T_{50} of CS were lower than HEACS and HPACS because acid containing in CS during dissolution can hydrolyze the chains. Therefore, T_{90} and T_{50} of CS and HAACSs could not be compared in this experiment.

Table 4.6 The T_{90} and T_{50} of CS and HAACSs films.

Formula	T_{90} (°C)	T_{50} (°C)
CS	195	321
HEACS	214	367
HPACS	200	345
HBACS	189	332

4.2.5 DMA thermograms

Thermal properties of CS and HAACSs films were also evaluated by DMA. The samples (2x0.5 cm^2) were kept in a humidity controlled chamber (25°C, 50% RH) before the experiment. Percent of water in the films after conditioned was determined by Karl-Fischer titration. The results are shown in Table 4.7.

Table 4.7 Percent of water in CS and HAACSs films.

Formula	%Water
CS	12.53±0.17
HEACS	8.76±1.90
HPACS	10.56±0.55
HBACS	10.74±0.25

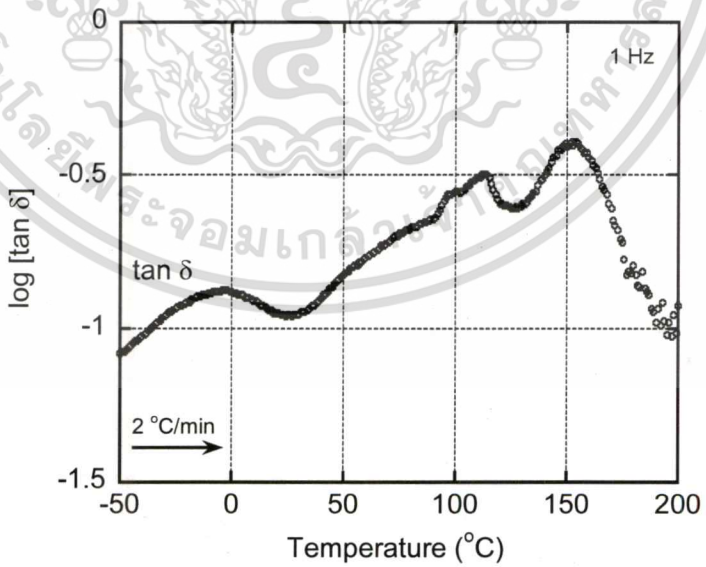

Figure 4.9 Loss tangent (tan δ) versus temperature of CS film.

From tan δ curve of CS film, it showed the peaks at -3, 114, and 154°C. For the peak at -3°C, it could be ascribed to ice melting [64]. The peak at 114°C related to water evaporation leading to reorganization of packing CS molecules. The peak at 154°C corresponded to the combination of structural reorganization of CS due to water loss and molecular degradation as well as local movement of the CS molecules in the pseudo-stable stage as reported by K. Sakurai et al. [65].

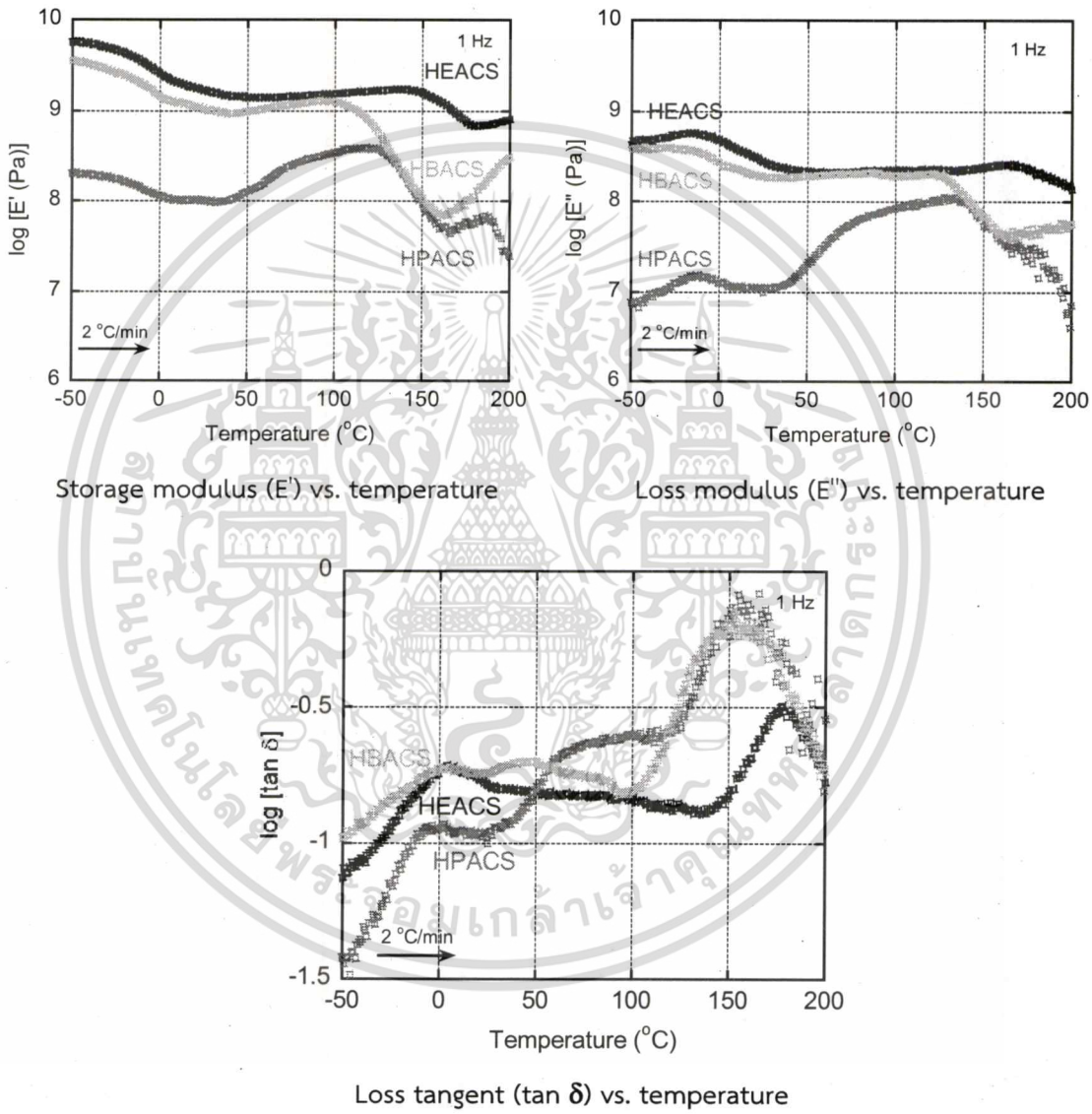

Figure 4.10 Temperature dependence of tensile moduli for HAACSs films.

From tan δ curves of HAACSs films, the main peak corresponded to the combination of the reorganization of molecules due to water loss and the local movement of the molecules in the pseudo-stable stage as well as molecular degradation of each of the films was observed at 178°C for HEACS, at 155°C for HPACS, and at 153°C for HBACS. For HBACS, its lowest main peak temperature in comparison with HEACS and HPACS was ascribed to its longest alkyl chain which facilitated molecular movement. In addition, it could be suggested that HPACS did not suitable for further application owing to its lowest mechanical properties comparing with HEACS and HBACS.

The peak assigned to ice melting was also exhibited in the curves at 4°C for HEACS, at -3°C for HPACS, and at -1°C for HBACS. In addition to the tan δ curve of HBACS, the peak involved with structural reorganization of the molecules due to an increase of remained water mobility, volume expansion and change of hydrogen bond strength [66] was observed at 49°C.

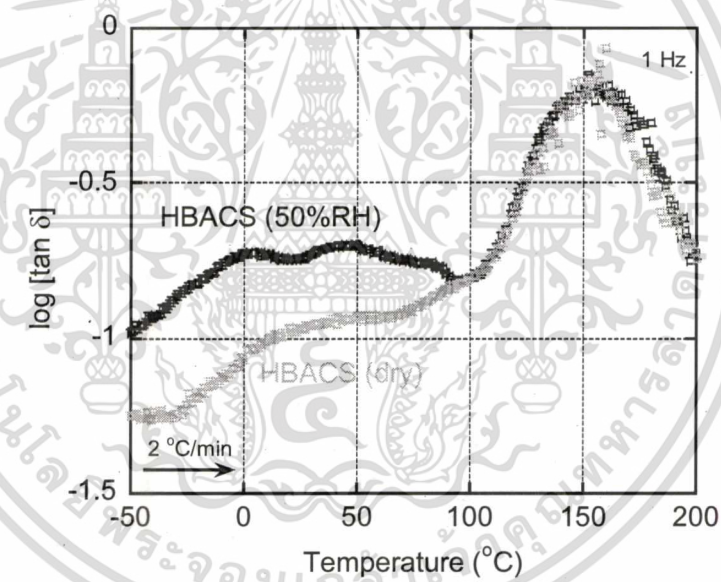

Figure 4.11 Loss tangent (tan δ) versus temperature of HBACS film with different storing conditions.

The effect of water content in the HBACS film on thermal properties was also investigated. The sample was dried in a vacuum oven at 60°C for 1 day before the experiment. The percent of water obtained from Karl-Fischer titration was lower from 10.74±0.25% (before drying) to 3.74±0.45%. The remained water in the sample could be owing to time used for drying was not enough to remove all water in the film and non-freezing bound water presented. Such type of bound water can bound through the polymer chain through hydrogen bonding and it cannot be totally removed under mild condition even vacuum is applied [67]. According to the tan δ curves, the main peak from the combination of the reorganization of molecules due

the local movement of the molecules in the pseudo-stable stage as well as molecular degradation between HBACS (50% RH) and HBACS (dry) films was detected at the similar temperature (ca. 157°C). This is because the amount of water in the films was not different enough to provide significant change of temperature range of the main peak. Nevertheless, the difference of the tan δ curves between HBACS (50% RH) and HBACS (dry) could be found in that the peak assigned to ice melting and structural reorganization due to residual water was not exhibited in the curve of HBACS film (dry).

In addition to all DMA experiments, it was observed that color of the samples changed from light yellow to dark yellow after the experiment as shown in Figure 4.12, indicating that the chains were degraded by heat. Therefore, a second run was not carried out.

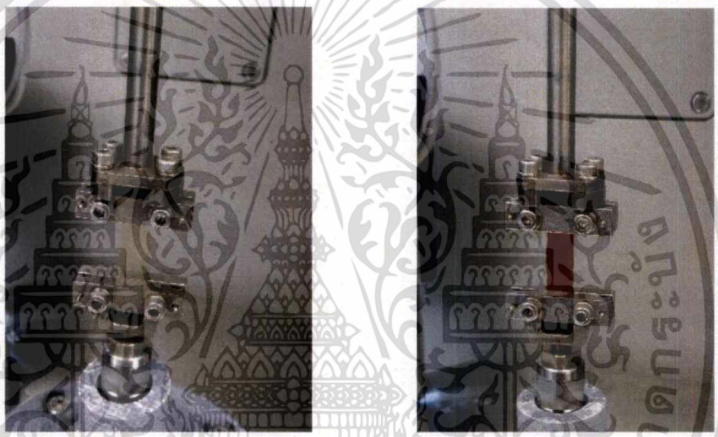

(a) (b)

Figure 4.12 Color of the films before DMA testing (a) and after DMA testing (b).

4.3 Synthesis and characterization of host polymers

The HAACSs-g-CDs as host polymers were prepared by the reaction between TsCD and HAACSs. The TsCD and HAACSs-g-CDs were characterized by a number of techniques. The results were discussed in details as below:

4.3.1 Properties of TsCD

TsCD was prepared by nucleophilic addition reaction between CD and TsCl in a presence of base. After the reaction, white solid was obtained (%Yield = 33). The product was further characterized in terms of its solubility, structure, and thermal properties and used as a reactant for preparing HAACSs-g-CDs. The synthetic scheme is depicted in Figure 4.13.

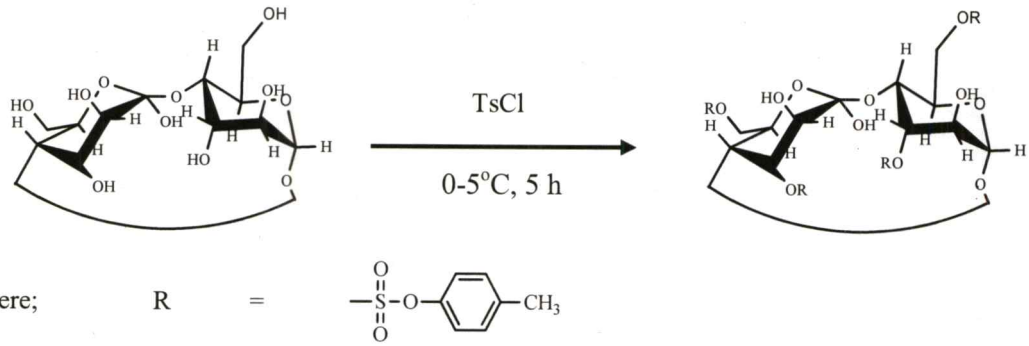

Figure 4.13 Synthetic scheme of TsCD.

4.3.1.1 Solubility results

Solubility of CD, TsCD, and TsOH was determined at a concentration of 1% w/v in various solvents. The results are depicted in Table 4.8.

Table 4.8 Solubility results of CD, TsCD, and TsOH.

Solvent	Polarity [68]	CD	TsCD	TsOH
H_2O	9.0	S	C	S
DMSO	7.2	S	S	S
DMF	6.4	S	PS	S
Acetone	5.1	I	I	S
EtOH	5.2	I	I	S
THF	4.0	I	I	S
i-PrOH	3.9	I	I	S
DCM	3.1	I	I	C

Where; S = Soluble, C = Cloudy, PS = Partial soluble, and I = Insoluble.

From the results, it showed that solubility of TsCD was difference from CD and TsOH. Unlike CD and TsOH, TsCD could well dissolve only in DMSO but it could not completely dissolve in distilled water and DMF because of tosyl group presented in the molecule.

4.3.1.2 FTIR spectra

FTIR spectra of CD and TsCD are depicted in Figure 4.14. The FTIR spectrum of CD showed the absorption band of –OH stretching vibration at 3500-3100 cm^{-1}. The peak at 2927 cm^{-1} corresponded to –CH and $-CH_2$ stretching vibration. The peak involved with hydrate bonds within CD molecules presented at 1647 cm^{-1}. The peak at 1158, 1028, 946 and 890 cm^{-1} corresponded to C-O-C stretching vibration, α-pyranyl vibration, and α-(1,4) glucopyranose in CD, respectively [56, 69]. These similar peaks were also observed in the spectrum of TsCD. Unlike the spectrum of CD, the additional peak due to the presence of tosyl group which corresponded to C=C stretching of aromatic group was found in TsCD spectrum at 1596 cm^{-1} [17]. This indicated that TsCD was successfully prepared. To confirm the results and calculate the degree of tosylation percentage (%DT) of TsCD, ^{1}H-NMR experiment was conducted.

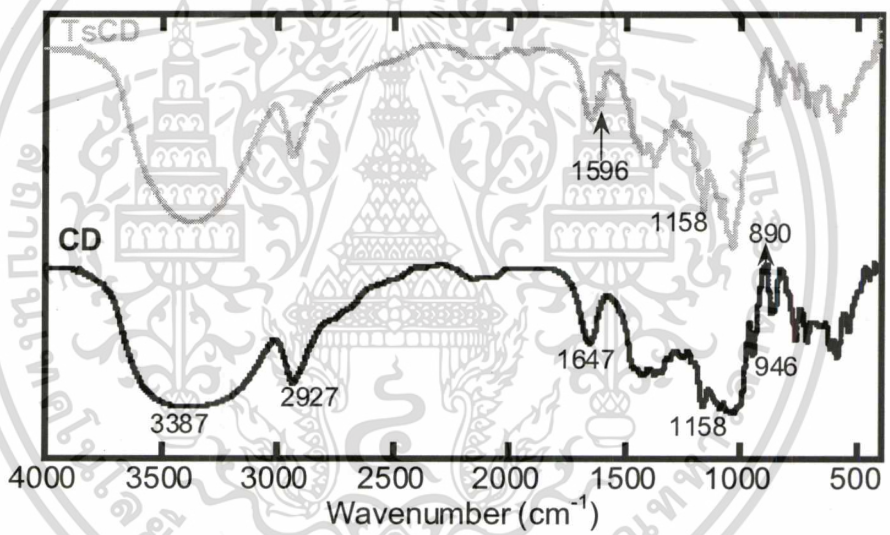

Figure 4.14 FTIR spectra of CD and TsCD.

4.3.1.3 ^{1}H-NMR spectrum

Figure 4.15 shows ^{1}H-NMR spectrum of TsCD in DMSO-d_6. The doublet of doublet signals at δ = 7.72 and 7.40 ppm assigned to aromatic protons of tosyl group, while the signals at δ = 7.50 and 7.10 ppm corresponded to *p*-toluenesulfonic acid (TsOH) as a by-product [70]. The appearance of TsOH in the spectra could be interpreted that the product was not stable and was hydrolyzed to form TsOH. The other signals were presented at δ = 4.85 (H_1), δ = 4.75 ($H_{1'}$), δ = 3.90-3.10 ($H_{2\text{-}6}$, $H_{2'\text{-}6'}$), and δ = 2.30 ppm (H_8) [17]. The %DT calculated from equation 3.3 was 201 (The method for calculating %DT is shown in Appendix B). This could be ascribed to ditosylation in the backbone because of high NaOH concentration usage [17]. Therefore, the tosylation reaction could be taken place at both C-6 and C-3 positions as purposed by S. Onozuka et al. [33].

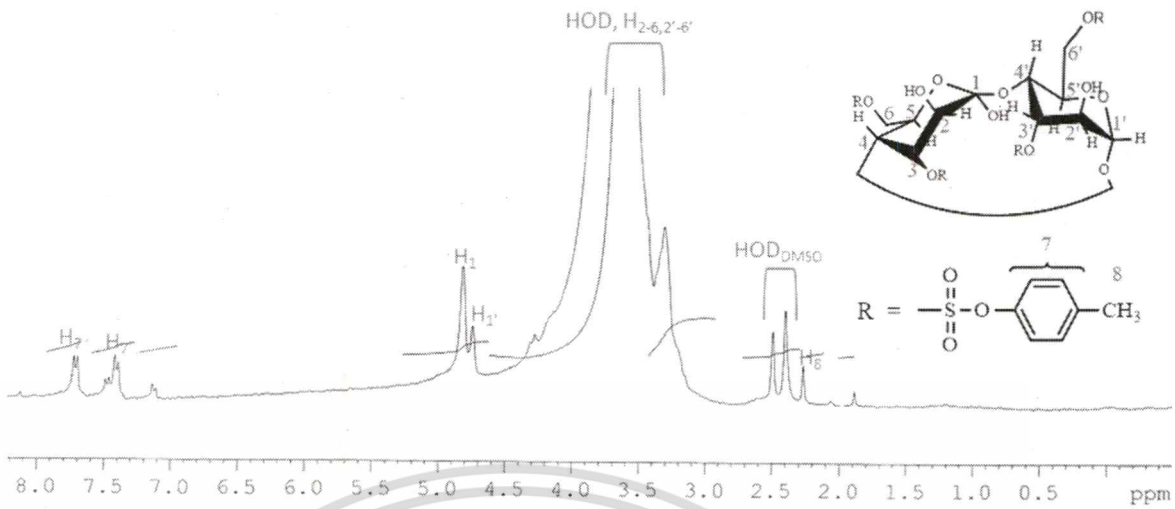

Figure 4.15 ^{1}H-NMR spectrum of TsCD.

From the above results, it could be concluded that ditosylated TsCD was successfully prepared. However, it should be further used instantly after the reaction due to TsOH as a by-product could be generated during storage.

4.3.1.4 UV-Vis spectra

UV-Vis spectra of CD, TsCD and TsOH in distilled water were recorded at a concentration of 0.001% w/v. The UV-Vis spectra are shown in Figure 4.16.

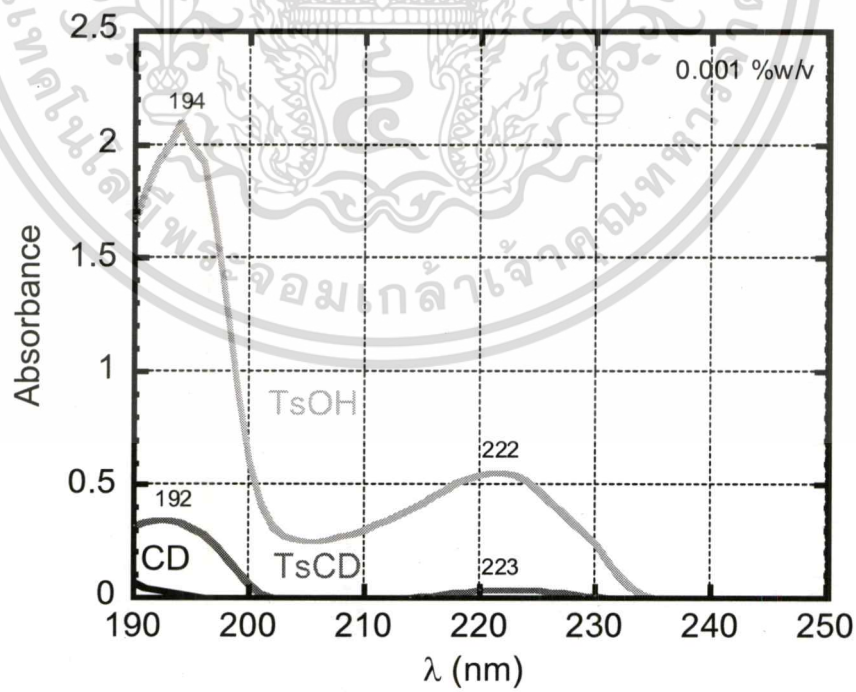

Figure 4.16 UV-Vis spectra of CD, TsCD, and TsOH.

From the spectra, there was no absorption peak found in CD spectrum because the $n \rightarrow \sigma^*$, which is the transition of hydroxyl group, was lower than 190 nm. For TsOH and TsCD spectra, the peak related to primary band found at 194 nm for TsOH and at 192 nm for TsCD and the peak corresponded to secondary band found at 222 nm for TsOH and at 223 nm for TsCD. Generally, the electronic transition of aromatic compounds is $\pi \rightarrow \pi^*$ transition [71]. The same absorbance peaks of TsCD in comparison with TsOH could be described by two reasons. For the first reason, those peaks could be attributed to TsOH which was a by-product from the reaction as discussed in previous section. The second reason was TsCD could undergo hydrolytic process at pH > 6 obtaining free CD and free tosyl group. This phenomenon was related to F. Djedaini-Pilard et al.'s work [72] who reported that TsCD could completely hydrolyze into free tosyl group and free CD when stirring at 35°C for 5 days in D_2O. In addition, the relatively low intensity of TsCD could be ascribed to its low water solubility.

4.3.1.5 Thermal properties

Thermal properties of CD and TsCD were investigated by using Gallenkamp melting point test apparatus and TGA. The results are shown below:

- Melting point test results

Melting point of CD and TsCD was determined using Gallenkamp melting point test apparatus. It showed that CD did not melt at 200°C, which was the highest temperature could be used in the experiment. Unlike CD, as shown in Figure 4.17, it was observed that TsCD changed from white solid to black solid at 140-142°C, which could be ascribed to the degradation of the molecule.

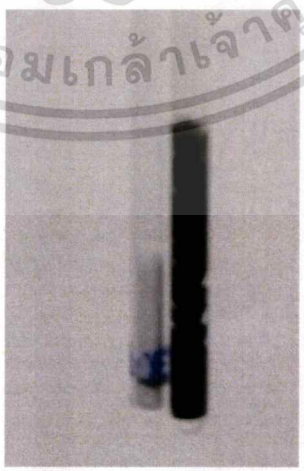

Figure 4.17 TsCD solid before experiment (left) and after experiment (right).

- TGA thermograms

Thermal stability of CD and TsCD was determined by TGA. The dried powder (5 mg) was heated from 30 to 500°C at a heating rate of 10°C/min under nitrogen purse. TGA thermograms of CD and TsCD are shown in Figure 4.18.

The CD thermogram showed three weight loss stages. The first stage, below 100°C, corresponded to the loss of absorbed water and the second stage at a temperature range of 300 – 350°C involved with thermal degradation and the formation of the char. For the third stage, over 400°C, it associated with degradation of the char [73]. For TsCD, the second weight loss stage shifted to lower temperature. This phenomenon could be interpreted that hydrogen bonds in CD molecule were disrupted after reacting with TsCl. The T_{90} and T_{50} of CD and TsCD are summarized in Table 4.9.

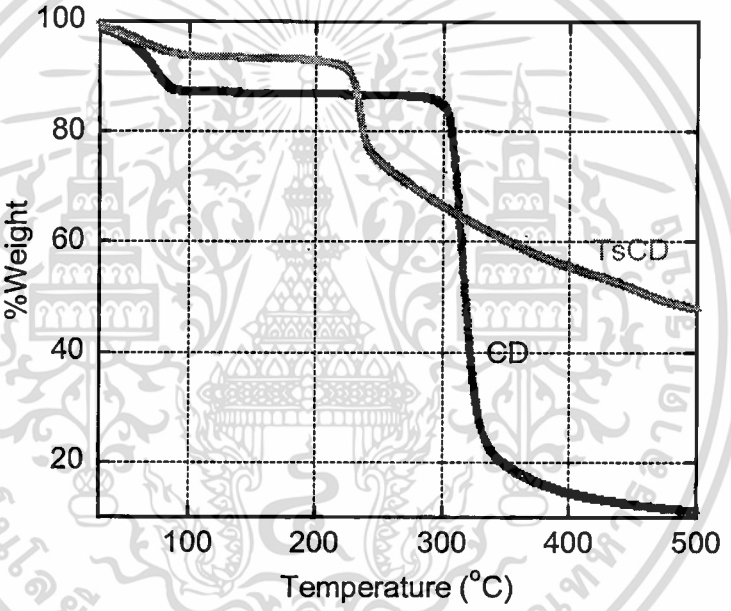

Figure 4.18 TGA thermograms of CD and TsCD.

Table 4.9 The T_{90} and T_{50} of CD and TsCD.

Formula	T_{90} (°C)	T_{50} (°C)
CD	75	315
TsCD	228	467

4.3.2 Properties of HAACSs-g-CDs

The HAACSs-g-CDs were prepared from the reaction between TsCD and HAACSs with varying type of HAACSs and amount of TsCD. The synthetic scheme of HAACSs-g-CDs is shown in Figure 4.19. After the reaction, the products were characterized in terms of their solubility, structure and molecular weight. The results are shown and discussed in details as below:

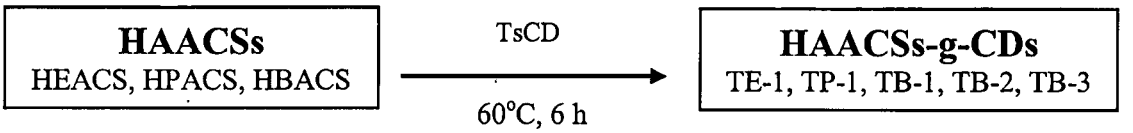

Note : Structures were depicted in Chapter 3.

Figure 4.19 Synthetic scheme of HAACSs-g-CDs.

4.3.2.1 Solubility results

Solubility of HAACSs-g-CDs was determined at 70°C using a concentration of 1% w/v. The solubility results of HAACSs-g-CDs are shown in Table 4.10.

Table 4.10 The solubility results of HAACSs-g-CDs.

Formula	Time used for completely dissolved at 70°C (1%w/v)
TE-1	2 hours
TP-1	50 minutes
TB-1	10 minutes
TB-2	
TB-3	

From the results, it showed that all HAACSs-g-CDs could dissolve in distilled water easier than HAACSs. This could be interpreted that grafting CD onto HAACSs could disrupt the formation of hydrogen bonds. In addition, owing to a number of hydroxyl groups presented in CD, hydrophilicity of HAACSs-g-CDs was changed significantly. Among these HAACSs-g-CDs, all TB series (TB-1, TB-2, and TB-3) could dissolve in distilled water very easily. This could be ascribed to its longest side chain comparing with TE-1 and TP-1.

4.3.2.2 FTIR spectra

FTIR spectra of HAACSs-g-CDs are depicted in Figure 4.20. From the spectra, it could be seen the combination of α-pyranyl stretching vibration from CD and β-pyranyl stretching vibration from HAACSs at 951 and 890 cm^{-1} for TE-1, at 949 and 898 cm^{-1} for TP-1, at 949 and 897 cm^{-1} for TB-1, at 947 and 839 cm^{-1} for TB-2, and at 945 and 862 cm^{-1} for TB-3. In addition, as summarized in Table 4.11, the C=O stretching vibration of these products shifted to lower wavenumbers in comparison with HAACSs spectra, indicating that the C=O stretching vibration was restricted after the formation of inclusion complex [74]. Hence it could

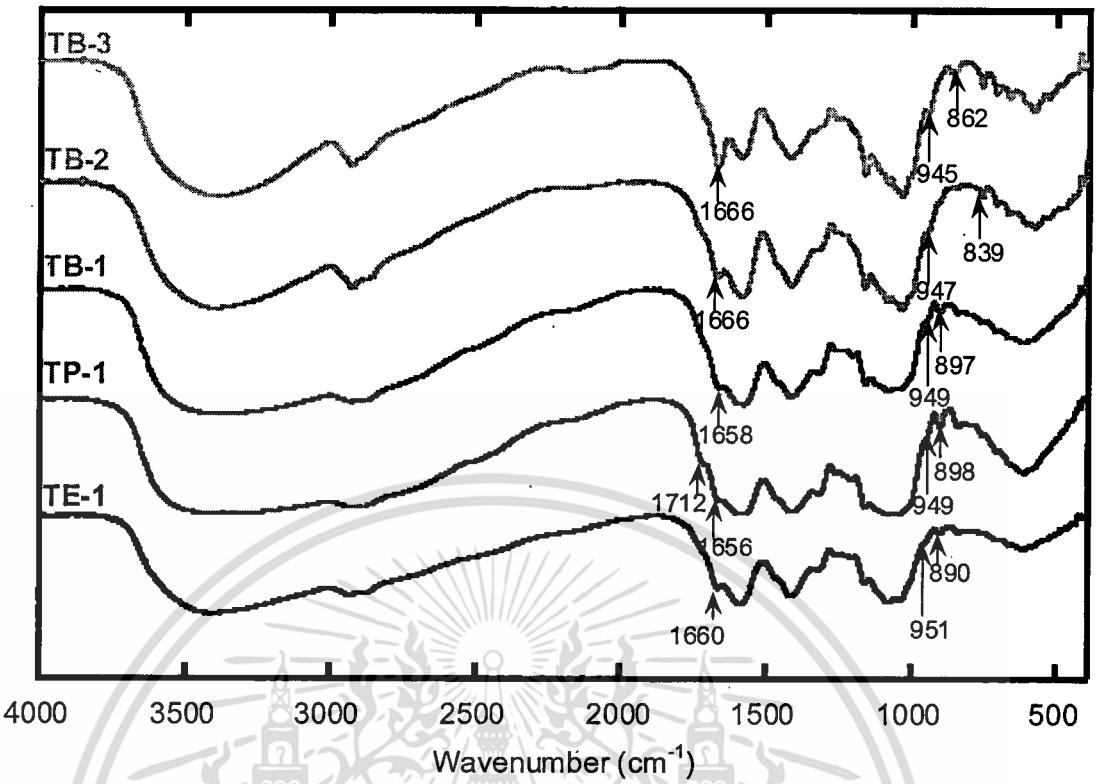

Figure 4.20 FTIR spectra of HAACSs-g-CDs.

be purposed that HAACSs-g-CDs were successfully prepared with the formation of both intra- and inter-molecular inclusion complexes between CD and hydroxyalkylacrylates moieties. The proposed model of self-inclusion complex of the molecules is depicted in Figure 4.21. Interestingly, the C=O stretching vibration peak was found at both 1712 and 1656 cm^{-1} in TP-1 spectrum. This is because the moieties were not fully included within the CD cavities [75]. Previously, it was reported by M. Rebarsky et al. [76] that equilibrium constant (K) of 2-alkanols (i.e., 2-propanol, 2-butanol) was lower than 1-alkanols (i.e., 1-propanol, 1-butanol). Therefore, the 1-alkanol structures (HEA and HBA) are more favorable to form inclusion complex with CD than the 2-alkanol structures (HPA).

Table 4.11 The C=O stretching vibration of HAACSs-g-CDs in comparison with HAACSs.

Formula	HAACSs used	$\nu_{C=O}$ (cm^{-1})	
		HAACSs	HAACSs-g-CDs
TE-1	HEACS	1728	1660
TP-1	HPACS	1724	1712, 1656
TB-1	HBACS	1726	1658
TB-2			1666
TB-3			

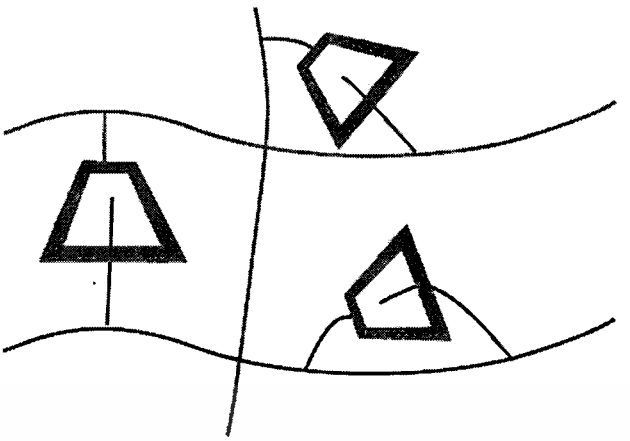

Figure 4.21 The proposed structural model of HAACSs-g-CDs.

Thereafter, structural analysis was further carried out using ^{1}H-NMR spectroscopy in order to confirm the results from FTIR spectra and calculate the degree of substitution percentage (%DS) of HAACSs-g-CDs. The results are shown and discussed in detail in next section.

4.3.2.3 ^{1}H-NMR spectra

Figure 4.22 shows ^{1}H-NMR spectra of HAACSs-g-CDs. It could be seen that all spectra exhibit the doublet of doublet signals of aromatic protons at 7.67 and 7.43 ppm due to tosyl group remained in the products as reported by P. Gonil et al. [17]. This is because TsCD used in the reaction contained more than one tosyl group in the structure as discussed earlier. The signals at 7.55 and 7.22 ppm were assigned to TsOH as a by-product [70]. In addition, the peaks assigned to DMF remained in the products were observed at 7.80, 2.88 and 2.73 ppm [77]. Generally, DMF cannot be removed from the products easily due to its high boiling point (155°C) [78]. The other important signals of each product were reported below:

- **TE-1** : δ = 4.94 (H_{1CD}), δ = 3.85 - 3.40 ($H_{2\text{-}6CD}$, $H_{3\text{-}6HEACS}$, $H_{c\text{-}d}$), δ = 3.10 (H_a), δ = 2.80 ($H_{2,2'}$), δ = 2.35 (H_b), δ = 2.28 (H_9), and δ = 1.94 ppm (H_7).
- **TP-1** : δ = 4.94 (H_{1CD}), δ = 4.45 ($H_{1,1'}$), δ = 3.85 - 3.40 ($H_{2\text{-}6\ CD}$, $H_{3\text{-}6\ HPACS}$, $H_{c\text{-}d}$), δ = 3.10 (H_a), δ = 2.75 ($H_{2,2'}$), δ = 2.37 (H_b), δ = 2.28 (H_9), δ = 1.94 (H_7), and δ = 1.50 ppm (H_e).
- **TB-1** : δ = 4.94 (H_{1CD}), δ = 4.45 ($H_{1,1'}$), δ = 3.85 - 3.40 ($H_{2\text{-}6\ CD}$, $H_{3\text{-}6\ HBACS}$, $H_{c,f}$), δ = 3.25 (H_a), δ = 2.70 ($H_{2,2'}$), δ = 2.34 (H_b), δ = 2.28 (H_9), and δ = 1.94 ppm (H_7).
- **TB-2** : δ = 4.94 (H_{1CD}), δ = 3.90 - 3.40 ($H_{2\text{-}6\ CD}$, $H_{3\text{-}6\ HBACS}$, $H_{c,f}$), δ = 3.10 (H_a), δ = 2.65 ($H_{2,2'}$), δ = 2.32 (H_b), δ = 2.28 (H_9), and δ = 1.94 ppm (H_7).

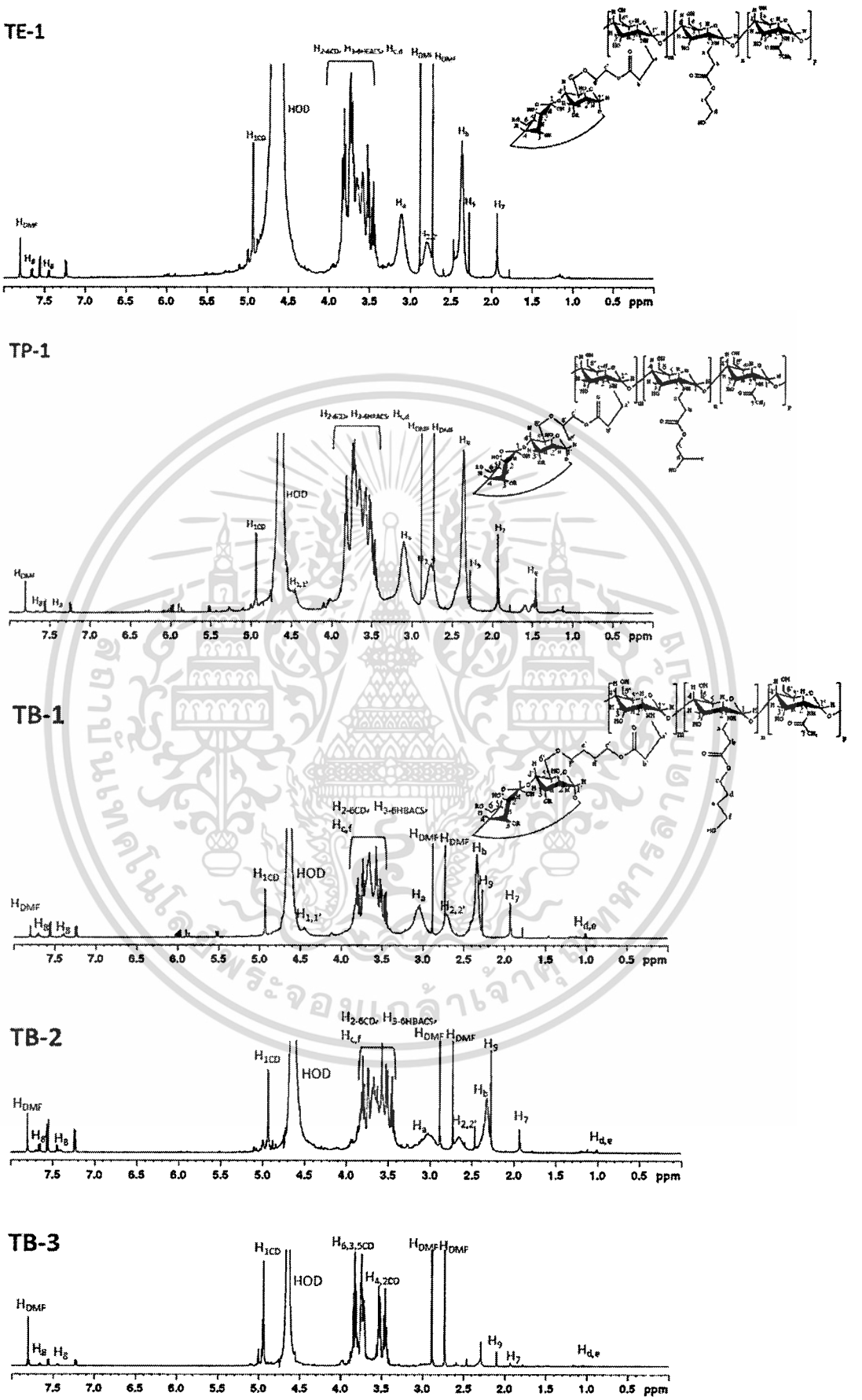

Figure 4.22 ^{1}H-NMR spectra of HAACSs-g-CDs.

- **TB-3** : δ = 4.94 (H_{1CD}), δ = 3.85 - 3.70 ($H_{6,3,5CD}$), δ = 3.55 – 3.40 ($H_{4,2CD}$), δ = 2.28 (H_9), and δ = 1.94 ppm (H_7).

From the above report, it could be suggested that HAACSs-g-CDs were successfully prepared. These results were confirmed FTIR results. However, an evidence about the formation of self-inclusion complex of HAACSs-g-CDs could not be observed from the ^{1}H-NMR spectra.

Additionally, it was interesting to point out that the trace signal of $H_{d,e}$ from HBACS at 1.02 ppm exhibited in TB-1 – TB-3 spectra decreased when increasing amount of TsCD in the reaction. The %DS and average molecular weight per repeating unit of HAACSs-g-CDs are summarized in Table 4.12.

Table 4.12 The %DS and average molecular weight per repeating unit of HAACSs-g-CDs.

Formula	%DS	Average molecular weight per repeating unit
TE-1	12	410
TP-1	3	301
TB-1	4	345
TB-2	10	412
TB-3	Could not be calculated	

* Methods for calculating the %DS and average molecular weight per repeating unit of HAACSs-g-CDs were presented in Appendix B.

4.3.2.4 GPC results

The weight average molecular weight (M_w), number average molecular weight (M_n), and polydispersive index (PDI, M_w/M_n) of HAACSs-g-CDs were determined by GPC using 0.1 M NaCl as an eluent. The results are shown in Table 4.13.

Table 4.13 The M_n, M_w, and PDI of HAACSs-g-CDs.

Formula	M_n	M_w	PDI
TE-1	14,900	49,900	3.34
TP-1	36,800	99,100	2.69
TB-1	24,200	69,200	2.86
TB-2	36,900	94,800	2.57
TB-3	32,800	80,400	2.45

* GPC chromatograms of HAACSs-g-CDs were depicted in Appendix C.

The results indicated that molecular weight of all HAACSs-g-CDs was lower than unmodified chitosan. However, the decrement in molecular weight after the reaction of HAACSs-g-CDs comparing with HAACSs was observed only TE-1, TB-1, and TB-3. This might be due to the competitive effect between chain hydrolysis by heat during the reaction and branching of the CD moieties.

4.4 Characterization and properties of TB-1 film

TB-1 was selected to prepare a solution-casted film. After drying in an oven, the film with average thickness of 117±22 μm was obtained. The appearance of the film is presented in Figure 4.23. Afterwards, the film was characterized by a number of methods as below:

Figure 4.23 The appearance of the TB-1 film.

4.4.1 Light transmittance

Light transmittance curves of the TB-1 film in comparison with the HBACS film are shown in Figure 4.24. It could be seen from the curves that the TB-1 film was more transparent than the HBACS film in visible region (400-700 nm). However, the results could not be discussed in detail because the thickness of the TB-1 film (117±22 μm) was not equal to the HBACS film (130±17 μm).

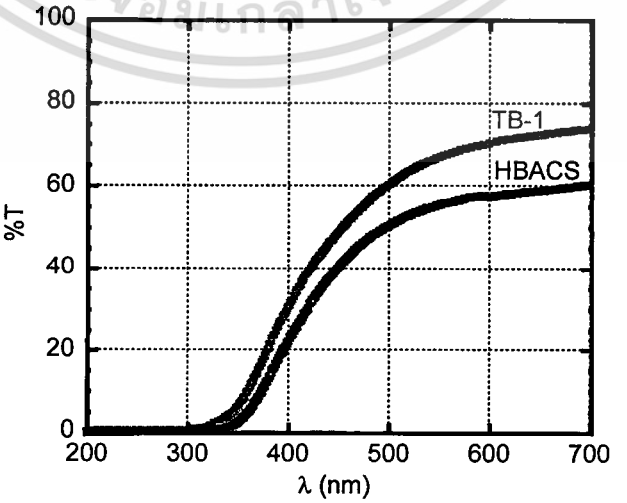

Figure 4.24 Light transmittance curves of TB-1 and HBACS films.

4.4.2 Refractive indexes

Refractive indexes of TB-1 and HBACS films at 589 nm are depicted in Figure 4.25. It showed that refractive index of the TB-1 film was lower than the HBACS film. This phenomenon could be interpreted that grafting CD onto HBACS could increase molar volume of the molecule, resulting in lower refractive index (see equation 4.1).

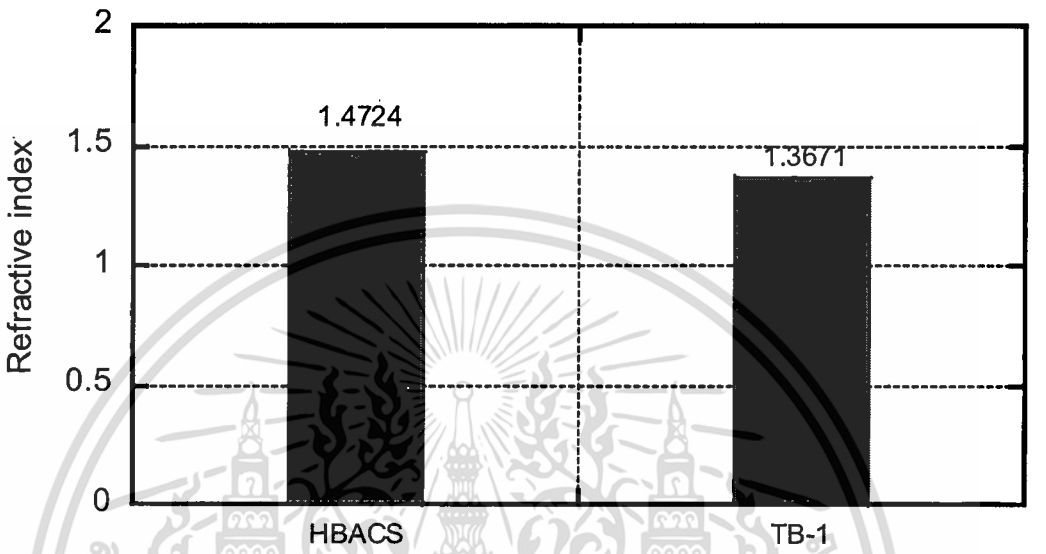

Figure 4.25 Refractive indexes of TB-1 and HBACS films at 589 nm.

4.4.3 WAXS patterns

The WAXS patterns of TB-1 and HBACS films are presented in Figure 4.26. It could be seen that the peak corresponding to crystal form II shifted from $2\theta = 20.7^{\circ}$ in HBACS to $2\theta = 19.0^{\circ}$ in TB-1. This was owing to the increment of *d*-spacing after grafting CD. In addition, the intensity of TB-1 pattern was lower than HBACS pattern, indicating that TB-1 film contained more amorphous region than HBACS film. The peaks corresponded to CD moieties were also observed at $2\theta = 6.04^{\circ}$ and 12.01°. This was slightly different from L. Liu and S. Zhu's work [79] who reported that the peaks of pure CD were observed in the XRD pattern at $2\theta = 12.5^{\circ}$ and 6.2° which is the depth of CD cavity and two times the depth of CD, respectively. However, from P. Gonil et al. work [17], they did not observe any peaks from CD side chains when they carried out the XRD experiment of CD-modified quaternized chitosan.

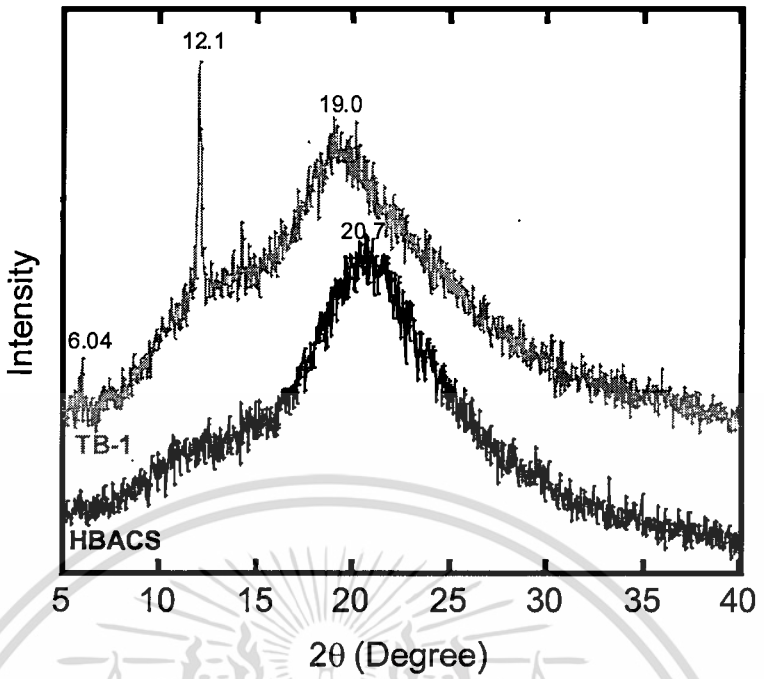

Figure 4.26 WAXS patterns of TB-1 and HBACS films.

4.4.4 TGA thermograms

Thermal behavior of TB-1 film was determined by TGA. Figure 4.27 shows TGA thermograms of TB-1 and HBACS films and Table 4.14 shows T_{90} and T_{50} obtained from the thermograms.

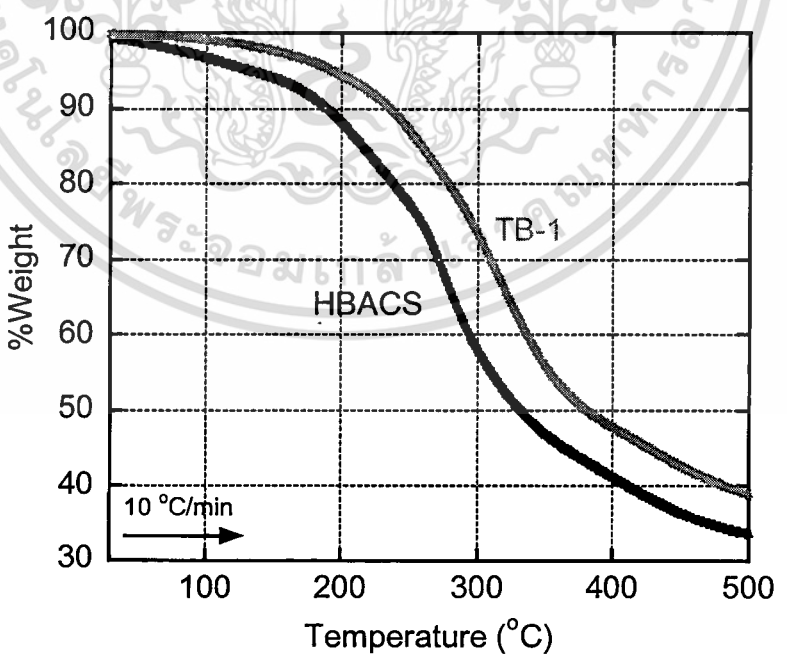

Figure 4.27 TGA thermograms of TB-1 and HBACS.

According to the thermograms, the two weight loss stages owing to dehydration of bound water (ca. 75 to 130°C) and degradation of the molecule (ca. 200 to 400°C) were found. From the results, as depicted in Table 4.14, TB-1 had higher thermal stability than HBACS. This phenomenon could be interpreted by two factors. The first factor involved with the loss of water molecules presented in CD cavities at the temperature above 100°C. These water molecules caused thermal lag in the measurement because they could reduce the actual temperature of the sample. The second factor attributed to the formation of self-inclusion complex in the molecule. It was reported that the thermal stability of inclusion complexes was higher than uncomplexed guest molecules [80].

Table 4.14 The T_{90} and T_{50} of TB-1 and HBACS films.

Formula	T_{90} (°C)	T_{50} (°C)
TB-1	216	359
HBACS	189	332

4.4.5 DMA thermograms

DMA was also used to determine the thermal properties of the TB-1 film. Before measuring, the sample (2x0.5 cm^2) was stored in a humidity controlled chamber (25°C, 50% RH). The percent of water of the film obtained from Karl-Fischer titration was 6.43±0.19, which was lower than HBACS film reported at 10.74±0.25.

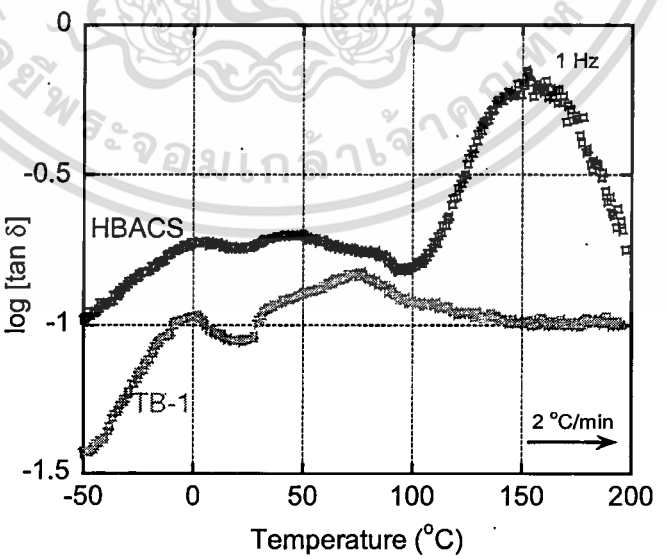

Figure 4.28 Loss tangent (tan δ) versus temperature of TB-1 and HBACS films.

From tan δ curve of TB-1 film, the peaks at 2°C and 77°C due to ice melting and structural reorganization of the molecules involved with an increase of remained water mobility, volume expansion, and change of hydrogen bond strength were observed. However, the peak assigned to water loss and local movement of the TB-1 molecules in the pseudo-stable stage as well as molecular degradation did not exhibit in the thermogram. This phenomenon could be described that the mobility of HBA moieties was restricted in the CD cavities. It was also reported by T. Mori et al. [81] that the tan δ peak of the film prepared from complexation between α-cyclodextrin and poly(ε-caprolactone) was higher than that of the uncomplexed film because only uncomplexed PCL segments could be relaxed in DMA measurement.

4.5 Preparation and properties of inclusion complex solutions

In this work, inclusion complex solutions containing CD or HAACSs-g-CDs (TE-1 and TB-1) as a host and MO as a guest with varying mole ratio were prepared and characterized by using UV-Vis spectroscopy. It was reviewed by M. Rekharsky and Y. Inoue [27] that the equilibrium constant of MO complexed with CD in both neutral and acidic conditions was higher than those of alkanols. Therefore, MO was acted as a competitive guest in this experiment. The UV-Vis spectra of the solutions were shown and discussed in details as below:

4.5.1 UV-Vis spectra of MO and inclusion complex between CD and MO solutions

The UV-Vis spectra of MO in different pH conditions at a concentration of 0.001% w/v are depicted in Figure 4.29. As can be seen from the spectra, the band attributed to the conjugated structure constructed via azo bond [82] was observed at 506 nm for pH 1, 497 nm for pH 4, and at 463 nm for pH 6 and pH 10. The variation in λ_{max} could be explained that MO can change to acid-stable form when pH below 3.2 and basic-stable form when pH above 4.4 (See Figure 2.33) [57].

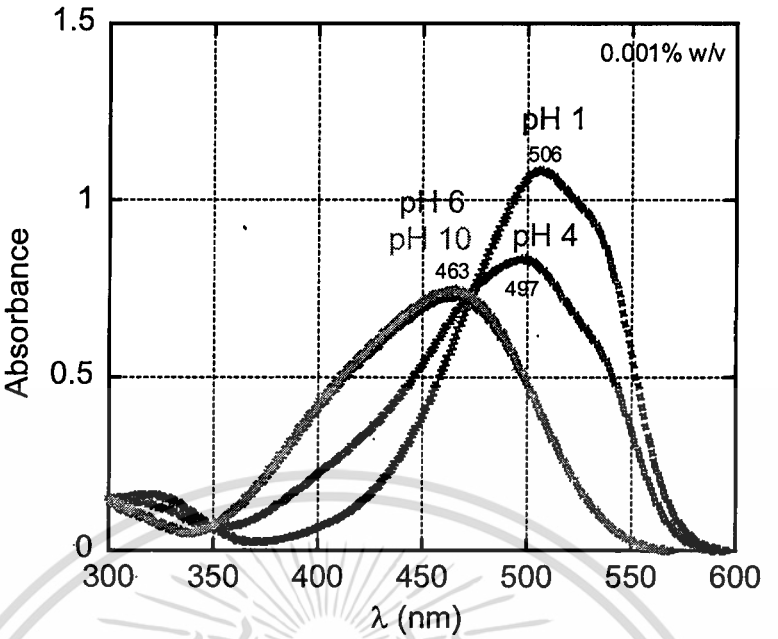

Figure 4.29 UV-Vis spectra of MO in different pH conditions.

Thereafter, the inclusion complex solutions containing an equimolar amount of CD and MO (CDMO-1) at different pH conditions were prepared to investigate the change of λ_{max} in UV-Vis spectra in comparison with pure MO solutions. From the spectra depicted in Figure 4.30, the hypsochromic shift (blue shift) of CDMO-1 solution (λ_{max} = 486 nm) comparing with MO solution (λ_{max} = 497 nm) was observed at pH 4. This could be ascribed to the depression of the acid-stable form and prominence of the basic-stable form when CD was added. However, it could not see any changes of λ_{max} in other pH conditions. Generally, CD can form inclusion complex with MO in various pH conditions, but the equilibrium constant indicating ability on forming inclusion complex of the 1:1 complex in acidic condition (pH 1) was lower than the complex in neutral condition [83].

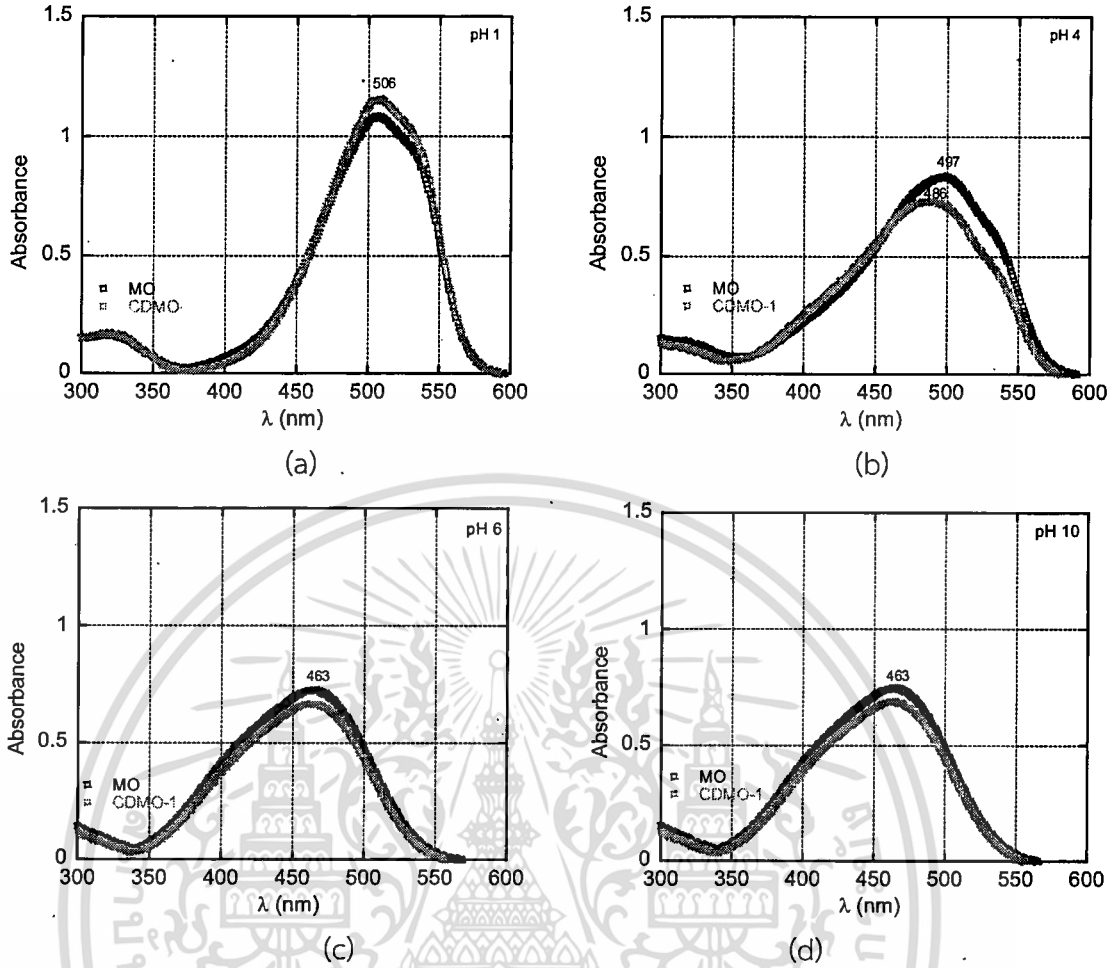

Figure 4.30 UV-Vis spectra of MO and CDMO-1 solutions at pH 1 (a), pH 4 (b), pH 6 (c) and at pH 10 (d).

The effect of MO content on the shift of λ_{max} was studied at pH 6. The formulae of inclusion complex solutions with varying amounts of CD are depicted in Table 3.4. From the UV-Vis spectra shown in Figure 4.31, the blue shift was observed when excess amount of CD was added into MO solution (CDMO-2, and CDMO-3). The λ_{max} shifted from 463 nm (CDMO-1) to 457 (CDMO-2) and 452 nm (CDMO-3). This phenomenon could be ascribed to the presence of the complexes at the stoichiometric ratio (CD:MO) of both 1:1 and 2:1 in the solutions [83].

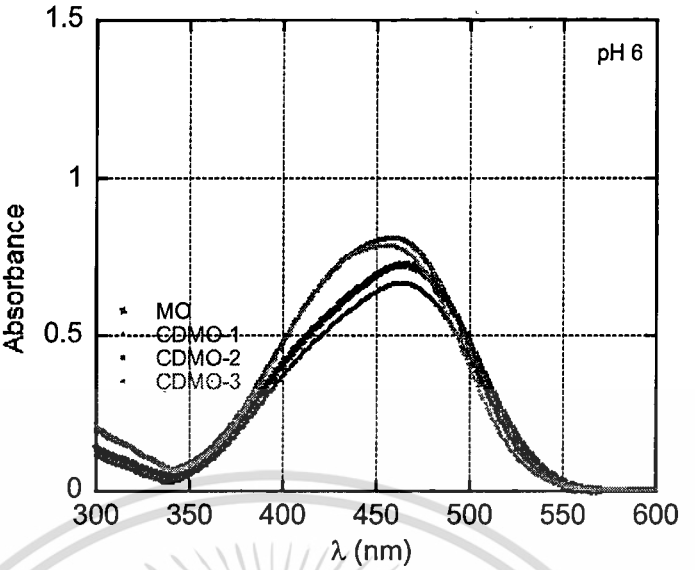

Figure 4.31 UV-Vis spectra of CDMO solutions with difference amounts of CD.

4.5.2 UV-Vis spectra of inclusion complex between HAACSs-g-CDs (TE-1 and TB-1) and MO solutions

The inclusion complex solutions containing host polymers (TE-1 and TB-1) and MO with varying mole ratio were prepared at pH 6 and 4. The formulae of the solutions are depicted in Table 3.5-3.6. The UV-Vis spectra of the solutions are shown and discussed in details as below:

Figures 4.32 and 4.33 show UV-Vis spectra of TE-1MO and TB-1MO solutions with varying mole ratio at pH 6, respectively. From the spectra, the dominant hypsochromic shift (λ_{max} shifted to lower wavelength more than 5 nm) from pure MO solution at 463 nm (Fig. 4.29) was observed at series A for both TE-1MO and TB-1MO. This could be attributed to high amount of CD moieties in comparison with MO leading to the formation of both 1:1 and 2:1 complexes as previous discussion. However, the significant blue shift of λ_{max} was not observed at series B, which contained relatively less amount of CD moieties in comparison with series A, because the CD moieties and MO molecules could not in contact easily [1]. Therefore, it could be suggested that TB-1 and TE-1 could form inclusion complex with MO at pH 6. Nonetheless, the concentration between MO and the host polymers should be considered.

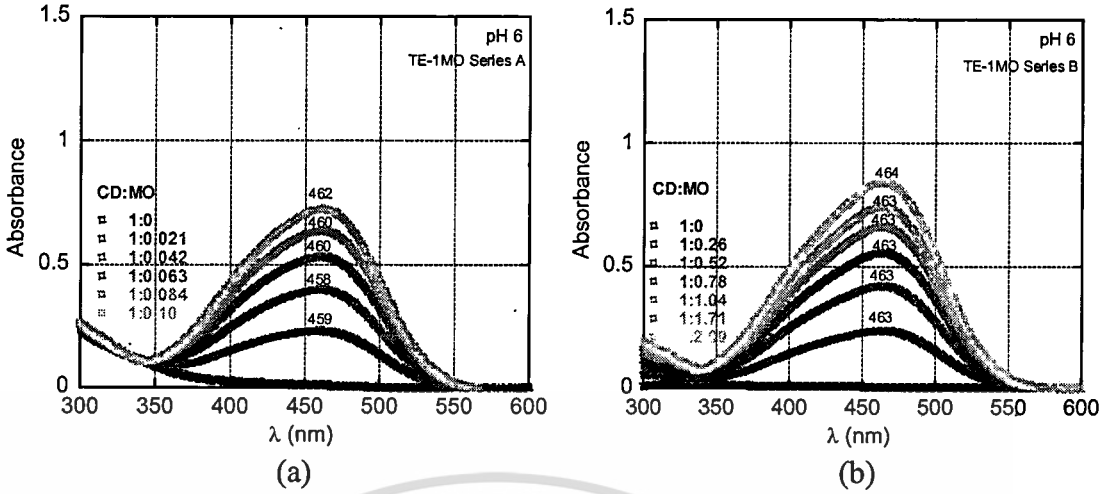

Figure 4.32 UV-Vis spectra of TE-1MO series A (a) and TE-1MO series B (b) at pH 6.

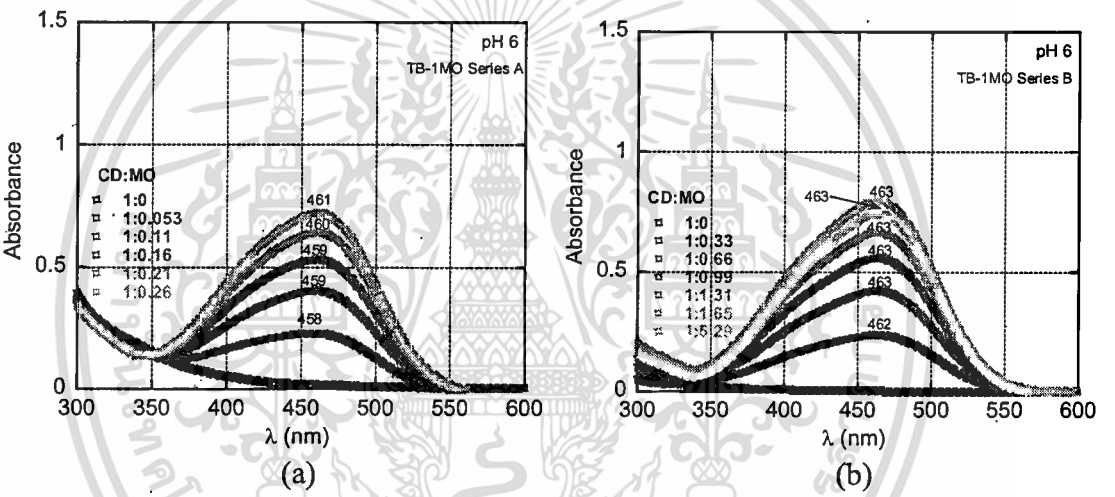

Figure 4.33 UV-Vis spectra of TB-1MO series A (a) and TB-1MO series B (b) at pH 6.

UV-Vis spectra of TE-1MO and TB-1MO solutions with varying mole ratio at pH 4 are depicted in Figure 4.34 and 4.35, respectively. From the spectra of TE-1MO and TB-1MO solutions, the significant blue shift of λ_{max} indicated the formation of inclusion complex, leading to the depressant of acid-stable form of MO from its based value at 497 nm was observed at both series A and B. However, the dominant hypsochromic shift could not be observed at the mole ratio between CD and MO of 1:2.09 (TE-1MO) and 1:5.29 (TB-1MO). As discussed above, no any shifts exhibited when the concentration of the host polymers was totally low in comparison with the guest because they could not contact to form the complex easily. Hence, it could be suggested that TB-1 and TE-1 could be able to form inclusion complex with MO at pH 4 as same as at pH 6.

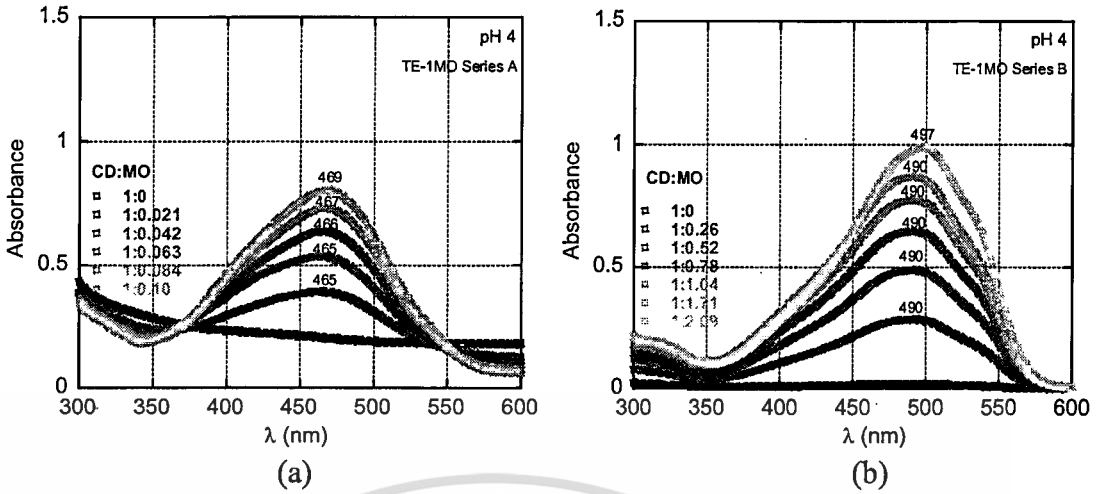

Figure 4.34 UV-Vis spectra of TE-1MO series A (a) and TE-1MO series B (b) at pH 4.

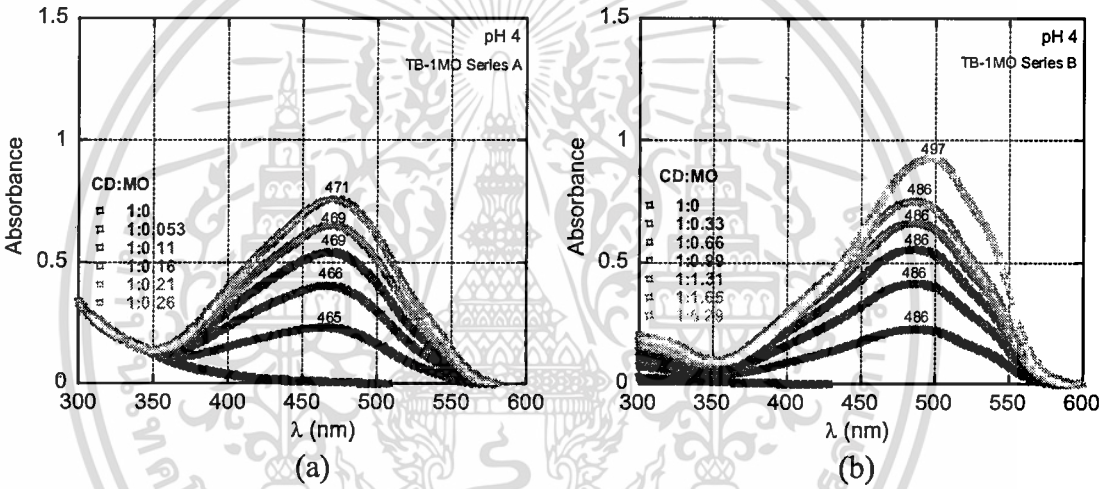

Figure 4.35 UV-Vis spectra of TB-1MO series A (a) and TB-1MO series B (b) at pH 4.

From the above results, it could be concluded that TE-1 and TB-1 as host polymers could form inclusion complex with MO as same manner as CD at both pH 6 and 4 due to the presence of blue shift as discussed earlier.

4.6 Characterization and properties of MO-incorporated TB-1 films

From previous section, the UV-Vis spectra showed that TE-1 and TB-1 could form inclusion complex with MO at both pH 4 and 6. Therefore, to study effect of MO as a competitive guest on film properties, solution-casted films from TB-1 with different amounts of MO were fabricated at pH 6. The formulae of MO-incorporated TB-1 films are summarized in Table 3.7. The appearance and average thickness of the films are depicted in Figure 4.36 and Table 4.15, respectively.

TB-1MO0.01 TB-1MO0.04 TB-1MO0.1

Figure 4.36 The appearance of MO-incorporated TB-1 films.

Table 4.15 The average thickness of MO-incorporated TB-1 films.

Formula	Average thickness (μm)
TB-1MO0.01	121±21
TB-1MO0.04	130±26
TB-1MO0.1	193±16

4.6.1 Light transmittance

Figure 4.37 shows the light transmittance curves of the films at wavelengths of 200-700 nm. From the curves, unlike the TB-1 film, it could be seen that transparency of the films was significantly declined when increasing amount of MO in the films. However, it should be considered that the thickness also plays a role of controlling light transparency of the films. Therefore, it could be suggested that the decrement of light transmittance in visible region (400-700 nm) of the films involved with methyl orange added and the increment in thickness in comparison with the TB-1 film reported at 117±22 μm.

In addition, it could be seen from the curves that the films could absorb entire energy at the wavelengths below 500 nm for TB-1MO0.01 film, 520 nm for TB-1MO0.04 film, and 528 nm for TB-1MO0.1 film.

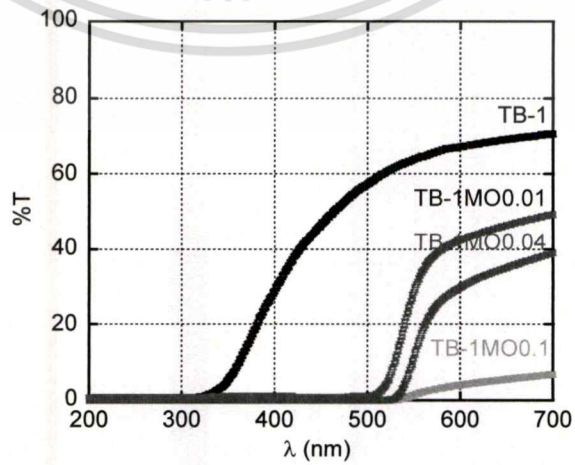

Figure 4.37 Light transmittance curves of TB-1 and MO-incorporated TB-1 films.

4.6.2 Refractive indexes

Figure 4.38 shows refractive indexes of TB-1 and MO-incorporated TB-1 films at 589 nm. From the graph, it shows that the refractive indexes of MO-incorporated TB-1 films were dominantly higher than TB-1 film. However, the significant difference in refractive index of each MO-incorporated TB-1 film was not observed. According to the light transmittance curves of TB-1 and MO-incorporated TB-1 films (Figure 4.37), the percent of transmittance (%T) of the films reduced when increasing amount of MO. Therefore, the relationship between %T and refractive index could be explained by equation 4.2 [84].

$$s = \frac{1}{T_s} + \sqrt{\left(\frac{1}{T_s^2} - 1\right)} \qquad (4.2)$$

Where s is the refractive index and T_s is the light transmission. Consequently, refractive index increases when light transmission of materials decreased.

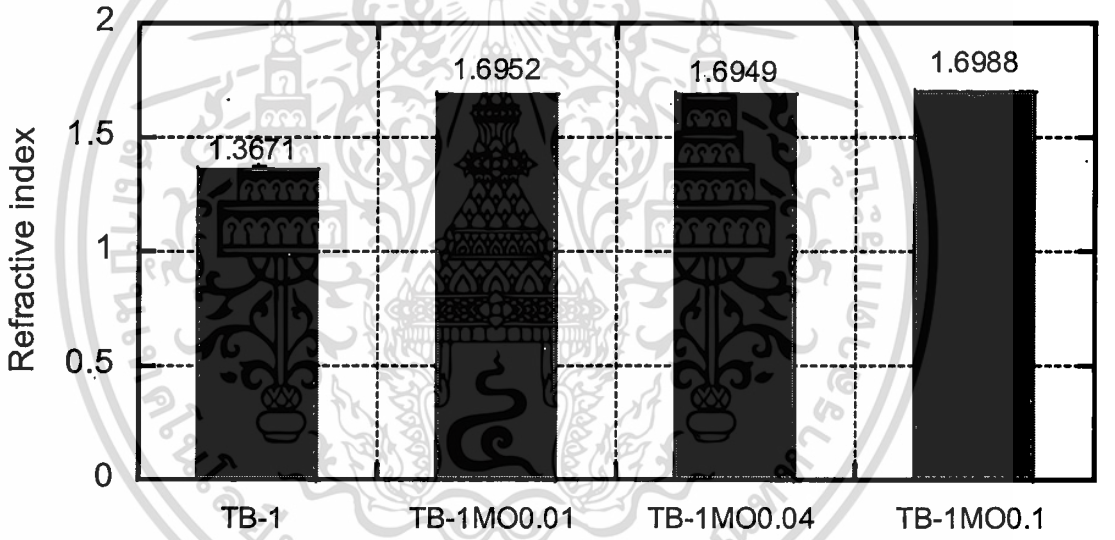

Figure 4.38 Refractive indexes of TB-1 and MO-incorporated TB-1 films at 589 nm.

4.6.3 FTIR spectra

Figure 4.39 shows FTIR spectra of MO and TB-1 powder, and MO-incorporated TB-1 films. From the FTIR spectrum of MO powder, the band at 2898 cm^{-1} assigned to –CH stretching vibration. The –N=N- stretching vibration of azo group was observed at 1607 cm^{-1}. The peaks at 1190 and 623 cm^{-1} corresponded to S=O stretching vibration, while the peak at 1037 cm^{-1} assigned to C-N stretching vibration. In addition, the C-O stretching vibration was found at 1119 cm^{-1} [85]. The FTIR spectra of the inclusion complex films were similar to TB-1 powder, due to low quantity of MO in the films. However, the variations of C=O stretching vibration were observed. The C=O stretching vibration observed in the spectrum of TB-1 powder at

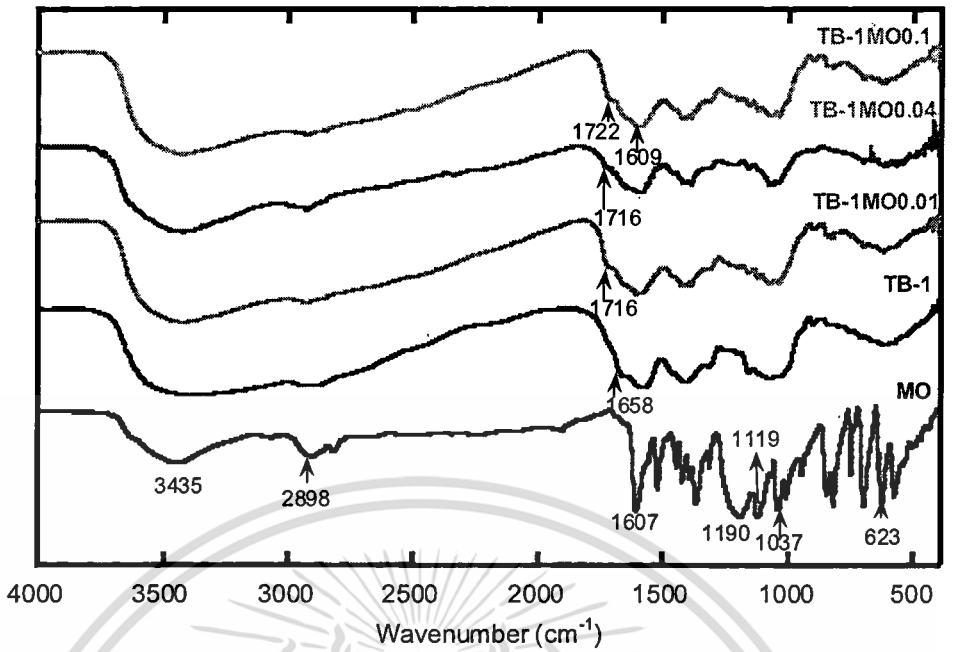

Figure 4.39 FTIR spectra of MO powder, TB-1 powder, and MO-incorporated TB-1 films.

1658 cm^{-1} shifted to higher wavenumbers at 1716 cm^{-1} for TB-1MO0.01 and TB-1MO0.04 films, and at 1722 cm^{-1} for TB-1MO0.1 film. According to Figure 4.2, the C=O stretching vibration of HBA moieties was observed at 1726 cm^{-1}. Therefore, from the above results, it could be suggested that C=O stretching vibration of HBA moieties would not restricted in CD cavities as TB-1 powder when MO acting as a competitive guest was added. This competitive guest could replace HBA moieties in CD cavities, leading to the shift of C=O stretching vibration to higher wavenumbers comparing with TB-1. This phenomenon could be ascribed to high equilibrium constant between MO and CD in comparison with those of alkanols [27]. The reaction scheme of the formation of inclusion complex between TB-1 and MO is illustrated in Figure 4.40.

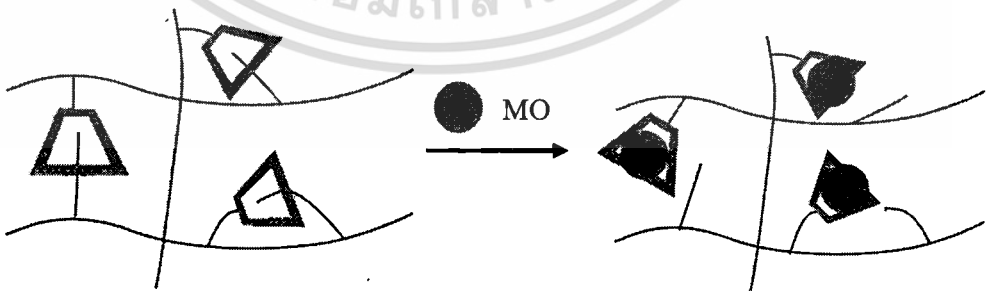

Figure 4.40 The reaction scheme of MO-incorporated TB-1.

4.6.4 WAXS patterns

WAXS patterns of TB-1 and TB-1MO0.01 films are shown in Figure 4.41. In WAXS pattern of TB-1 film, the peaks were observed at $2\theta = 6.04^{\circ}$, 12.1° and 19.0°. It

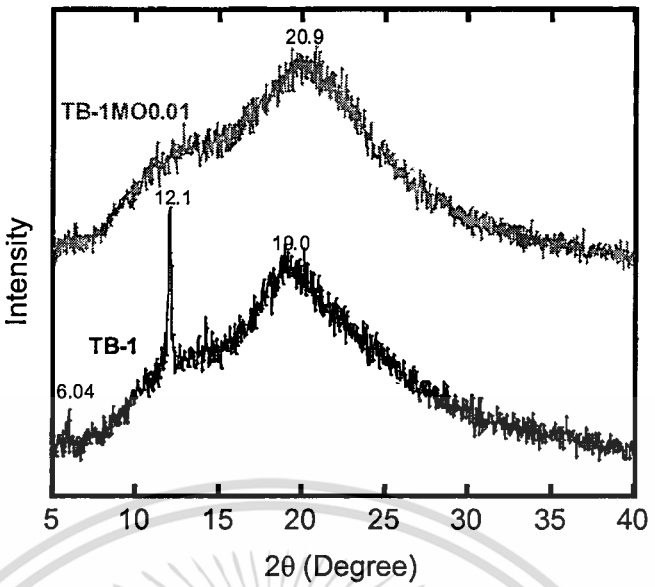

Figure 4.41 WAXS patterns of TB-1 and TB-1MO0.01 films.

was earlier mentioned that the peaks at $2\theta = 6.04^{\circ}$ and 12.1° were assigned to CD. However, as shown in the WAXS pattern of TB-1MO0.01 film, the peaks involved with CD were disappeared and the peak was exhibited only at $2\theta = 20.9^{\circ}$. Such changes of the WAXS pattern suggested the formation of inclusion complex between CD moieties in TB-1 molecules and MO molecules [86].

4.6.5 TGA thermograms

Thermal behavior of MO-incorporated TB-1 films was also studied using TGA. The thermograms of the films are depicted in Figure 4.42. The T_{90} and T_{50} of the films are summarized in Table 4.16.

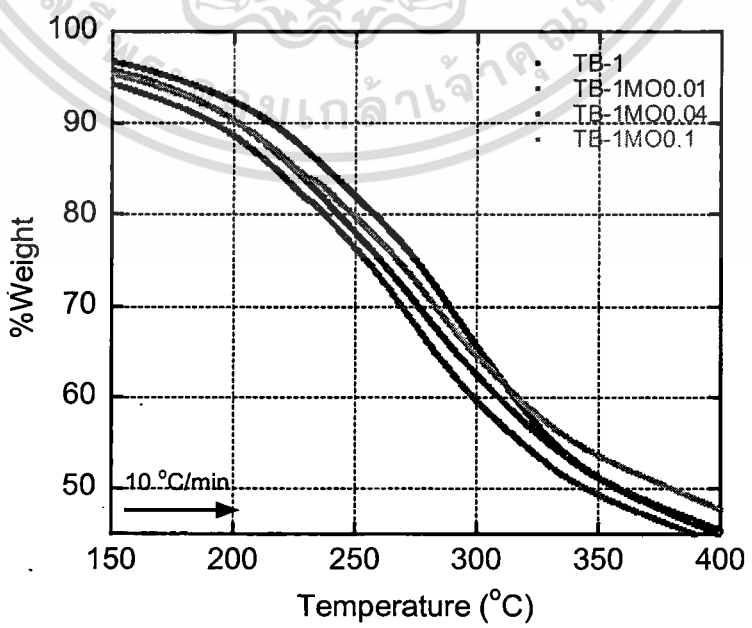

Figure 4.42 TGA thermograms of TB-1 and MO-incorporated TB-1 films.

Table 4.16 The T_{90} and T_{50} of TB-1 and MO-incorporated TB-1 films.

Formula	T_{90} (°C)	T_{50} (°C)
TB-1	216	359
TB-1MO0.01	202	358
TB-1MO0.04	193	346
TB-1MO0.1	203	381

From Figure 4.42 and Table 4.16, it could be seen that T_{90} of all inclusion complex films was higher than TB-1 film. This could be attributed to the substitution of MO molecules in CD cavities as discussed earlier. In addition, it was found that the T_{90} of TB-1MO0.1film was higher than both TB-1MO0.01 and TB-1MO0.04 films. In terms of TB-1MO0.1 film, its relatively high T_{90} and T_{50} comparing with TB-1MO0.01 and TB-1MO0.04 films could be owing to free MO molecules remained in the film. According to TGA thermogram of MO depicted in Appendix F, it was observed that T_{90} of MO was 346°C, which was higher than TB-1 film at 216°C. Therefore, the free MO molecules could play an important role to increase T_{90} and T_{50} of the film. For TB-1MO0.01 film, it was observed that the T_{90} and T_{50} were lower than TB-1MO0.1 film, but they were still higher than those of TB-1MO0.04 film. This phenomenon could be interpreted that self-inclusion molecules were still remain due to the mole of MO added was lower than the mole of CD moieties. As mentioned in Section 4.4.4, the occurrence of self-inclusion complex could improve thermal stability of molecules. Lastly, for TB-1MO0.04 film, it was observed that the T_{90} and T_{50} of the film were lower than TB-1MO0.01 and TB-1MO0.1 films. However, the T_{90} and T_{50} of the film were still higher than HBACS film observed at 189 and 332°C, respectively. This could be interpreted that self-inclusion molecules were still exhibited even adding equimolar amount of MO in the solutions.

4.6.6 DMA thermograms

DMA was also used to study thermal properties of MO-incorporated TB-1 films. The samples were stored in a humidity controlled chamber (25°C, 50% RH) before the experiment. The percent of water in the films determined by Karl-Fischer titration is shown in Table 4.17.

Table 4.17 Percent of water in MO-incorporated TB-1 films.

Formula	%Water
TB-1MO0.01	10.00±0.91
TB-1MO0.04	7.00±0.19
TB-1MO0.1	6.44±0.50

Figures 4.43 and 4.44 show DMA thermograms of TB-1 and MO-incorporated TB-1 films. From Figure 4.43, the significant drop in storage modulus assigned to ice melting was observed at 14°C for TB-1MO0.01 film and at 12°C for TB-1MO0.04 film. The slightly drop in storage modulus assigned to ice melting was also observed in TB-1MO0.1 film at 17°C. According to the tan δ curves illustrated in Figure 4.44, the main peak corresponded to water loss and local movement of the molecules in the pseudo-stable stage as well as molecular degradation of inclusion complex films was found. From the tan δ curve of TB-1 film, unlike the inclusion complex films, the main peak could not be observed because the mobility of HBA moieties was restricted in the CD cavities. Therefore, it could be suggested that MO as a competitive guest could substitute HBA moieties in CD cavities, leading to the re-appearance of the main peak because HBA moieties could be able to move after MO was added. This results confirmed FTIR and TGA results.

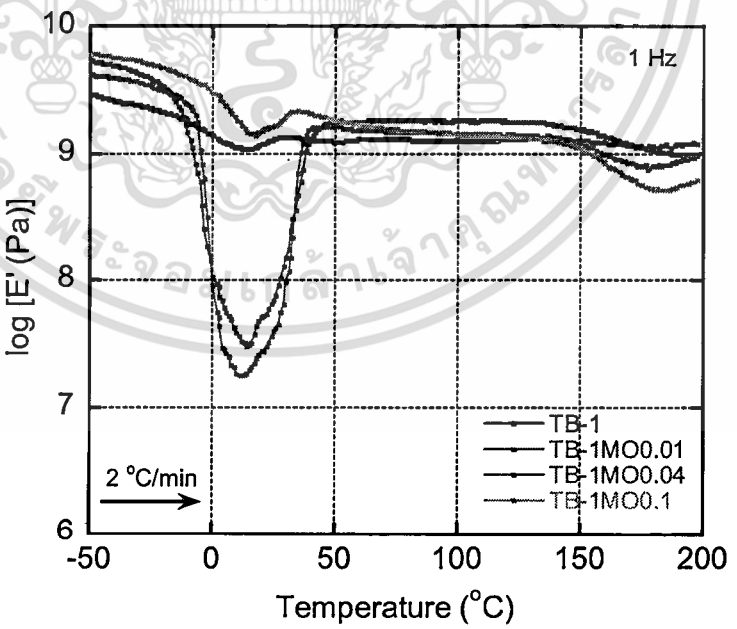

Figure 4.43 Storage modulus (E') versus temperature of TB-1 and MO-incorporated TB-1 films.

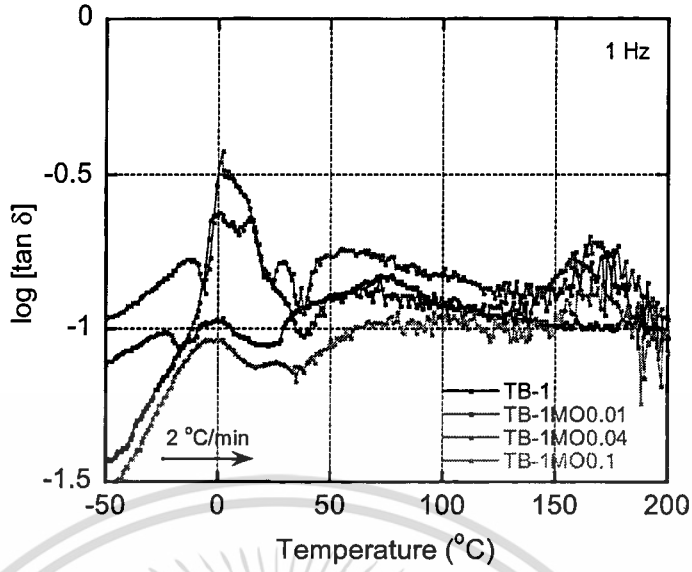

Figure 4.44 Loss tangent (tan δ) versus temperature of TB-1 and MO-incorporated TB-1 films.

The effect of a competitive guest on the properties of the materials has been reported by several works. One of those works is Y. Jia and X. Zhu.'s work [87]. They prepared Poly(*N,N'*-dimethylacrylamide) containing cholic acid ((P(DMA-CAM)) and CD pendents (P(DMA-CMA)). After that, those polymers were mixed altogether to prepare a supramolecular hydrogel. To investigate effect of a competitive guest, potassium 1-adamantylcarboxylate which has a much higher equilibrium constant toward CD than cholic acid was added to the hydrogel. The results showed that viscosity of the hydrogel dramatically decreased, and viscous sol was obtained. Therefore, the supramolecular networks could be dissociated when a competitive guest, which has higher equilibrium constant than the former was added.

Therefore, from all above discussions, it could be concluded that properties of TB-1 film could be affected by the addition of MO acting as a competitive guest.

Chapter 5
Conclusions and Suggestions

5.1 Conclusions

This research studied on inclusion complex solutions and films of β-cyclodextrin modified hydroxyalkylacrylchitosans (HAACSs-g-CDs) and methyl orange (MO). Properties of the reactants i.e., hydroxyalkylacrylchitosans (HAACSs), tosyl-modified β-cyclodextrin (TsCD), and HAACSs-g-CDs were investigated in terms of their solubility, molecular weight, and structure. Inclusion complex solutions from HAACSs-g-CD and MO were prepared and characterized by UV-Vis spectroscopy. The solution-casted films of CS, HAACSs, β-cyclodextrin-modified hydroxybutylacrylchitosan (TB-1), and inclusion complex between TB-1 and different amounts of MO were characterized and tested by UV-Vis, Abbe refractometer, WAXS, TGA, and DMA. In addition, the structural results of the inclusion complex films were obtained by FTIR. All results were summarized as below:

Synthesis and characterization of HAACSs

HAACSs (i.e., hydroxyethylacrylchitosan (HEACS), hydroxypropylacrylchitosan (HPACS), and hydroxybutylacrylchitosan (HBACS)) were prepared via Michael addition reaction between different hydroxyalkylacrylates and chitosan (CS). The solubility test showed that all HAACSs could dissolve in distilled water at 70°C. Among these HAACSs, HBACS used the least time to dissolve in distilled water (1 day). The FTIR spectra of HAACSs showed the additional peaks from C=O stretching and asymmetric and symmetric stretching of COO^- of hydroxyalkylacrylates pendants. Additional signals from hydroxyalkylacrylates moieties were observed in ^{1}H-NMR spectra of HAACSs. Lastly, data obtained from GPC chromatograms showed that the molecular weight of all HAACSs was lower than pristine chitosan.

Therefore, HAACSs were successfully prepared. For HBACS, it was the most suitable candidate for using in further reaction.

Characterization and properties of HAACSs films

Solution-casted films from CS and HAACSs were fabricated. In terms of photo properties, data obtained from light transmittance curves suggested that all films were transparent in visible region (400-700 nm). The WAXS pattern of CS film showed the peaks at 2θ = 12.4° and 21.1°, while the WAXS patterns of HEACS, HPACS and HBACS films showed the peaks at 2θ = 20.8, 20.6° and 20.7°, respectively. The TGA thermograms of all films showed two weight loss stages corresponded to the loss of

bound water and molecular degradation. From the thermograms, the T_{90} and T_{50} of HBACS was lower than HPACS and HEACS. However, the T_{90} and T_{50} of HAACSs and CS could not be compared because solvent used for preparing the films was different. In addition to tan δ curves obtained from DMA thermograms of HAACSs films, the main peak temperature involved with the combination of the reorganization of molecules due to water loss and the local movement of the molecules in the pseudo-stable stage as well as molecular degradation of HBACS was detected at 153°C, which was lower than HEACS (178°C) and HPACS (155°C). The DMA experiments of HBACS films with varying storing conditions (dry and 50%RH) were also performed. The tan δ curves showed that the main peak temperature of HBACS film (dry) and HBACS film (50% RH) was not different.

Synthesis and characterization of host polymers

HAACSs-g-CDs as host polymers were prepared by nucleophilic addition between TsCD and HAACSs with varying types of HAACSs and amounts of TsCD. In terms of TsCD, it was prepared by reaction between β-cyclodextrin (CD) and TsCl. The results were summarized as follow:

-TsCD

The solubility results revealed that TsCD could dissolve in DMSO, partial dissolve in DMF, and cloudy in H_2O, which difference from CD and TsOH. The FTIR spectrum of TsCD showed the additional peak of C=C stretching vibration from tosyl group at 1596 cm^{-1}. This suggested that TsCD was successfully prepared. Data obtained from the ^{1}H-NMR spectrum showed that the degree of tosylation percentage (%DT) of TsCD was 201, indicating that ditosylation product was obtained. The UV-Vis spectra showed that the bands related to the transition of aromatic compounds of TsOH and TsCD were observed at the same wavelength. In terms of thermal properties, the results obtained from Gallenkamp melting point test apparatus showed that the appearance of TsCD was changed from white to black solid at 140-142°C, while the appearance of CD was not changed even heating to 200°C. The TGA thermograms of CD and TsCD showed three weight loss stages: loss of absorbed water, thermal degradation of the molecule and the formation of the char, and the degradation of the char. In addition to the thermograms, it showed that the second weight loss stage temperature of TsCD was lower than CD.

-HAACSs-g-CDs

The solubility results showed that the time used for dissolving HAACSs-g-CDs in distilled water at 70°C was less than HAACSs. For β-cyclodextrin-modified

hydroxybutylacrylchitosans (TB-1, TB-2, and TB-3), it used only 10 min to dissolve in the medium. The FTIR spectra of HAACSs-g-CDs showed the combination of α-pyranyl stretching vibration from CD and β-pyranyl stretching vibration from HAACSs. In addition, the shift of C=O stretching vibration was observed, indicating that the self-inclusion complex was formed. The ^{1}H-NMR spectra of HAACSs-g-CDs showed the additional signals from CD moieties and tosyl groups.

Consequently, the HAACSs-g-CDs were successfully prepared. It was suggested that TB-1 was the interesting candidate for using in further step.

Characterization and properties of TB-1 film

The TB-1 film was prepared using solution casting method. The light transmittance curve showed that TB-1 film was more transparent than HBACS film. Data obtained from Abbe refractometer showed that the refractive index of TB-1 film was lower than HBACS film. From WAXS analysis of TB-1 film, the additional peaks corresponded to CD moieties were observed at $2\theta = 6.04^{\circ}$ and 12.1°. In addition, it was observed from the WAXS pattern that the peak involved with crystal form II structure was shifted from $2\theta = 20.7^{\circ}$ exhibited in the WAXS pattern of HBACS film to $2\theta = 19.0^{\circ}$. Data obtained from the TGA thermogram indicated that the thermal stability of TB-1 film was higher than HBACS film. In addition to the tan δ curve of TB-1 film, the main peak temperature related to the combination of the reorganization of molecules due to water loss and the local movement of the molecules in the pseudo-stable stage as well as molecular degradation was not observed.

Preparation and properties of inclusion complex solutions

Inclusion complex solutions between MO and various hosts (CD, TE-1, and TB-1) were prepared. UV-Vis spectroscopy was used to study behavior of the solutions. In terms of solutions prepared from equimolar amount of CD and MO, the blue shift from 497 to 486 nm was observed at pH 4. The blue shift was also observed at pH 6 when high amount of CD was complexed with MO. According to UV-Vis spectra of TE-1MO and TB-1MO at pH 6, the slightly blue shift was only observed in the series A which contained high amount of the host polymers. In addition to the spectra of these host polymers complexed with MO at pH 4, the blue shift was observed in both series A and B.

Characterization and properties of MO-incorporated TB-1 films

TB-1 was mixed with different amounts of methyl orange and then casted into films using solution casting method. The light transmittance curves showed that the transparency of the films was decreased when the amount of MO in the films was

increased. In addition, the refractive indexes of the films increased when MO was added. FTIR spectra of the films showed the shift of C=O stretching vibration from lower wavenumbers to higher wavenumbers. The WAXS pattern of TB-1MO0.01 film showed the peak at $2\theta = 20.9^{\circ}$, which was difference from the WAXS pattern of TB-1 film. From TGA thermograms, it was seen that the T_{90} of all MO-incorporated TB-1 films was lower than TB-1 film. In terms of DMA results, the significant drop in storage modulus assigned to ice melting was observed in TB-1MO0.01 film at 14°C and TB-1MO0.04 film at 12°C. According to the tan δ curves of the films, unlike TB-1 film, the main peak temperature involved with the combination of the reorganization of molecules due to water loss and the local movement of the molecules in the pseudo-stable stage as well as molecular degradation was observed.

5.2 Suggestions

1. The drying process such as lyophilization should be performed in order to reduce remained solvents presented in the products.

2. The mechanism of self-inclusion complex of HAACSs-g-CDs should be further investigated using the combination of 1D NMR and 2D NMR data.

3. Equilibrium constant between HAACSs-g-CDs and various guests should be quantitatively determined using Benesi-Hildebrand's method or Isothermal calorimetric titration (ITC) method.

4. DMA experiment of all films should be performed in various moisture contents to determine effect of water content on thermal properties of the films.

5. The HBACS should be grafted with the molecule which provides high equilibrium constant with CD (i.e., adamantanecarboxylic acid) and then mixed the product with TB-1 to prepare supramolecular hydrogels crosslinked by the formation of inclusion complexes.

References

[1] Martin, E.M. 2004. "Cyclodextrins and Their Uses: a Review." *Process Biochemistry.* 39 : 1033-1046.

[2] Szejtli, J. 1998. "Introduction and General Overview of Cyclodextrin Chemistry." *Chemical reviews.* 98 : 1743-1754.

[3] Zhao, P. Xin, M. Li, M. and Deng, J. 2015. "Adsorption of Methyl Orange from Aqueous Solution Using Chitosan Microspheres Modified by β-Cyclodextrin." *Desalination and Water Treatment.* 55 : 1-9.

[4] Williams III, O.R. Mahaguna, V. and Sriwongjanya, M. 1998. "Characterization of an Inclusion Complex of Cholesterol and Hydroxypropyl-β-Cyclodextrin." European Journal of Pharmaceutics and Biopharmaceutics. 46 : 355-360.

[5] Szente, L. Szejtli, J. Szeman, J. and Kato, L. 1993. "Fatty acid-cyclodextrin complexes: Properties and applications." *Journal of Inclusion Phenomena and Molecular Recognition in Chemistry.* 16 : 339-354.

[6] Abrahaet, E. 1977. **Dyes and Their Intermediates.** 2nd ed. Oxford : Pergamon Press.

[7] Hunger, K. 2003. **Industrial Dyes.** Weinheim : Wiley-VCH.

[8] Tawarah, K. 1992. "A Thermodynamic Study of the Inclusion Processes of α- and β-Cyclodextrins with The Acid Forms of Methyl Orange and Methyl Yellow." *Journal of Inclusion Phenomena and Macrocyclic Chemistry.* 14 : 195-204..

[9] Kompany-Zareh, M. Mokhtari, Z. and Abdollahi, H. 2012. "Spectrophotometric Thermodynamic Study of Orientational Isomers Formed by Inclusion of Methyl Orange Into β-Cyclodextrin Nanocavity." *Chemometrics and Intelligent Laboratory Systems.* 118 : 230-238.

[10] Rinaudo, M. 2006. "Chitin and Chitosan: Properties and Applications." *Progress in Polymer Science.* 31 : 603-632.

[11] Pillai, C.K.S. Paul, W. and Sharma, P.C. 2009. "Chitin and Chitosan Polymers: Chemistry, Solubility and Fiber Formation." *Progress in Polymer Science.* 34 : 641-678.

[12] Kumar, R.V.N.V. Muzzarelli, A.A.R. Muzzarelli, C. Sashiwa, H. and Domb, J.A. 2004. "Chitosan Chemistry and Pharmaceutical Perspectives." *Chemical Reviews.* 104 : 6017-6084.

[13] Prabaharan, M. and Mano, J.F. 2006. "Chitosan Derivatives Bearing Cyclodextrin Cavitiesas Novel Adsorbent Matrices." *Carbohydrate Polymers.* 63 : 153-166.

[14] Chen, S. and Wang, Y. 2001. Study on β-cyclodextrin Grafting with Chitosan and Slow Release of its Inclusion Complex with Radioactive Iodine. *Journal of Applied Polymer Science.* 82 : 2414-2421.

[15] Aoki, N. Nishikawa, M. and Hattori, K. 2003. "Synthesis of Chitosan Derivatives Bearing Cyclodextrin and Adsorption of *p*-Nonylphenol and Bisphenol A." *Carbohydrate Polymers.* 52 : 219-223.

[16] Lu, L. Shao, X. Jiao, Y. and Zhou, C. 2014. "Synthesis of Chitosan-graft-β-Cyclodextrin for Improving the Loading and Release of Doxorubicin in the Nanopaticles." *Journal of Applied Polymer Science.* 131 : 1-7.

[17] Gonil, P. Sajomsang, W. Ruktanonchai, R.U. Pimpha, N. Sramala, I. Nuchuchua, O. Saesoo, S. Chaleawlert-umpon, S. and Puttipipatkhachorn, S. 2011. "Novel Quaternized Chitosan Containing β-Cyclodextrin Moiety: Synthesis, Characterization and Antimicrobial Activity," *Carbohydrate Polymers.* 83 : 905-913.

[18] Tanida, F. Tojima, T. Han, S. M. Nishi, N. Tokura, S. Sakairi, N. Seino, H. and Hamada, K. 1998. "Novel Synthesis of a Water-Soluble Cyclodextrin-Polymer Having a Chitosan Skeleton." *Polymer.* 39 : 5261-5263.

[19] Ma, G. Yang, D. Zhou, Y. Xiao, M. Kennedy F.J. and Nie, J. 2008. "Preparation and Characterization of Water-Soluble *N*-Alkylated Chitosan." *Carbohydrate Polymers.* 74 : 121-126.

[20] Treenate, P. Monvisade, P. and Yamaguchi, M. 2015. "Development of Hydroxyethylacryl Chitosan/Alginate Hydrogel Films for Biomedical Application." *Journal of Polymer Research.* 21 : 1-12.

[21] Davis, F. and Higson, S. 2011. *Macrocycles.* Hoboken : Wiley.

[22] Bilensoy, E. 2011. **Cyclodextrins in Pharmaceutics, Cosmetics, and Biomedicine.** Hoboken, N.J. : Wiley.

[23] Crini, G. 2014. "Review: A History of Cyclodextrins." *Chemical Reviews.* 114 : 10940-10975.

[24] Biwer, A. Antranikian, G. and Heinzle, E. 2002. "Enzymatic Production of Cyclodextrins." *Applied Microbiology and Biotechnology.* 59 : 609-617.

[25] Park, J. 2006. "Kinetics and Mechanism of Cyclodextrin Inclusion Complexation Incorporating Bidirectional Inclusion and Formation of Orientational Isomers." *The Journal of Physical Chemistry B.* 110 : 24915-24922.

[26] Connors, K. 1997. "The Stability of Cyclodextrin Complexes in Solution." *Chemical Reviews.* 97 : 1325-1358.

[27] Rekharsky, M. and Inoue, Y. 1998. "Complexation Thermodynamics of Cyclodextrins." *Chemical Reviews.* 98 : 1875-1918.

[28] Khan, A. Forgo, P. Stine, K. and D'Souza, V. 1998. "Methods for Selective Modifications of Cyclodextrins." *Chemical Reviews.* 98 : 1977-1996.

[29] Liu, Y. Zhang, Y. Qi, A. Chen, R. Yamamoto, K. Wada, T. and Inoue, Y. 1997. "Molecular Recognition Study on a Supramolecular System. 10. 1 Inclusion Complexation of Modified β-Cyclodextrins with Amino Acids: Enhanced Enantioselectivity for l / d -Leucine." *The Journal of Organic Chemistry.* 62 : 1826-1830.

[30] Ashton, P. Ellwood, P. Staton, I. and Stoddart, J. 1991. "Per-3,6-Anhydro-α-Cyclodextrin and Per-3,6-Anhydro-β-Cyclodextrin." *The Journal of Organic Chemistry.* 56 : 7274-7280.

[31] De Rango, C. Charpin, P. Navaza, J. Keller, N. Nicolis, I. Villain, F. and Coleman, A. 1992. "β-Cyclodextrin/Pyridine Gel Systems. The Crystal Structure of a First β-Cyclodextrin-Pyridine Water Compound." *Journal of the American Chemical Society.* 114 : 5475-5476.

[32] Vizitiu, D. Walkinshaw, C. Gorin, B. and Thatcher, G. 1997. "Synthesis of Monofacially Functionalized Cyclodextrins Bearing Amino Pendent Groups." *The Journal of Organic Chemistry.* 62 : 8760-8766.

[33] Onozuka, S. Kojima, M. Hattori, K. and Toda, F. 1980. "The Regiospecific Mono tosylation of Cyclodextrins." *Bulletin of the Chemical Society of Japan.* 53 : 3221-3224.

[34] Brady, B. Lynam, N. O'sullivan, T. Ahern, C. and Darcy, R. 2000. "6^{A}-*O*-*p*-TOLUENESULFONYL-β-CYCLODEXTRIN." *Organic Syntheses.* 77 : 220-221.

[35] Ravi Kumar, M. 2000. "A Review of Chitin and Chitosan Applications." *Reactive and Functional Polymers.* 46 : 1-27.

[36] Harish Prashanth, K. and Tharanathan, R. 2007. "Chitin/Chitosan: Modifications and Their Unlimited Application Potential—an Overview." *Trends in Food Science & Technology.* 18 : 117-131.

[37] Gorochovceva, N. and Makuška, R. 2004. "Synthesis and Study of Water-Soluble Chitosan-*O*-Poly(Ethylene Glycol) Graft Copolymers." *European Polymer Journal.* 40 : 685-691.

[38] Yoshifuji A. Noishiki, Y. Wada, M. Heux, L. and Kuga, S. 2006. "Esterification of β-Chitin via Intercalation by Carboxylic Anhydrides." *Biomacromolecules.* 7 : 2878-2881.

[39] Harish Prashanth, K. and Tharanathan, R. 2006. "Crosslinked chitosan—Preparation and Characterization." *Carbohydrate Research.* 341 : 169-173.

[40] Jayakumar, R. Prabaharan, M. Reis, R. and Mano, J. 2005. "Graft Copolymerized Chitosan—Present Status and Applications." Carbohydrate Polymers. 62 : 142-158.

[41] Fei Liu, X. Lin Guan, Y. Zhi Yang, D. Li, Z. and De Yao, K. 2000. "Antibacterial Action of Chitosan and Carboxymethylated Chitosan." *Journal of Applied Polymer Science.* 79 : 1324-1335.

[42] Yi, H. Wu, L. Bentley, W. Ghodssi, R. Rubloff, G. Culver, J. and Payne, G. 2005. "Biofabrication with Chitosan." *Biomacromolecules.* 6 : 2881-2894.

[43] Mather, B. Viswanathan, K. Miller, K. and Long, T. 2006. "Michael Addition Reactions in Macromolecular Design for Emerging Technologies." *Progress in Polymer Science.* 31 : 487-531.

[44] Smith Gorzynski, J. 1977. *Organic Chemistry.* 3rd ed. Singapore : McGraw-Hill.

[45] Sashiwa, H. Kawasaki, N. Nakayama, A. Muraki, E. Yajima, H. Yamamori, N. and Ichinose, Y. Sunamoto, J. and Aiba, S. 2003. "Chemical Modification of Chitosan. Part 15: Synthesis of Novel Chitosan Derivatives by Substitution of Hydrophilic Amine using *N*-Carboxyethylchitosan Ethyl Ester as an Intermediate." *Carbohydrate Research.* 338 : 557-561.

[46] Sashiwa, H. Yamamori, N. Ichinose, Y. Sunamoto, J. and Aiba, S. 2003. "Chemical Modification of Chitosan, 17[a] : Michael Reaction of Chitosan with Acrylic Acid in Water." *Macromolecular Bioscience.* 3 : 231-233.

[47] Sashiwa, H. Yamamori, N. Ichinose, Y. Sunamoto, J. and Aiba, S. 2003. "Michael Reaction of Chitosan with Various Acryl Reagents in Water." *Biomacromolecules.* 4 : 1250-1254.

[48] Wang, K. Yin, R. Tong, Z. Yu, Q. and Nie, J. 2011. "Synthesis and Characterization of Water-Soluble Glucosyloxyethyl Acrylate Modified Chitosan." *International Journal of Biological Macromolecules.* 48 : 753-757.

[49] Gao, X. Zhou, Y. Ma, G. Shi, S. Yang, D. Lu, F. and Nie, J. 2010. "A Water-Soluble Photocrosslinkable Chitosan Derivative Prepared by Michael-Addition Reaction as a Precursor for Injectable Hydrogel." *Carbohydrate Polymers.* 79 : 507-512.

[50] Mourya, V. and Inamdar, N. 2008. "Chitosan-Modifications and Applications: Opportunities Galore." *Reactive and Functional Polymers.* 68 : 1013-1051.

[51] Zhang, X. Wang, Y. and Yi, Y. 2004. "Synthesis and Characterization of Grafting β-Cyclodextrin with Chitosan." *Journal of Applied Polymer Science.* 94 : 860-864..

[52] Auzély-Velty, R. and Rinaudo, M. 2001. "Chitosan Derivatives Bearing Pendant Cyclodextrin Cavities: Synthesis and Inclusion Performance." *Macromolecules.* 34 : 3574-3580.

[53] Martel, B. Devassine, M. Crini, G. Weltrowski, M. Bourdonneau, M. and Morcellet, M. 2000. "Preparation and Sorption Properties of β-Cyclodextrin-Linked Chitosan Derivative. *Journal of Polymer Science Part A: Polymer Chemistry.* 39 : 169-176.

[54] Prabaharan, M. and Jayakumar, R. 2009. "Chitosan-graft-β-Cyclodextrin Scaffolds with Controlled Drug Release Capability for Tissue Engineering Applications." *International Journal of Biological Macromolecules.* 44 : 320-325.

[55] El-Tahlawy, K. Gaffer, M. and Elrafie, S. 2006. "Novel Method for Preparation of β-Cyclodextrin/Grafted Chitosan and It's Application." Carbohydrate Polymers. 63 : 385-392.

[56] Yuan, Z. Ye, Y. Gao, F. Yuan, H. Lan, M. Lou, K. and Wang, W. 2013. "Chitosan-graft-β-Cyclodextrin Nanoparticles as a Carrier for Controlled Drug Release." *International Journal of Pharmaceutics.* 446 : 191-198.

[57] Williamson, K. 1989. *Macroscale and Microscale Organic Experiments.* USA : Heath.

[58] Valentin, R. Bonelli, B. Garrone, E. Di Renzo, F. and Quignard, F. 2007. "Accessibility of the Functional Groups of Chitosan Aerogel Probed by FT-IR-Monitored Deuteration." *Biomacromolecules.* 8 : 3646-3650.

[59] Machell, J. Greener, J. and Contestable, B. 1990. "Optical Properties of Solvent-Cast Polymer Films." *Macromolecules.* 23 : 186-194.

[60] Jiang, H. Su, W. Caracci, S. Bunning, T. Cooper, T. and Adams, W. 1996. "Optical Waveguiding and Morphology of Chitosan Thin Films." *Journal of Applied Polymer Science.* 61 : 1163-1171.

[61] Yang, C. and Jenekhe, S. 1994. "Effects of Structure on Refractive Index of Conjugated Polyimines." *Chemistry of Materials.* 6 : 196-203.

[62] Zong, Z. Kimura, Y. Takahashi, M. and Yamane, H. 2000. "Characterization of Chemical and Solid State Structures of Acylated Chitosans." *Polymer.* 41 : 899-906.

[63] Nunthanid, J. Puttipipatkhachorn, S. Yamamoto, K. and Peck, G. 2001. "Physical Properties and Molecular Behavior of Chitosan Films." *Drug Development and Industrial Pharmacy.* 27 : 143-157.

[64] Lee, E. Chung, H. and Lim, S. 2001. "Change in Thermal Transition of Korean Rice Cake (Karedduk) During Storage." *Food Science and Biotechnology.* 10 : 583-589.

[65] Sakurai, K. Maegawa, T. and Takahashi, T. 2000. "Glass Transition Temperature of Chitosan and Miscibility of Chitosan/Poly(*N*-vinyl pyrrolidone) Blends." *Polymer.* 41 : 7051-7056.

[66] Mucha, M. and Pawlak, A. 2005. "Thermal Analysis of Chitosan and Its Blends." *Thermochimica Acta.* 427 : 69-76.

[67] Ferreira, P. Coelho, J. dos Santos, K. Ferreira, E. and Gil, M. 2006. "Thermal Characterization of Chitosan-Grafted Membranes to be Used as Wound Dressings." *Journal of Carbohydrate Chemistry* 25 : 233-251.

[68] Phenomenex. 2016. **Solvent Miscibility Table.** [Online]. Available : https://www.erowid.org/archive/rhodium/pdf/solvent.miscibility.pdf.

[69] Badr-Eldin, S. Elkheshen, S. and Ghorab, M. 2008. "Inclusion complexes of tadalafil with natural and chemically modified **β**-cyclodextrins. I: Preparation and *in-vitro* evaluation." European Journal of Pharmaceutics and Biopharmaceutics. 70 : 819-827.

[70] Tripodo, G. Wischke, C. Neffe, A. and Lendlein, A. 2013. "Efficient Synthesis of Pure Monotosylated Beta-Cyclodextrin and Its Dimers." *Carbohydrate Research*. 381 : 59-63.

[71] Lampman, G. and Pavia, D. 2010. *Spectroscopy*. Belmont, CA : Brooks/Cole.

[72] Djedaini-Pilard, F. Gosnat, M. Steinbruckner, S. Dalbiez, J. Crini, G. Perly, B. and Gadelle, A. 1999. "Mono-6-Tosyl-β-Cyclodextrin: Preparation, Hydrolysis and Self-Inclusion Studies in Aqueous Solution." *Proceedings of the Ninth International Symposium on Cyclodextrins*. 73-76.

[73] Trotta, F. Zanetti, M. and Camino, G. 2000. "Thermal Degradation of Cyclodextrins." *Polymer Degradation and Stability*. 69 : 373-379.

[74] Yuan, C. Jin, Z. and Xu, X. 2012. "Inclusion Complex of Astaxanthin with Hydroxypropyl-β-Cyclodextrin: UV, FTIR, ^{1}H NMR and Molecular Modeling Studies." *Carbohydrate Polymers*. 89 : 492-496.

[75] Salústio, P. Feio, G. Figueirinhas, J. Pinto, J. and Cabral Marques, H. 2009. The Influence of the Preparation Methods on the Inclusion of Model Drugs in a β-Cyclodextrin Cavity." *European Journal of Pharmaceutics and Biopharmaceutics*. 71 : 377-386.

[76] Rekharsky, M. Schwarz, F. Tewari, Y. and Goldberg, R. 1994. "A Thermodynamic Study of the Reactions of Cyclodextrins with Primary and Secondary Aliphatic Alcohols, with D- and L-Phenylalanine, and with L-Phenylalanine Amide." *The Journal of Physical Chemistry*. 98 : 10282-10288.

[77] Gottlieb, H. Kotlyar, V. and Nudelman, A. 1997. "NMR Chemical Shifts of Common Laboratory Solvents as Trace Impurities." *The Journal of Organic Chemistry*. 62 : 7512-7515.

[78] Dimethylformamide [MAK Value Documentation]. 2012. *Annual Thresholds and Classifications for the Workplace*. 1-44.

[79] Liu, L. and Zhu, S. 2007. "A Study on the Supramolecular Structure of Inclusion Complex of **β**-Cyclodextrin with Prazosin Hydrochloride." *Carbohydrate Polymers*. 68 : 472-476.

[80] Shen, Y. Yang, S. Wu, L. and Ma, X. 2005. "Study on Structure and Characterization of Inclusion Complex of Gossypol/Beta Cyclodextrin." *Spectrochimica Acta Part A: Molecular and Biomolecular Spectroscopy*. 61 : 1025-1028.

[81] Mori, T. Dong, T. Yazawa, K. and Inoue, Y. 2007. "Preparation of Highly Transparent and Thermally Stable Films of α-Cyclodextrin/Polymer Inclusion Complexes." Macromolecular Rapid Communications. 28 : 2095-2099.

[82] Chen, Y. Liu, S. Yu, H. Yin, H. and Li, Q. 2008. "Radiation-Induced Degradation of Methyl Orange in Aqueous Solutions." *Chemosphere*. 72 : 532-536.

[83] Carrazana, J. Reija, B. Cabrer, P. Al-Soufi, W. Novo, M. and Tato, J. 2004. "Complexation of Methyl Orange with β-cyclodextrin: Detailed Analysis and Application to Quantification of Polymer-bound Cyclodextrin." *Supramolecular Chemistry*. 16 : 549-559.

[84] Swanepoel, R. 1983. "Determination of the Thickness and Optical Constants of Amorphous Silicon." *Journal of Physics E: Scientific Instruments*. 16 : 1214-1222.

[85] Ayed, L. Khelifi, E. Jannet, H. Miladi, H. Cheref, A. Achour, S. and Bakhrouf, A. 2010. "Response Surface Methodology for Decolorization of Azo Dye Methyl Orange by Bacterial Consortium: Produced Enzymes and Metabolites Characterization." *Chemical Engineering Journal*. 165 : 200-208.

[86] Wang, J. Cao, Y. Sun, B. and Wang, C. 2011. "Physicochemical and Release Characterisation of Garlic Oil-β-cyclodextrin Inclusion Complexes." *Food Chemistry*. 127 : 1680-1685.

[87] Jia, Y. and Zhu, X. 2015. "Self-Healing Supramolecular Hydrogel Made of Polymers Bearing Cholic Acid and β-Cyclodextrin Pendants." *Chemistry of Materials*. 27 : 387-393.

Appendices

Appendix A

FTIR spectra

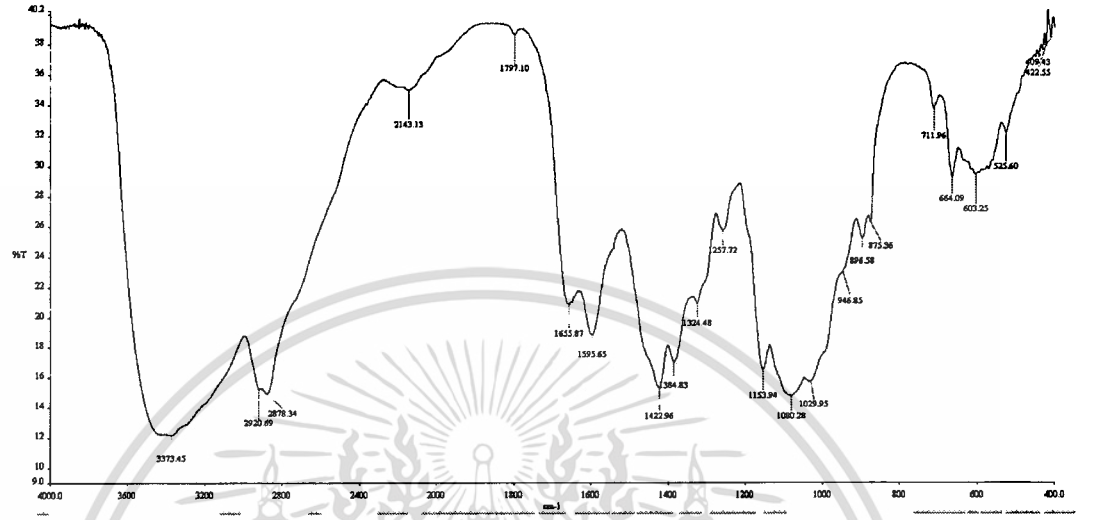

Figure A-1 FTIR spectrum of CS.

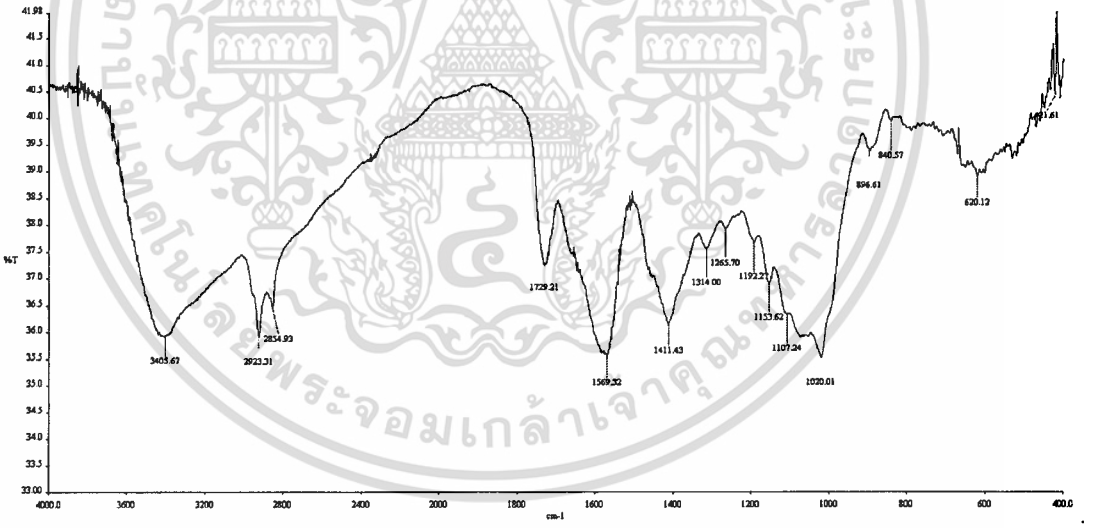

Figure A-2 FTIR spectrum of HEACS.

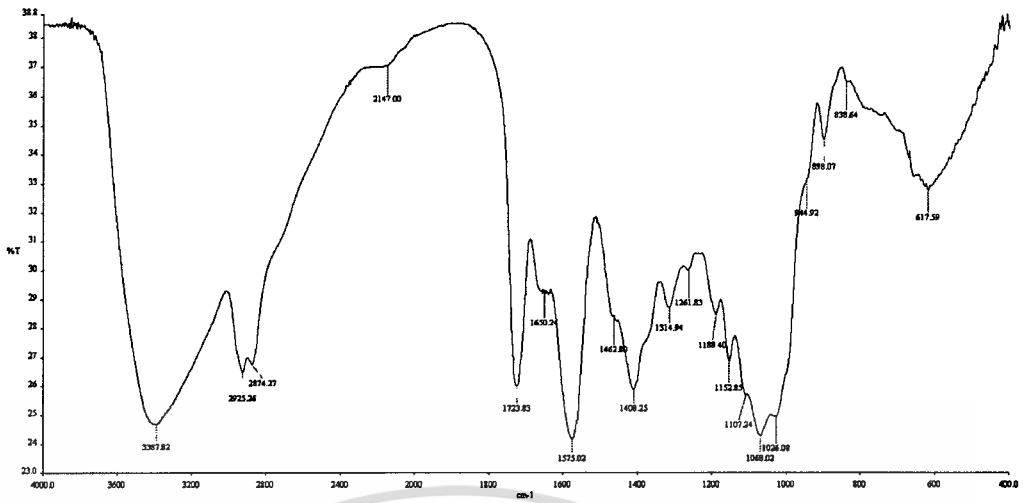

Figure A-3 FTIR spectrum of HPACS.

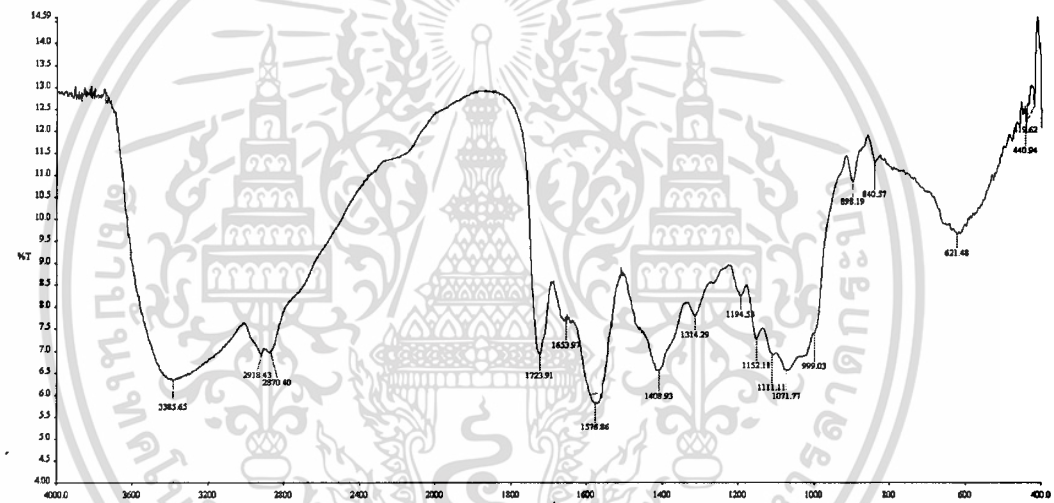

Figure A-4 FTIR spectrum of HBACS.

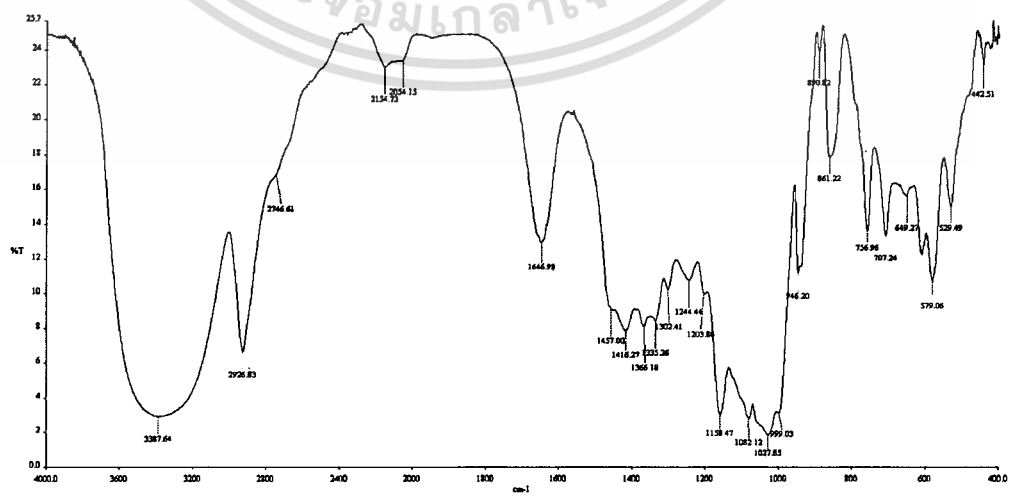

Figure A-5 FTIR spectrum of CD.

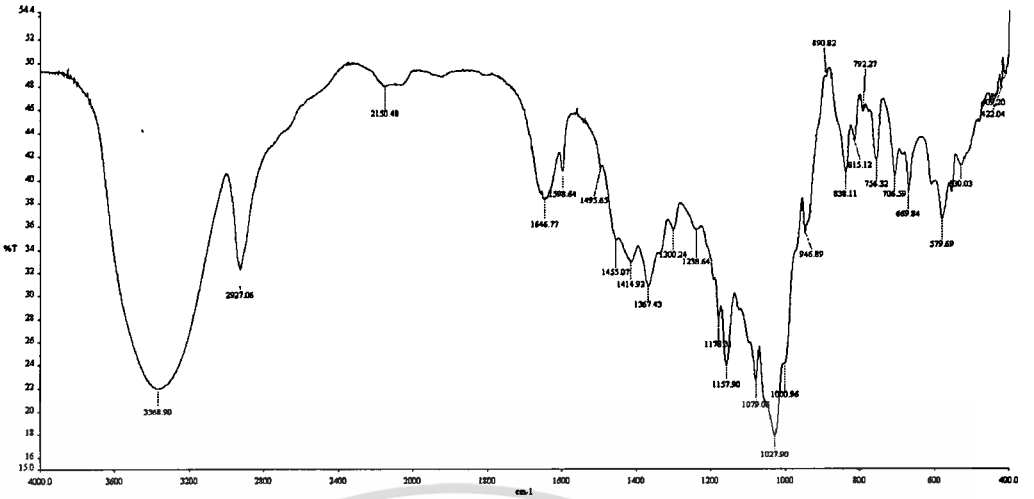

Figure A-6 FTIR spectrum of TsCD.

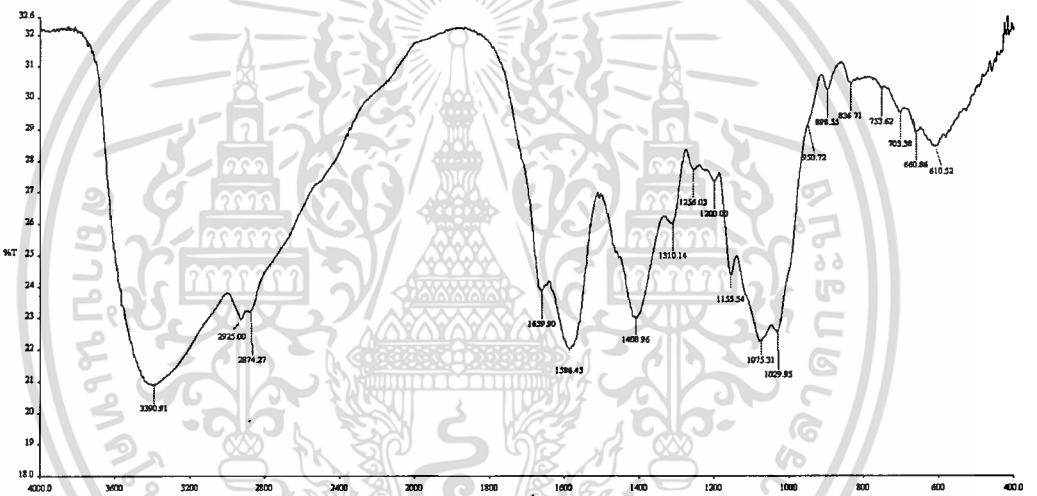

Figure A-7 FTIR spectrum of TE-1.

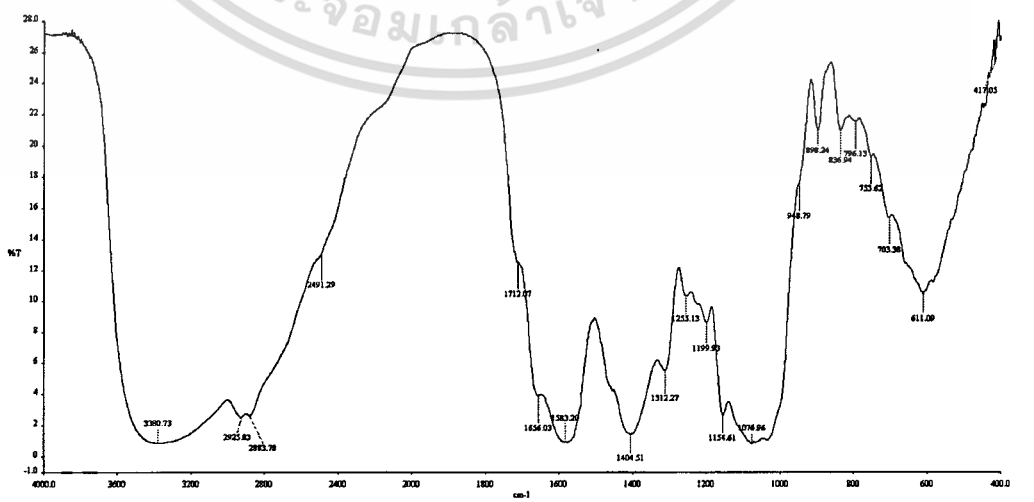

Figure A-8 FTIR spectrum of TP-1.

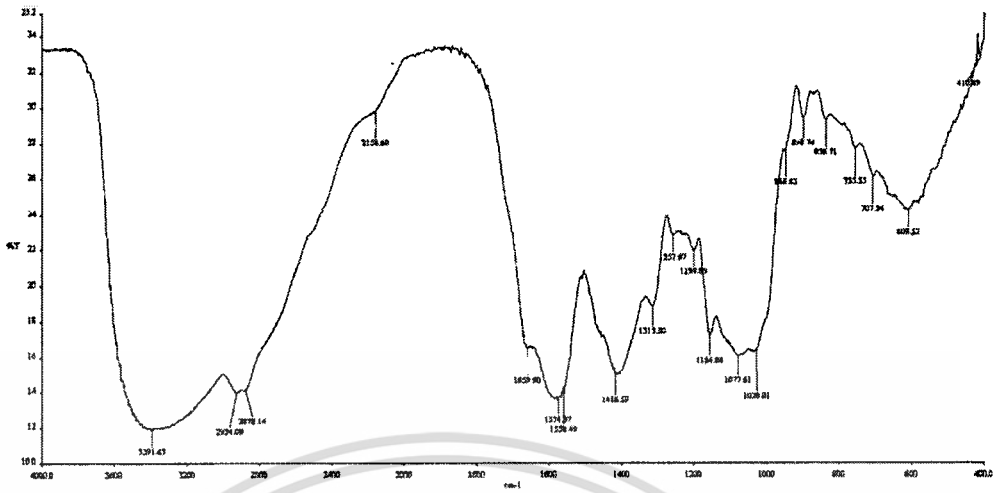

Figure A-9 FTIR spectrum of TB-1.

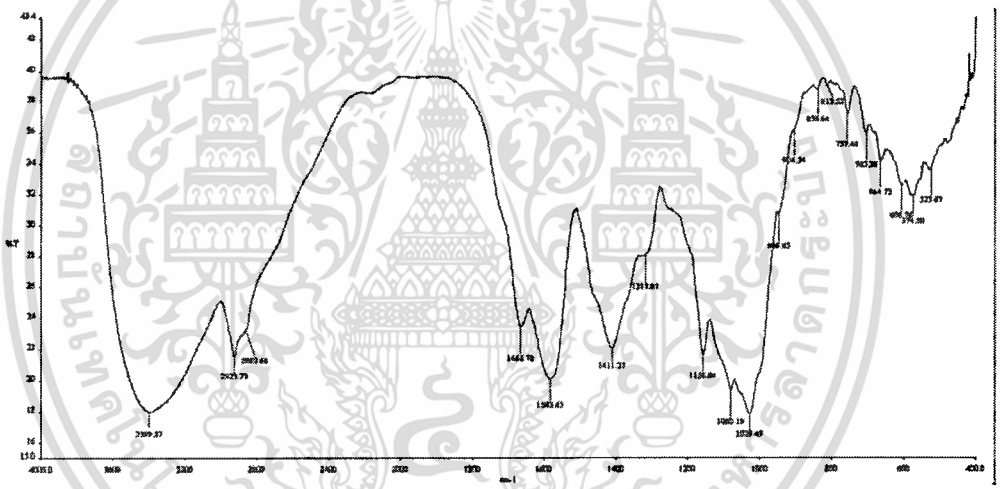

Figure A-10 FTIR spectrum of TB-2.

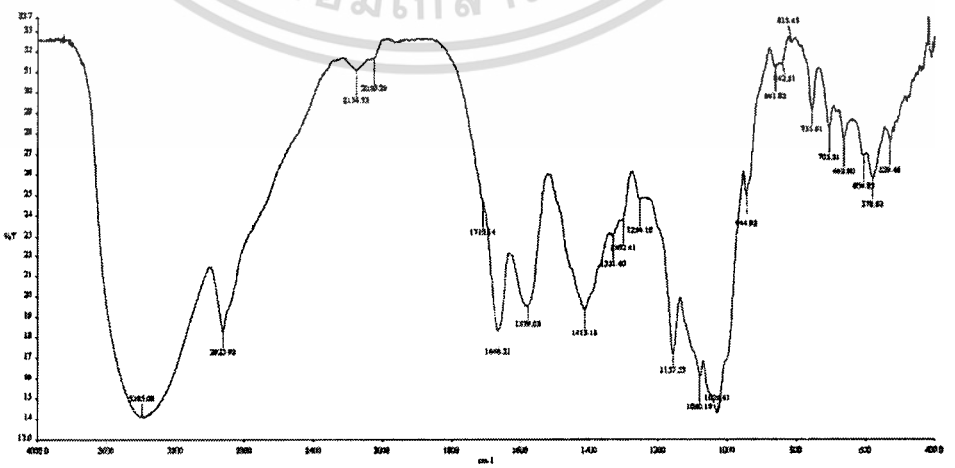

Figure A-11 FTIR spectrum of TB-3.

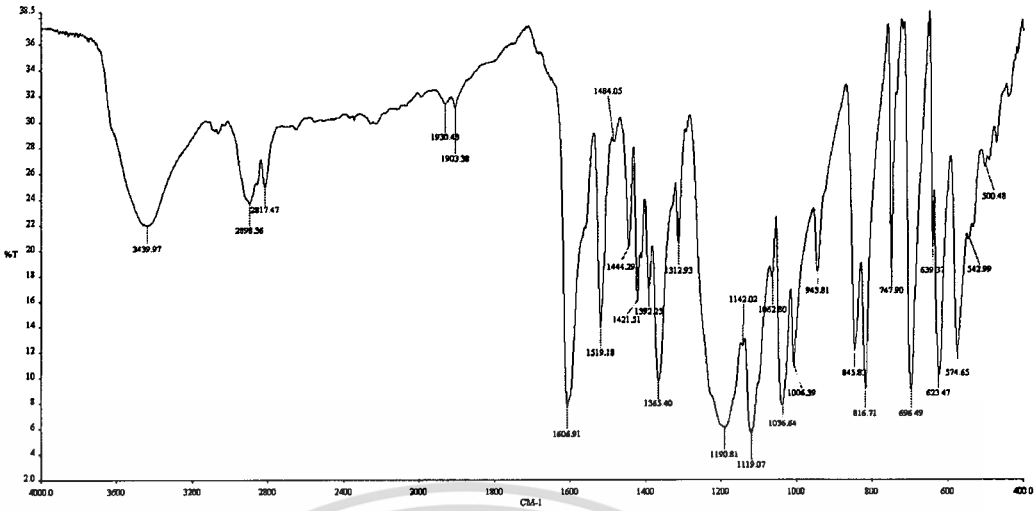

Figure A-12 FTIR spectrum of MO.

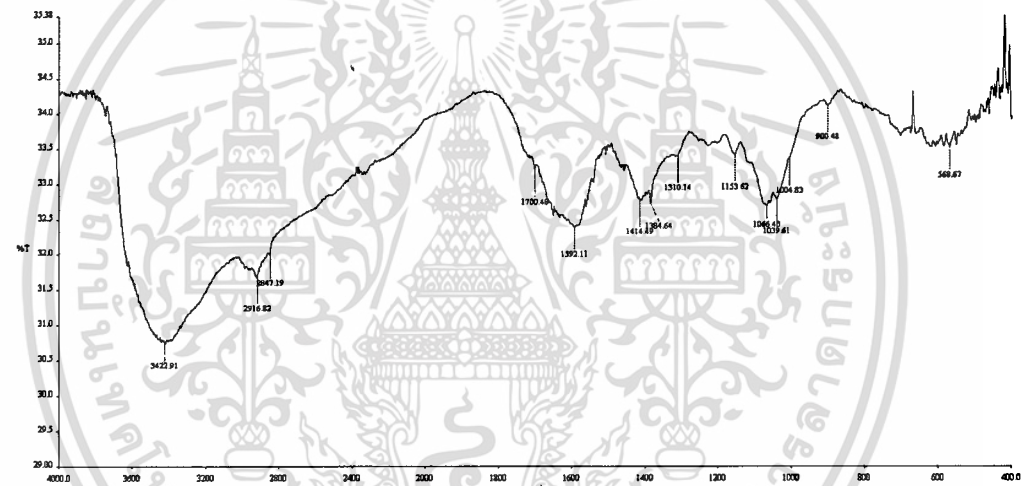

Figure A-13 FTIR spectrum of TB-1MO0.01 film.

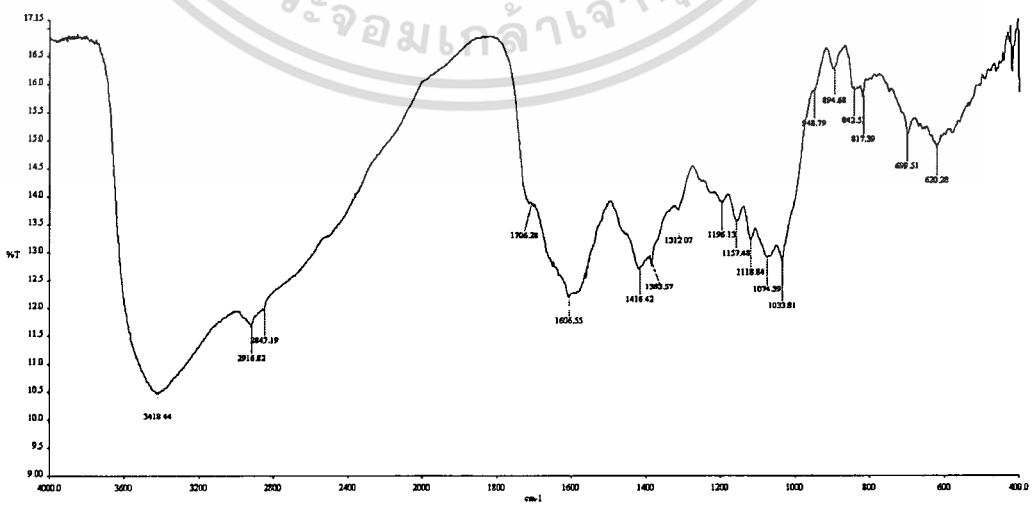

Figure A-14 FTIR spectrum of TB-1MO0.04 film.

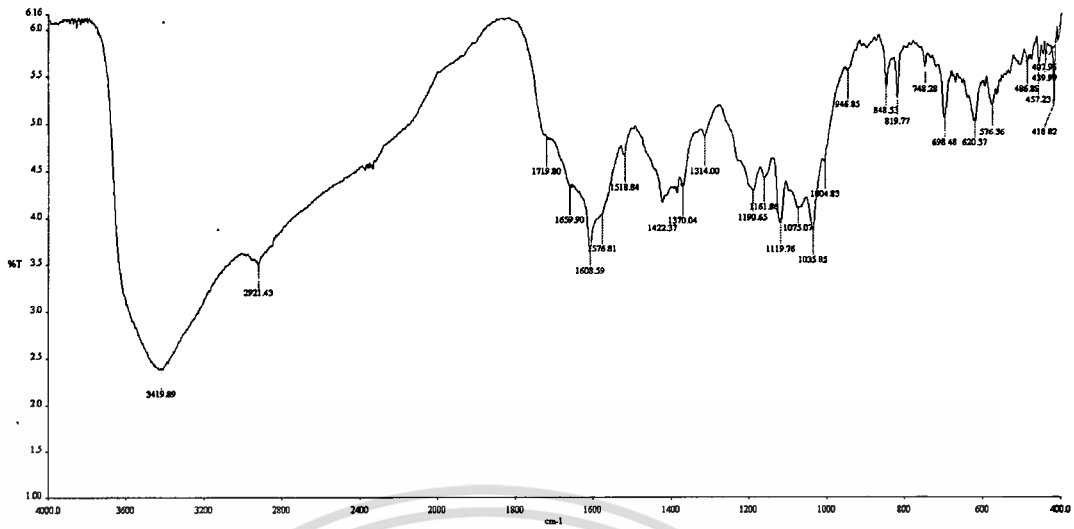

Figure A-15 FTIR spectrum of TB-1MO0.1 film.

Appendix B

Calculation of %DS, average molecular weight per repeating unit and %yield using data from ^{1}H-NMR spectra.

In this section, methods for calculating %DS, average molecular weight per repeating and %yield of each product were reported. Integration data from ^{1}H-NMR spectra was used for calculation.

1. HEACS

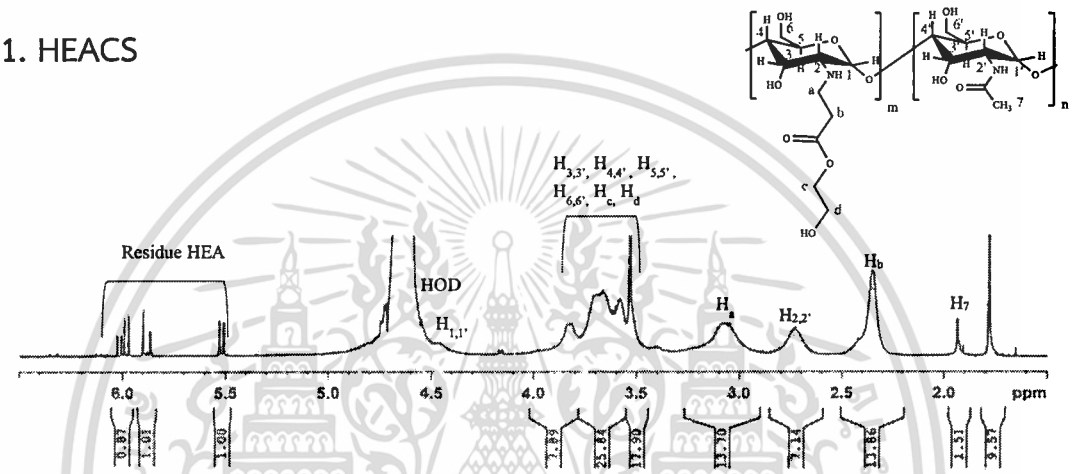

Figure B-1 ^{1}H-NMR spectrum of HEACS.

1.1 %DS

Before calculating the %DS of HEACS, degree of deacetylation percentage (%DD) of CS as a reactant was firstly determined from the integral area of acetyl protons (-COCH_3) of CS at δ = 1.94 ppm (H_7) against the integral area of CS proton at δ = 2.73 ppm ($H_{2,2'}$) as below:

$$\%DD = 100 - \left(\frac{H_7/3}{H_{(2,2')}} \times 100\right) \quad \text{(B-1)}$$

$$= 100 - \left(\frac{1.51/3}{7.14} \times 100\right)$$

$$= 93\ \%$$

Subsequently, %DS of HEACS can be calculated by using equation 3.1.

$$\%DS\ (HEACS) = \frac{H_b/2}{H_{(2,2')}} \times 100 \quad (3.1)$$

From the spectrum depicted in Figure B-1, the integral area of HEA moiety protons (-CH_2-CO-) at δ = 2.35 ppm (H_b) was 13.86, and the integral area of CS proton at δ = 2.73 ppm ($H_{2,2'}$) was 7.14. Therefore,

$$\%DS\ (HEACS) = \frac{13.86/2}{7.14} \times 100$$

$$= 97\ \%$$

1.2 Average molecular weight per repeating unit

Before calculating average molecular weight per repeating unit of HEACS, average molecular weight per repeating unit of CS used in the reaction was needed to be firstly determined. It should be mentioned again that CS is the product from deacetylation of chitin as illustrated in Figure B-2.

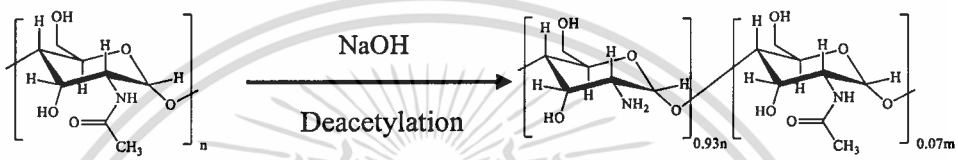

Chitin (M_w = 203) Chitosan (CS)

Figure B-2 Deacetylation reaction of chitin.

Therefore, average molecular weight per repeating unit of CS could be determined as equation B-2:

$$M_w \text{ per repeating unit of CS} = (Mw_{acetyl} - (43 \times 0.93)) + (Mw_H \times 0.93) \quad \text{(B-2)}$$

$$= (203 - 40) + (1 \times 0.93)$$

$$= 164$$

Thereafter, average molecular weight per repeating unit of HEACS could be determined using equation B-3.

$$M_w \text{ per repeating unit of HEACS} = (Mw_{CS} - (Mw_H \times 0.97)) + (Mw_{HEA} \times 0.97) \quad \text{(B-3)}$$

$$= (164 - (1 \times 0.97)) + (116 \times 0.97)$$

$$= 276$$

1.3 %Yield

Determining theoretical weight of HEACS;

$$W_{HEACS} = 6\ g\ CS \times \frac{1 mol\ CS}{164\ g\ CS} \times \frac{276\ g\ HEACS}{1\ mol\ HEACS}$$

$$= 10.10\ g$$

%Yield of products could be calculated by equation B-4:

$$\%\text{Yield} = \frac{\text{Actual weight}}{\text{Theroretical weight}} \times 100 \quad \text{(B-4)}$$

After the reaction, 9.43 g of product was obtained. Therefore,

$$\%\text{Yield} = \frac{9.43}{10.10} \times 100$$

$$\%\text{Yield} = 93\ \%$$

2. HPACS

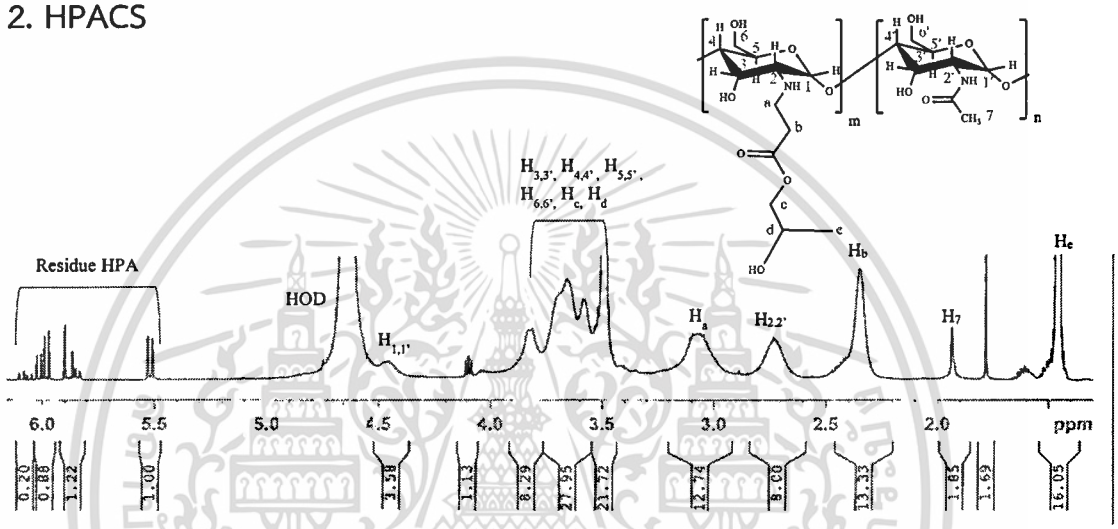

Figure B-3 ^{1}H-NMR spectrum of HPACS.

2.1 %DS

The %DD of CS as a reactant was firstly determined again from the ^{1}H-NMR spectrum of HPACS using equation B-1. It could be observed from the spectrum that the integral area of H_7 at δ = 1.94 ppm was 1.85 and the integral area of $H_{(2,2')}$ at δ = 2.73 ppm was 8. Therefore,

$$\%\text{DD} = 100 - \left(\frac{H_7/3}{H_{(2,2')}} \times 100\right) \quad \text{(B-1)}$$

$$= 100 - \left(\frac{1.85/3}{8} \times 100\right)$$

$$= 92\ \%$$

Thereafter, %DS of HPBACS was calculated by using equation 3.2.

$$\%\text{DS (HPACS or HBACS)} = \frac{H_a/2}{H_{(2,2')}} \times 100 \quad \text{(3.2)}$$

From the spectrum, the integral area of HPA moiety protons (-NH-CH_2-) at δ = 3.05 ppm (H_a) was 12.74 and the integral area of $H_{(2,2')}$ at δ = 2.73 ppm was 8.00. Consequently,

$$\%DS\ (HPACS\ or\ HBACS) = \frac{12.74/2}{8.00} \times 100$$

$$= 80\ \%$$

2.2 Average molecular weight per repeating unit

Average molecular weight per repeating unit of CS was calculated using %DD obtained from previous section. Therefore,

$$M_w \text{ per repeating unit of CS} = (Mw_{acetyl} - (43 \times 0.92)) + (Mw_H \times 0.92) \quad \text{(B-2)}$$

$$= (203 - 40) + (1 \times 0.92)$$

$$= 164$$

To determine average molecular weight per repeating unit of HPACS, equation B-5 was used.

$$M_w \text{ per repeating unit of HPACS} = (Mw_{CS} - (Mw_H \times 0.80)) + (Mw_{HPA} \times 0.80) \quad \text{(B-5)}$$

$$= (164 - (1 \times 0.80)) + (130 \times 0.80)$$

$$= 267$$

2.3 %Yield

Calculating theoretical weight;

$$W_{HPACS} = 6\ g\ CS \times \frac{1\ mol\ CS}{164\ g\ CS} \times \frac{267\ g\ HPACS}{1\ mol\ HPACS}$$

$$= 9.77\ g$$

The weight of the obtained product was 6.80 g. Hence,

$$\%Yield = \frac{6.80}{9.77} \times 100$$

$$= 70\ \%$$

3. HBACS

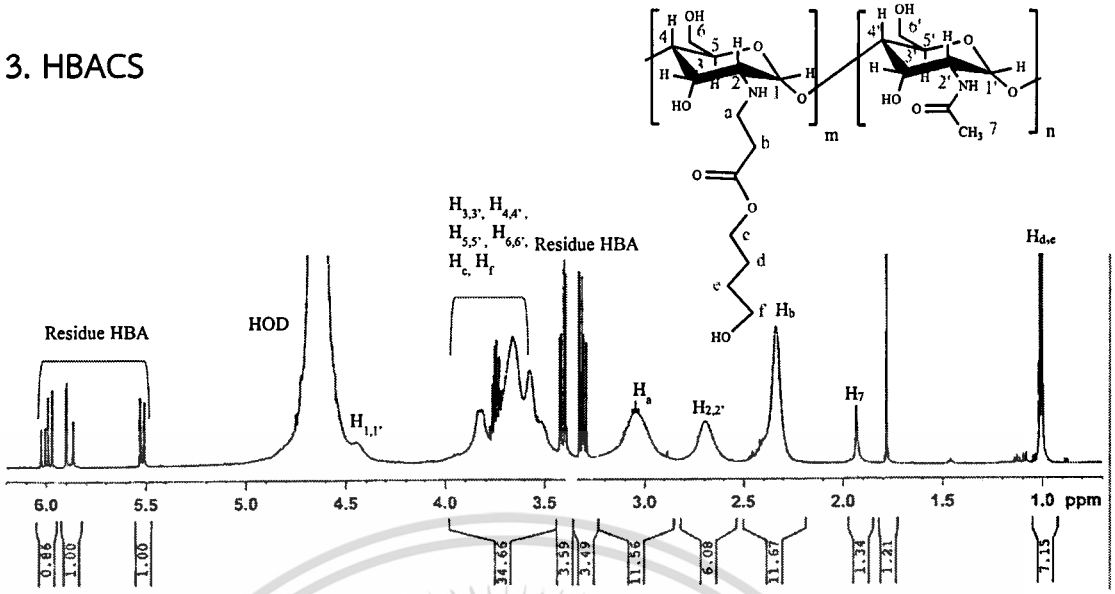

Figure B-4 ^{1}H-NMR spectrum of HBACS.

3.1 %DS

The %DD of CS was firstly calculated using data obtained from the spectrum depicted in Figure B-4. It could be seen from the spectrum that the integral area of H_7 at δ = 1.94 ppm was 1.34 and the integral area of $H_{(2,2')}$ at δ = 2.73 ppm was 6.08. Therefore,

$$\%DD = 100 - \left(\frac{H_7/3}{H_{(2,2')}} \times 100\right) \quad \text{(B-1)}$$

$$= 100 - \left(\frac{1.34/3}{6.08} \times 100\right)$$

$$= 93\ \%$$

After that, %DS of HBACS was calculated using equation 3.2.

$$\%DS\ (HPACS\ or\ HBACS) = \frac{H_a/2}{H_{(2,2')}} \times 100 \quad (3.2)$$

Data obtained from the spectrum showed that the integral area of H_a at δ = 3.05 ppm was 11.56 and the integral area of $H_{(2,2')}$ at δ = 2.73 ppm was 6.08. Thus,

$$\%DS\ (HPACS\ or\ HBACS) = \frac{11.56/2}{6.08} \times 100$$

$$= 95\ \%$$

3.2 Average molecular weight per repeating unit

Before calculating average molecular weight per repeating unit of HBACS, average molecular weight per repeating unit of CS was firstly determined using %DD obtained from previous section. Therefore,

M_w per repeating unit of CS $= (Mw_{acetyl} - (43 \times 0.93)) + (Mw_H \times 0.93)$ (B-2)

$= (203 - 40) + (1 \times 0.92)$

$= 164$

After that, equation B-6 was applied to calculate average molecular weight per repeating unit of HBACS.

M_w per repeating unit of HBACS $= (Mw_{CS} - (1 \times Mw_H)) + (Mw_{HBA} \times 0.95)$ (B-6)

$= (164 - (1 \times 0.95)) + (144 \times 0.95)$

$= 300$

3.3 %Yield

Theoretical weight of HBACS was firstly calculated;

$$W_{HBACS} = 6 \text{ g CS} \times \frac{1 \text{ mol CS}}{164 \text{ g CS}} \times \frac{300 \text{ g HBACS}}{1 \text{ mol HBACS}}$$

$$= 10.98 \text{ g}$$

The weight of the product was 9.59 g. Therefore,

$$\%\text{Yield} = \frac{9.59}{10.98} \times 100$$

$$= 87\ \%$$

4. TsCD

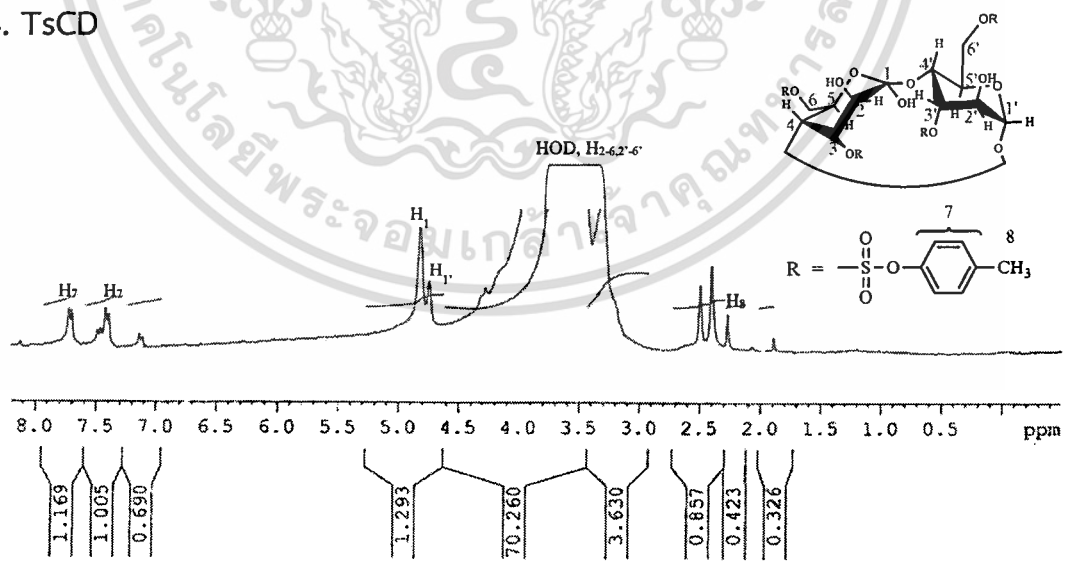

Figure B-5 ^{1}H-NMR spectrum of TsCD.

4.1 %DT

%DT of TsCD can be calculated from equation 3.3.

$$\%DT\ (TsCD) = \frac{H_{Ar}/4}{(H_1+H_{1'})/7} \times 100 \quad (3.3)$$

Figure B-5 shows ^{1}H-NMR spectrum of TsCD. From the spectrum, the integral area of H_{Ar} which is aromatic protons from tosyl group at δ = 7.72 and 7.40 ppm was 1.484 and the integral area of H_1 and $H_{1'}$ protons from CD was 1.293. Hence,

$$\%DT\ (TsCD) = \frac{1.484/4}{1.293/7} \times 100$$

$$= 201\ \%$$

4.2 Average molecular weight per repeating unit

Average molecular weight per repeating unit of TsCD could be calculated using the following equation:

$$M_w \text{ per repeating unit of TsCD} = (Mw_{CD} - (Mw_H \times 2.01)) + ((Mw_{TsCl} - 35.5) \times 2.01) \quad (B\text{-}7)$$

$$= (1135 - (1 \times 2.01)) + ((190.5 - 35.5) \times 2.01)$$

$$= 1132.99 + 311.55$$

$$= 1445$$

4.3 %yield

Calculating theoretical weight of TsCD;

$$W_{TsCD} = 10\ g\ CD \times \frac{1\ mol\ CD}{1135\ g\ CD} \times \frac{1445\ g\ TsCD}{1\ mol\ TsCD}$$

$$= 12.73\ g$$

The weight of the product was 4.25 g. Thus,

$$\%Yield = \frac{4.25}{12.73} \times 100$$

$$= 33\ \%$$

5. TE-1

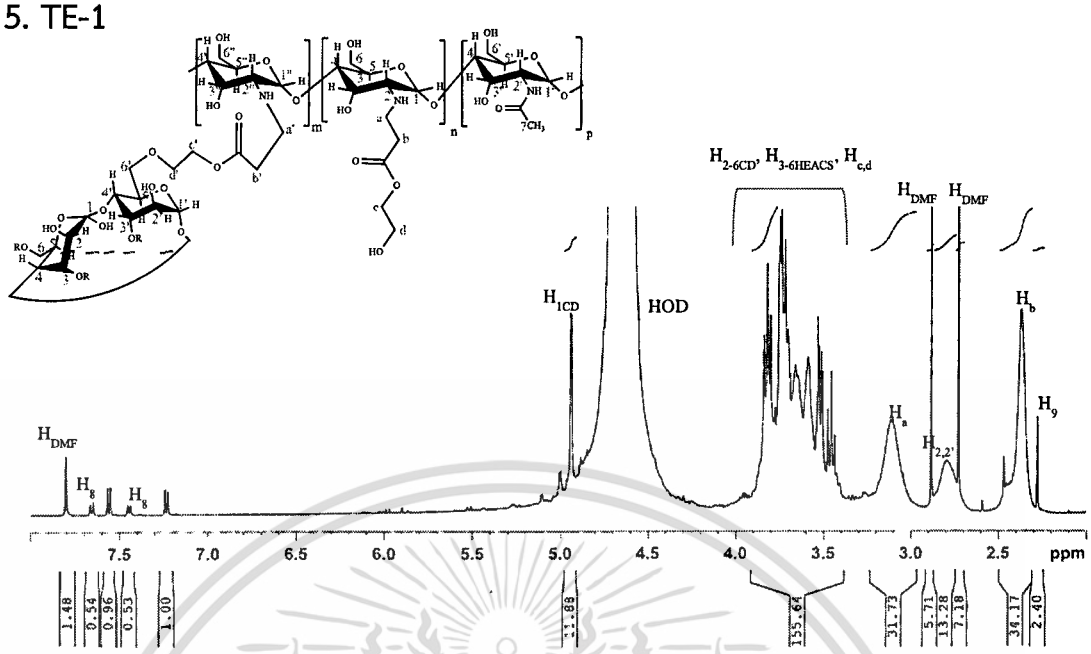

Figure B-6 ^{1}H-NMR spectrum of TE-1.

5.1 %DS

To calculate %DS of TE-1, equation 3.4 was used.

$$\%DS\ (TE\text{-}1) = \frac{H_{1CD}/7}{H_{(2,2')}[\%DS=100]} \times 100 \qquad (3.4)$$

From the spectrum illustrated in Figure B-6, the integral area of H_{1CD} which is the H_1 proton of CD at δ = 4.94 ppm was 11.68 and the integral area of $H_{(2,2')}$ from CS skeleton at δ = 2.73 ppm was 13.28.

Because the %DS of HEACS used as a reactant was 97. Therefore, the integral area of $H_{(2,2')}$ has to be converted to %DS = 100 in order to obtain the accurate value of the %DS of TE-1. Hence,

$$H_{(2,2')}[\%DS=100] = 13.28 \times \frac{100}{97}$$

$$= 13.68$$

Substituted the value of $H_{(2,2')}$[%DS=100] and H_{1CD} into equation 3.4;

$$\%DS\ (TE\text{-}1) = \frac{11.68/7}{13.68} \times 100$$

$$= 12\ \%$$

5.2 Average molecular weight per repeating unit

Equation B-8 was used to calculate average molecular weight per repeating unit of TE-1.

M_w per repeating unit of TE-1 = $(Mw_{HEACS} - (Mw_H \times 0.12)) + ((Mw_{CD} - 17) \times 0.12)$ (B-8)

= $(276 - (1 \times 0.12)) + ((1135 - 17) \times 0.12)$

= 275.88 + 134.16

= 410

6. TP-1

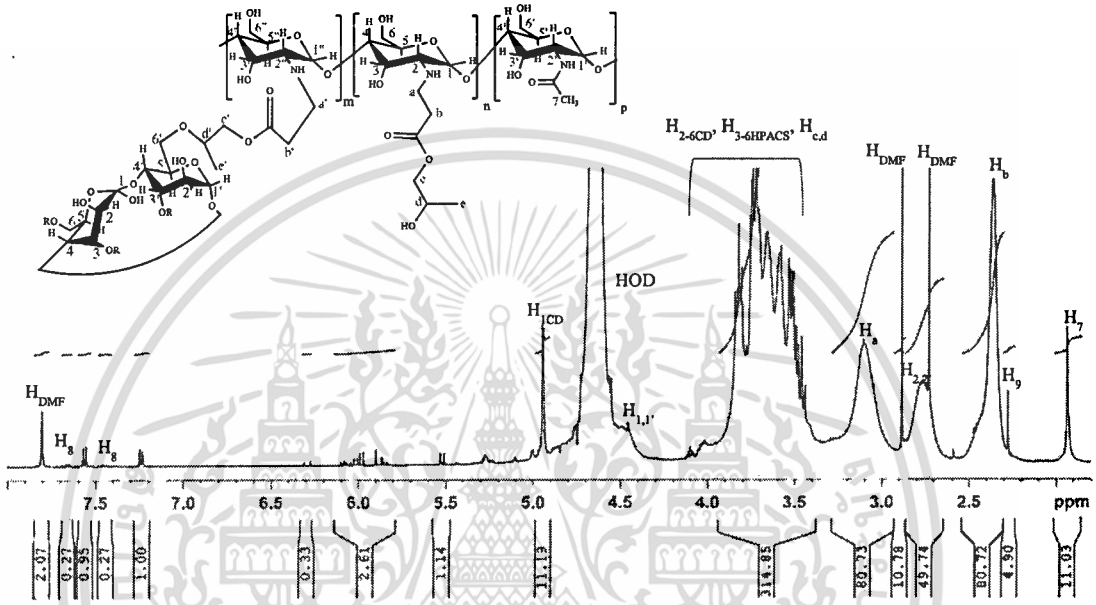

Figure B-7 ^{1}H-NMR spectrum of TP-1.

6.1 %DS

Equation 3.5 was used for calculating %DS of TP-1.

$$\%DS\ (TP\text{-}1, TB\text{-}1\text{-}3) = \frac{H_{1CD}/7}{H_a/2[\%DS=100]} \times 100 \quad (3.5)$$

Figure B-7 shows the ^{1}H-NMR spectrum of TP-1. The integral area of H_{1CD} at δ = 4.94 ppm was 11.19 and the integral area of HPA moiety protons (H_a) at δ = 3.10 ppm was 80.73.

Data from section 2.1 showed that the %DS of HPACS was 80. Therefore, the integral area of H_a has to be converted to %DS = 100 as below:

$$H_a[\%DS=100] = 80.73 \times \frac{100}{80}$$

$$= 100.91$$

Substituted the values into equation 3.5;

$$\%DS\ (TP\text{-}1,TB\text{-}1\text{-}3) = \frac{11.19/7}{100.91/2} \times 100$$

$$= 3\ \%$$

6.2 Average molecular weight per repeating unit

Average molecular weight per repeating unit of TP-1 could be calculated using equation B-9.

$$M_w \text{ per repeating unit of TP-1} = (Mw_{HPACS} - (Mw_H \times 0.03)) + ((Mw_{CD} - 17) \times 0.03) \quad \text{(B-9)}$$

$$= (267 - (1 \times 0.03)) + ((1135 - 17) \times 0.03)$$

$$= 266.97 + 33.54$$

$$= 301$$

7. TB-1

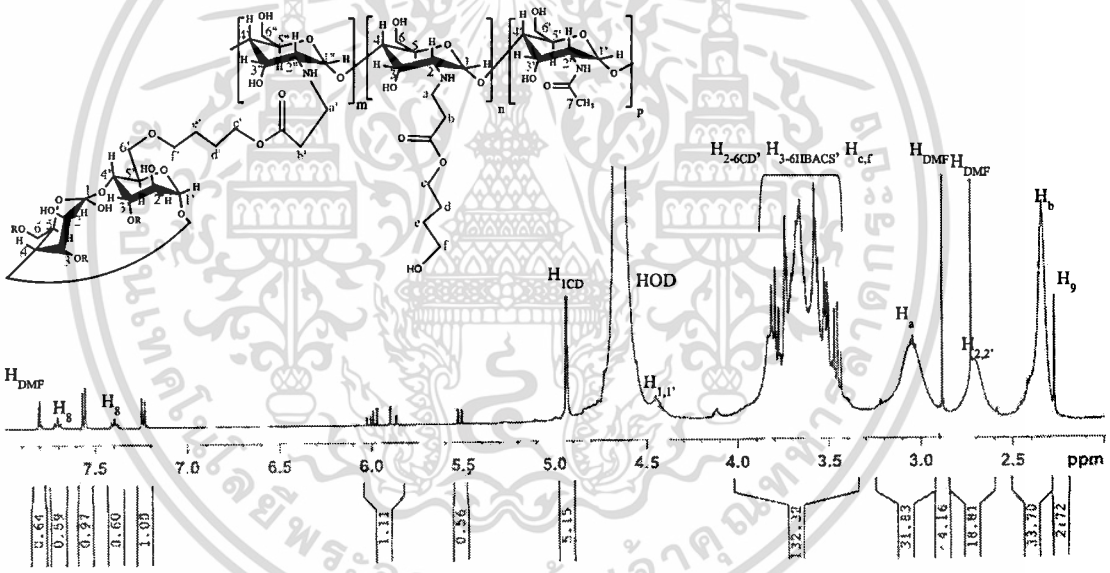

Figure B-8 ^{1}H-NMR spectrum of TB-1.

7.1 %DS

%DS of TB-1 could be also calculated using equation 3.5. From Figure B-8, the integral area of H_{1CD} at δ = 4.94 ppm was 5.15 and the integral area of H_a at δ = 3.25 ppm was 31.83.

To calculate the %DS of TB-1, the integral area of H_a was needed to be converted to %DS = 100 because %DS of HBACS used in the reaction was 95. Consequently,

$$H_a[\%DS=100] = 31.83 \times \frac{100}{95}$$

$$= 33.51$$

Substituted the integral values into equation 3.5;

$$\%DS\ (TP\text{-}1,TB\text{-}1\text{-}3) = \frac{5.15/7}{33.51/2} \times 100$$

$$= 4\ \%$$

7.2 Average molecular weight per repeating unit

To calculate average molecular weight per repeating unit of TB-1, equation B-10 was used.

$$M_w \text{ per repeating unit of TB-1} = (Mw_{HBACS} - (Mw_H \times 0.04)) + ((Mw_{CD} - 17) \times 0.04) \quad \text{(B-10)}$$

$$= (300 - (1 \times 0.04)) + ((1135 - 17) \times 0.04)$$

$$= 299.96 + 44.72$$

$$= 345$$

8. TB-2

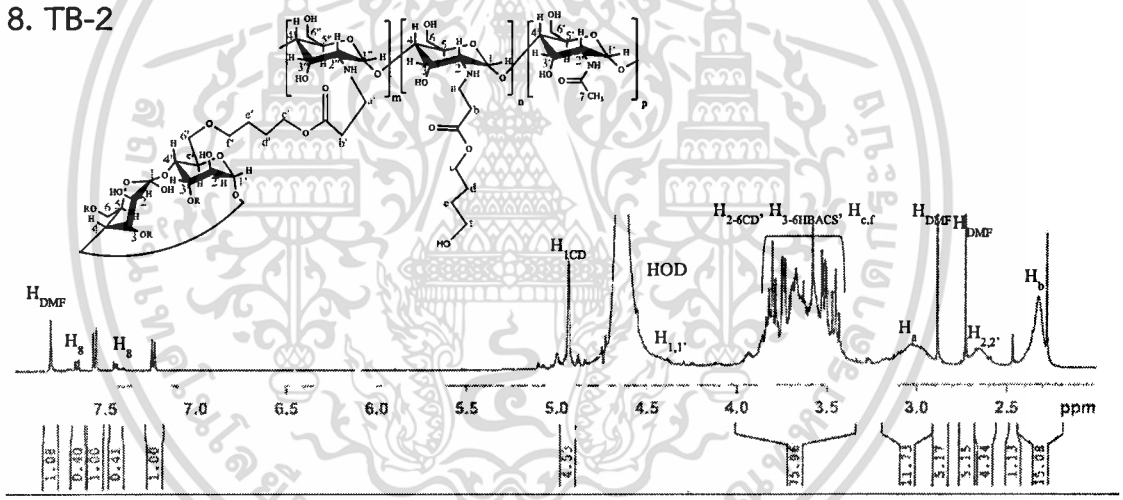

Figure B-9 ^{1}H-NMR spectrum of TB-2.

8.1 %DS

Equation 3.5 was also used for calculating %DS of TB-2. From the above spectrum, the integral area of H_{1CD} at δ = 4.94 ppm was 4.53 and the integral area of H_a at δ = 3.10 ppm was 11.73.

Converting the integral area of H_a to %DS = 100;

$$H_a[\%DS=100] = 11.73 \times \frac{100}{95}$$

$$= 12.35$$

Substituted the values into equation 3.5;

$$\%DS\ (TP\text{-}1,TB\text{-}1\text{-}3) = \frac{4.53/7}{12.35/2} \times 100$$

$$= 10\ \%$$

8.2 Average molecular weight per repeating unit

Equation B-11 was used for calculating average molecular weight per repeating unit of TB-2.

$$M_w \text{ per repeating unit of TB-2} = (Mw_{HBACS} - (Mw_H \times 0.1)) + ((Mw_{CD} - 17) \times 0.1) \quad \text{(B-11)}$$

$$= (300 - 0.1) + ((1135 - 17) \times 0.1)$$

$$= 299.9 + 111.8$$

$$= 412$$

9. TB-3

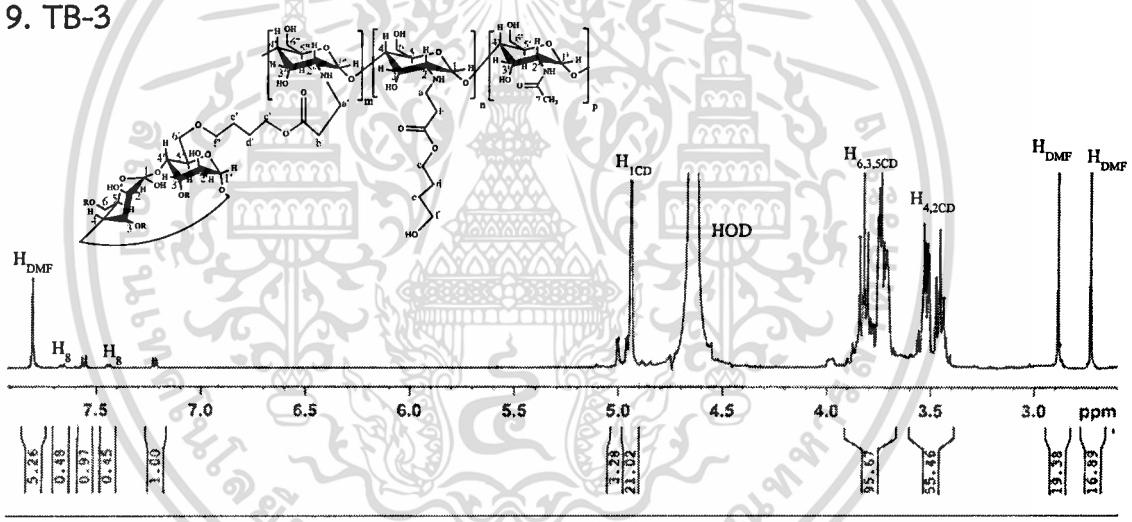

Figure B-10 ^{1}H-NMR spectrum of TB-3.

The %DS and other values of TB-3 could be calculated because there was no any signals from HBACS in the spectrum.

Appendix C

GPC chromatogram of CS, HAACSs, and HAACSs-g-CDs

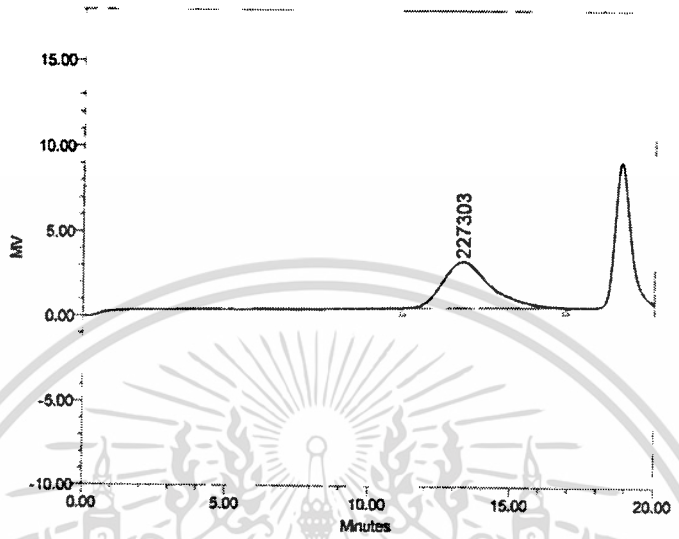

	Mn (Daltons)	Mw (Daltons)	MP (Daltons)	Mz (Daltons)	Mz+1 (Daltons)	Polydispersity
1	82729	269685	227303	541791	889903	3.259869

Figure C-1 GPC chromatogram of CS.

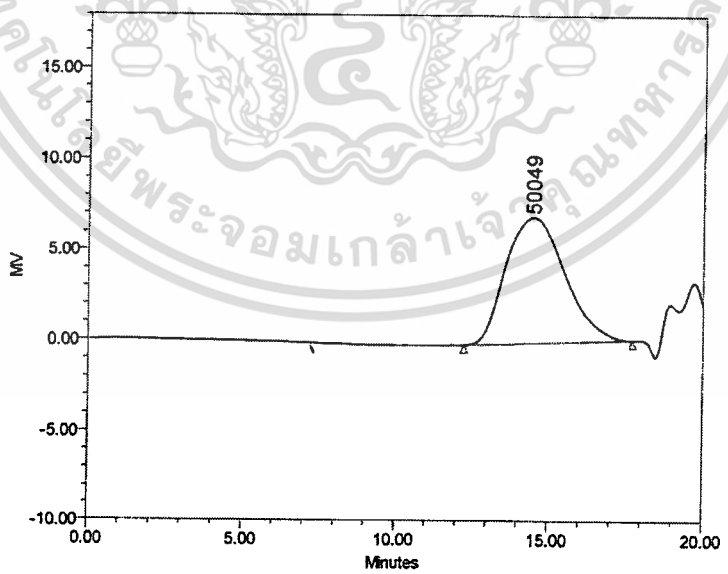

	Mn (Daltons)	Mw (Daltons)	MP (Daltons)	Mz (Daltons)	Mz+1 (Daltons)	Polydispersity
1	22734	69209	50049	141153	218730	3.044245

Figure C-2 GPC chromatogram of HEACS.

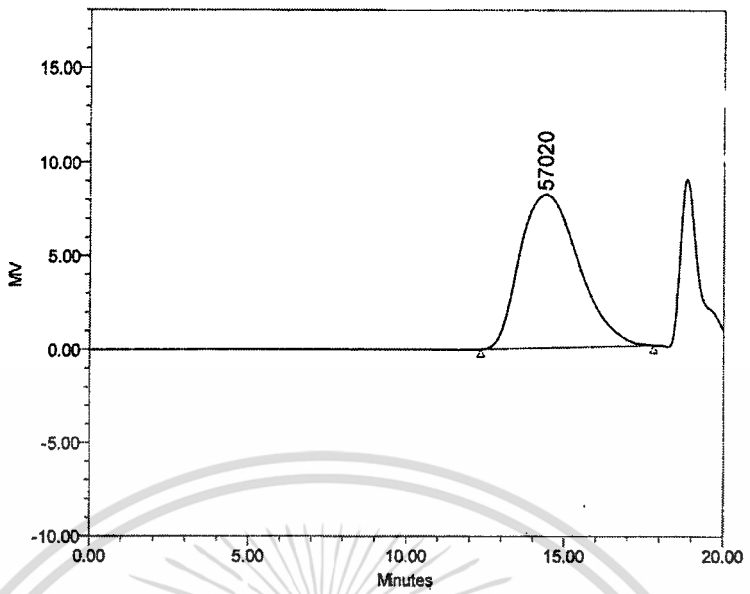

	Mn (Daltons)	Mw (Daltons)	MP (Daltons)	Mz (Daltons)	Mz+1 (Daltons)	Polydispersity
1	23581	69886	57020	135918	203735	2.963707

Figure C-3 GPC chromatogram of HPACS.

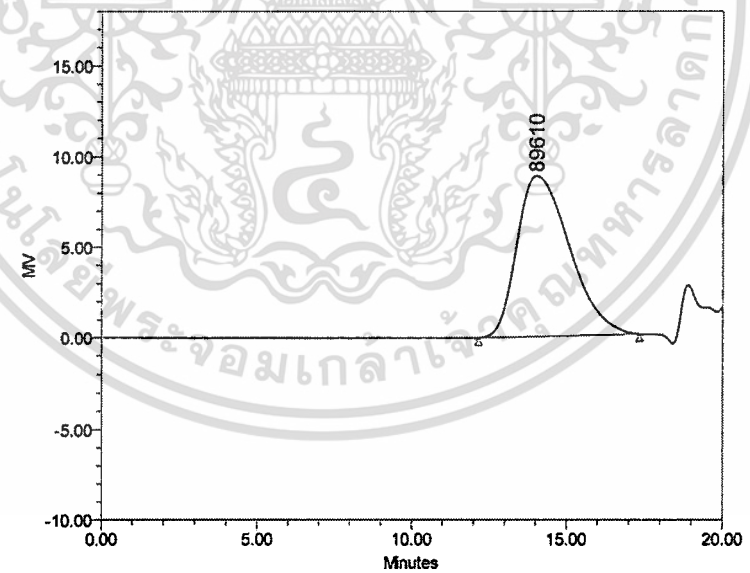

	Mn (Daltons)	Mw (Daltons)	MP (Daltons)	Mz (Daltons)	Mz+1 (Daltons)	Polydispersity
1	33879	90046	89610	165339	247520	2.657856

Figure C-4 GPC chromatogram of HBACS.

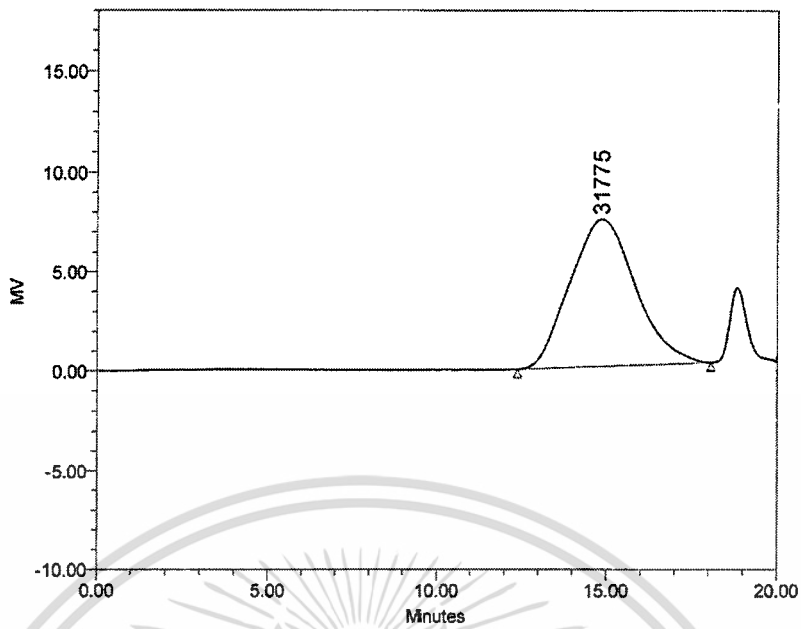

	Mn (Daltons)	Mw (Daltons)	MP (Daltons)	Mz (Daltons)	Mz+1 (Daltons)	Polydispersity
1	14928	49931	31775	114424	189982	3.344802

Figure C-5 GPC chromatogram of TE-1.

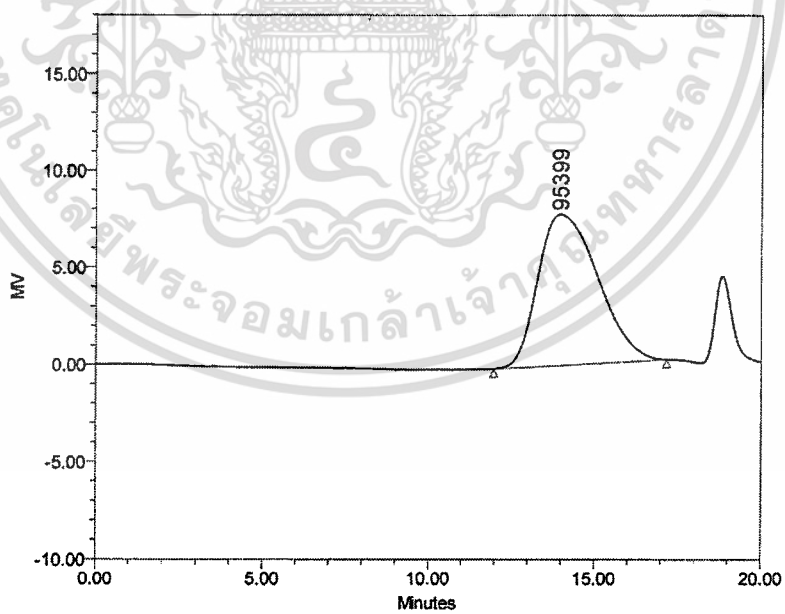

	Mn (Daltons)	Mw (Daltons)	MP (Daltons)	Mz (Daltons)	Mz+1 (Daltons)	Polydispersity
1	36815	99080	95399	190510	295047	2.691317

Figure C-6 GPC chromatogram of TP-1.

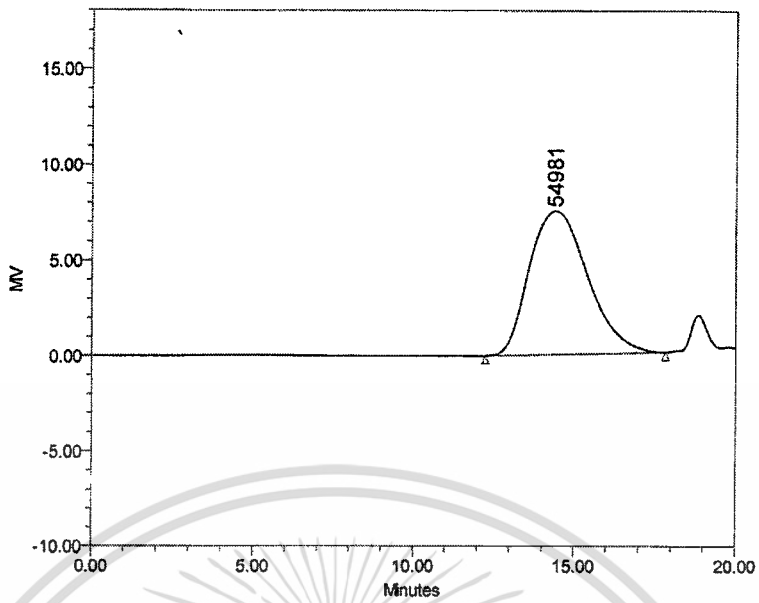

	Mn (Daltons)	Mw (Daltons)	MP (Daltons)	Mz (Daltons)	Mz+1 (Daltons)	Polydispersity
1	24217	69223	54981	134348	205126	2.858474

Figure C-7 GPC chromatogram of TB-1.

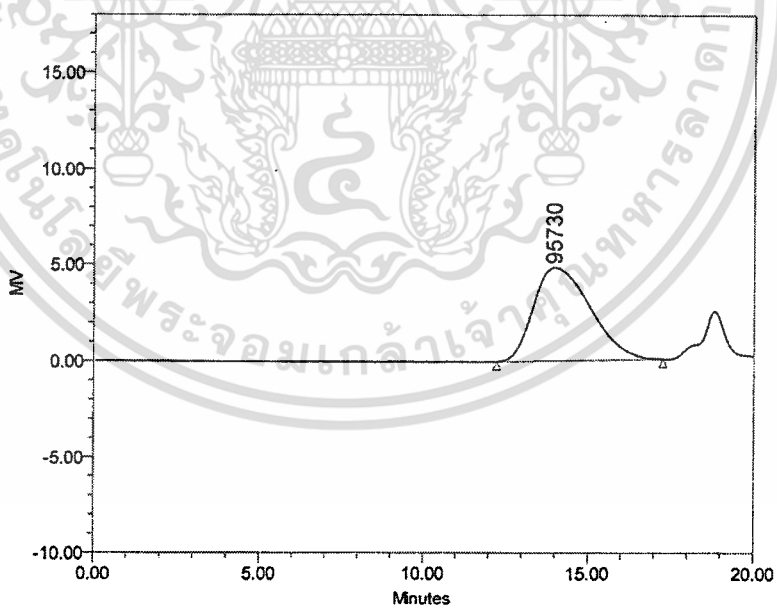

	Mn (Daltons)	Mw (Daltons)	MP (Daltons)	Mz (Daltons)	Mz+1 (Daltons)	Polydispersity
1	36940	94766	95730	172354	253005	2.565408

Figure C-8 GPC chromatogram of TB-2.

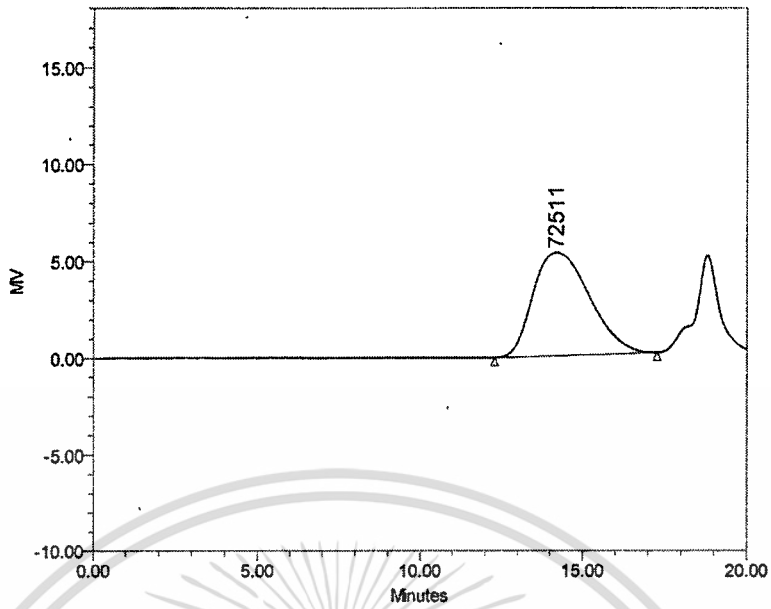

	Mn (Daltons)	Mw (Daltons)	MP (Daltons)	Mz (Daltons)	Mz+1 (Daltons)	Polydispersity
1	32809	80404	72511	146124	215527	2.450687

Figure C-9 GPC chromatogram of TB-3.

Appendix D

Examples of mole ratio calculation of inclusion complex solutions and films

In this section, the method for calculating mole ratio of inclusion complex solutions and films was presented. The examples used for calculating were from Table 3.5-3.7.

1. Inclusion complex solutions of TE-1MO

From data depicted in Table 3.5, the inclusion complex solution from series A with 25 mL of TE-1 and 25 mL of MO solutions was used to be an example for showing calculation method.

Calculating mmol of TE-1

In series A, 0.05 g of TE-1 was dissolved in 25 mL of water. Therefore, mmol of TE-1 could be calculated using average molecular weight per repeating unit from Appendix B as below:

$$\text{mmol}_{\text{TE-1}} = 0.05 \text{ g TE-1} \times \frac{1 \text{ mol TE-1}}{410 \text{ g TE-1}} \times \frac{1000 \text{ mmol TE-1}}{1 \text{ mol TE-1}}$$

$$= 0.122 \text{ mmol}$$

Calculating mmol of CD

From ^{1}H-NMR spectrum of TE-1 depicted in Appendix B, it showed that the %DS of TE-1 was 12%. This indicated that 12 units of CD were grafted onto 100 units of HBACS. Hence,

$$\text{mmol}_{\text{CD}} = 0.122 \text{ mmol TE-1} \times \frac{0.12 \text{ mmol CD}}{1 \text{ mmol TE-1}}$$

$$= 0.0146 \text{ mmol}$$

Calculating mmol of MO

The 50 mL of mixture contained 25 mL of 0.002% w/v of MO. Thus, mmol of MO could be calculated as follow:

$$\text{mmol}_{\text{MO}} = 25 \text{ mL MO} \times \frac{0.002 \text{ g MO}}{100 \text{ mL MO}} \times \frac{1 \text{ mmol MO}}{327 \text{ g MO}} \times \frac{1000 \text{ mmol MO}}{1 \text{ mol MO}}$$

$$= 1.53 \times 10^{-3} \text{ mmol}$$

Calculating mole ratio

The mole ratio of MO to CD of the example could be calculated as below:

$$\text{mmol}_{MO/CD} = \frac{1.53\text{x}10^{-3}\ \text{mmol MO}}{0.0146\ \text{mmol CD}}$$

$$= 0.10:1$$

2. Inclusion complex solutions of TB-1MO

From Table 3.6, the inclusion complex solution from series B contained 25 mL of TB-1 and 10 mL of MO solutions was used as an example for presenting the method for calculation.

Calculating mmol of TB-1

From the Table 3.6, 0.008 g of TB-1 was dissolved in 25 mL of water. Thus, mmol of TB-1 could be calculated using average molecular weight per repeating unit from Appendix B as follow:

$$\text{mmol}_{TB\text{-}1} = 0.008\ \text{g TB-1} \times \frac{1\ \text{mol TB-1}}{345\ \text{g TB-1}} \times \frac{1000\ \text{mmol TB-1}}{1\ \text{mol TB-1}}$$

$$= 0.023\ \text{mmol}$$

Calculating mmol of CD

From the calculation as depicted in Appendix B, the %DS of TB-1 was 4%. Consequently, mmol of CD could be obtained as below:

$$\text{mmol}_{CD} = 0.023\ \text{mmol TB-1} \times \frac{0.04\ \text{mmol CD}}{1\ \text{mmol TB-1}}$$

$$= 9.28 \times 10^{-4}\ \text{mmol}$$

Calculating mmol of MO

The 35 mL of mixture contained 10 mL of 0.002% w/v of MO. Therefore, mmol of MO could be calculated as follow:

$$\text{mmol}_{MO} = 10\ \text{mL MO} \times \frac{0.002\ \text{g MO}}{100\ \text{mL MO}} \times \frac{1\ \text{mmol MO}}{327\ \text{g MO}} \times \frac{1000\ \text{mmol MO}}{1\ \text{mol MO}}$$

$$= 6.12 \times 10^{-4}\ \text{mmol}$$

Calculating mole ratio

The mole ratio between MO and CD of the example could be calculated as below:

$$\text{mmol}_{MO/CD} = \frac{6.12\text{x}10^{-4}\ \text{mmol MO}}{9.28\text{x}10^{-4}\ \text{mmol CD}}$$

$$= 0.66:1$$

3. Inclusion complex films

The formulae of MO-incorporated TB-1 films were previously presented in Table 3.7. The TB-1MO0.04 film was selected to exemplify the method for calculation mole ratio of MO to CD.

From the Table 3.7, the TB-1MO0.04 film contained 1 g of TB-1 and 0.04 g of MO. The method for calculating the mole ratio was depicted as below:

Calculating mmol of TB-1

$$\text{mmol}_{\text{TB-1}} = 1\text{ g TB-1} \times \frac{1\text{ mol TB-1}}{345\text{ g TB-1}} \times \frac{1000\text{ mmol TB-1}}{1\text{ mol TB-1}}$$

$$= 2.90\text{ mmol}$$

Calculating mmol of CD

$$\text{mmol}_{\text{CD}} = 2.90\text{ mmol TB-1} \times \frac{0.04\text{ mmol CD}}{1\text{ mmol TB-1}}$$

$$= 0.116\text{ mmol}$$

Calculating mmol of MO

$$\text{mmol}_{\text{MO}} = 0.04\text{ g MO} \times \frac{1\text{ mmol MO}}{327\text{ g MO}} \times \frac{1000\text{ mmol MO}}{1\text{ mol MO}}$$

$$= 0.122\text{ mmol}$$

Calculating mole ratio

$$\text{mmol}_{\text{MO/CD}} = \frac{0.122\text{ mmol MO}}{0.116\text{ mmol CD}}$$

$$= 1.05{:}1$$

Appendix E

DMA thermograms

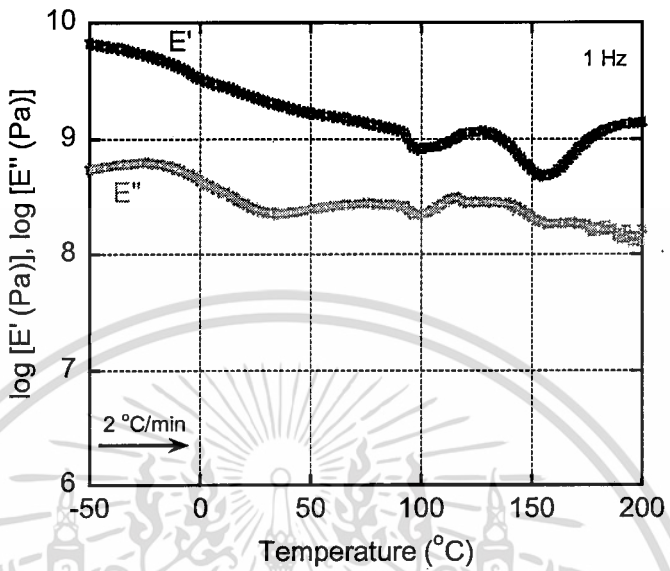

Figure E-1 Storage modulus (E') and loss modulus (E") versus temperature of CS film.

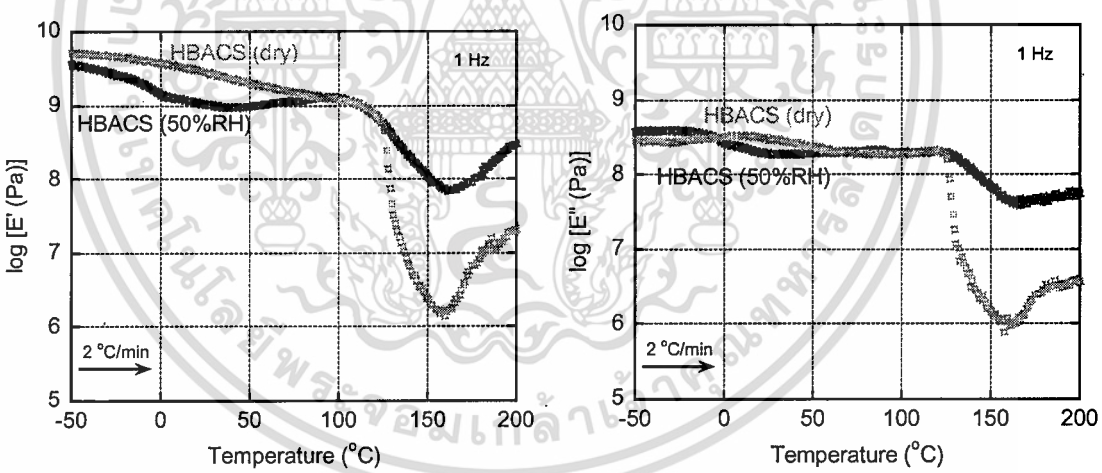

Figure E-2 Temperature dependence of tensile moduli for HBACS film with different storing conditions.

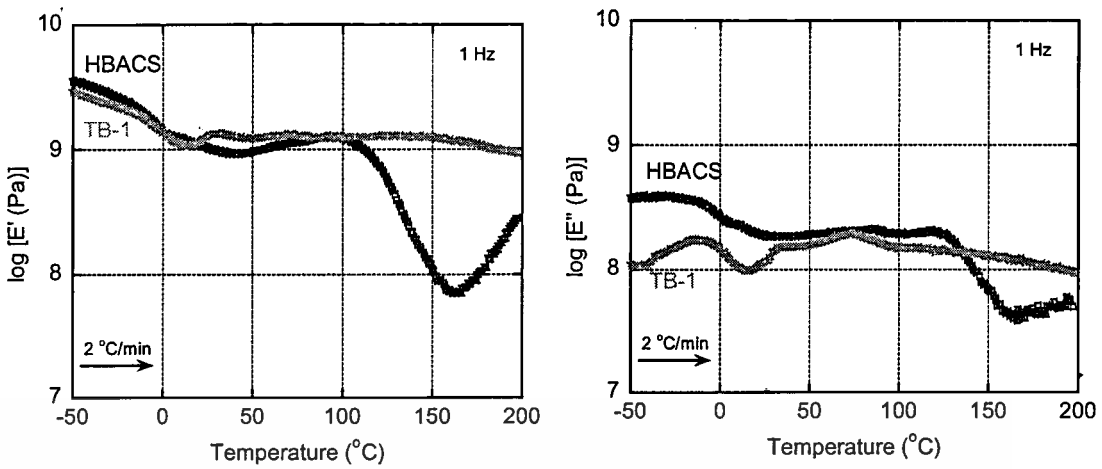

Storage modulus (E') vs. temperature Loss modulus (E") vs. temperature

Figure E-3 Temperature dependence of tensile moduli for TB-1 and HBACS films.

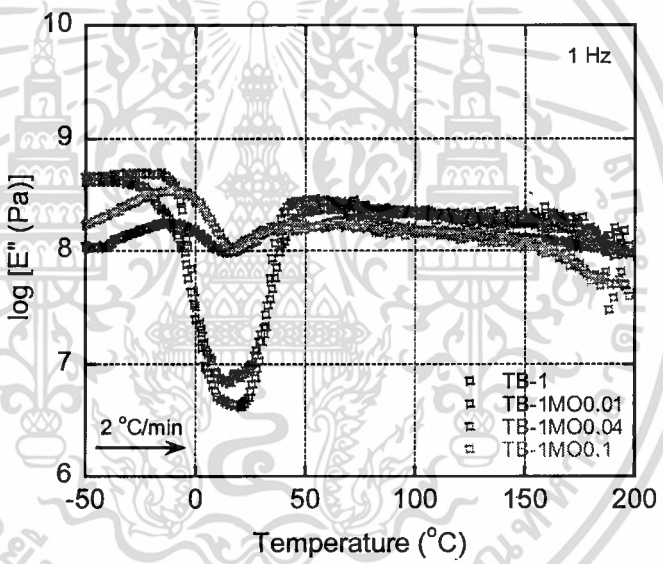

Figure E-4 Loss modulus (E") versus temperature of TB-1 and MO-incorporated TB-1 films.

Appendix F

TGA thermogram of methyl orange powder

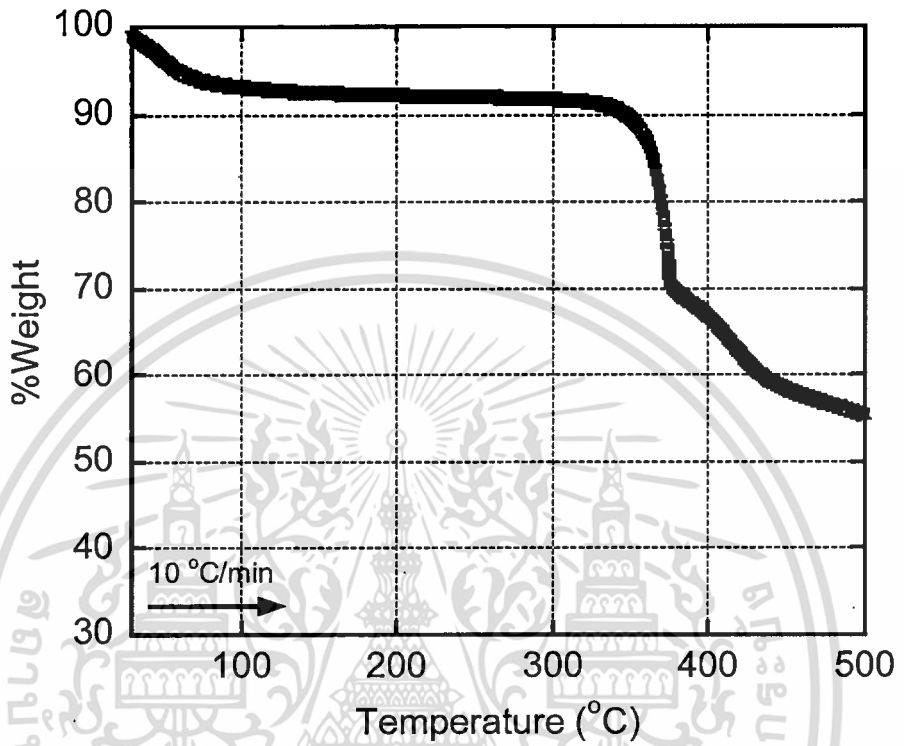

Figure F-1 TGA thermogram of methyl orange powder.

Author Biography

Name	Mr. Mongkhol Prawatborisut
Date of Birth	21 November 1991
Address	479/185 Soi Suttiporn Prachasongkhor road Dindang Bangkok 10400
Education	(2013) Bachelor of Science in Industrial Chemistry GPA 3.79 King Mongkut's Institute of Technology Ladkrabang (2015) Master of Science in Polymer Technology GPA 4.00 King Mongkut's Institute of Technology Ladkrabang
Scholarship	JAIST's Asian short-term stay program granted by Japan Student Services Organization (JASSO)

Academic Publication

[1] Mongkhol Prawatborisut and Pathavuth Monvisade, Preparation and characterization of β-cyclodextrin-modified hydroxyethylacrylchitosan and its inclusion complexes with methyl orange, Pure and applied chemistry international conference (PACCON) 2016, Bangkok international trade & exhibition centre (BITEC), Bangkok, Thailand, February 9-11, 2016, POL-0916, p 1176-1180.